National Library of Canada

Acquisitions and Bibliographic Services Branch

395 Wellington Street
Ottawa, Ontario
K1A 0N4

Bibliothèque nationale du Canada

Direction des acquisitions et des services bibliographiques

395, rue Wellington
Ottawa (Ontario)
K1A 0N4

Your file Votre référence

Our file Notre référence

NOTICE

The quality of this microform is heavily dependent upon the quality of the original thesis submitted for microfilming. Every effort has been made to ensure the highest quality of reproduction possible.

If pages are missing, contact the university which granted the degree.

Some pages may have indistinct print especially if the original pages were typed with a poor typewriter ribbon or if the university sent us an inferior photocopy.

AVIS

La qualité de cette microforme dépend grandement de la qualité de la thèse soumise au microfilmage. Nous avons tout fait pour assurer une qualité supérieure de reproduction.

S'il manque des pages, veuillez communiquer avec l'université qui a conféré le grade.

La qualité d'impression de certaines pages peut laisser à désirer, surtout si les pages originales ont été dactylographiées à l'aide d'un ruban usé ou si l'université nous a fait parvenir une photocopie de qualité inférieure.

Canada

MISFIRE OF SPARK IGNITED LEAN MIXTURE OF PROPANE - AIR IN A CONSTANT VOLUME VESSEL

by

ALI BONDOK

A thesis
submitted to the University of Ottawa,
March, 1993
in partial fulfillment of the
requirement for the degree of

MASTER OF APPLIED SCIENCE
in
MECHANICAL ENGINEERING

Department of Mechanical Engineering
University of Ottawa
OTTAWA, CANADA, 1993

ISBN 0-315-82582-0

UNIVERSITÉ D'OTTAWA
UNIVERSITY OF OTTAWA

Abstract

Misfire occurs when operating an internal combustion engine with air fuel ratio near the lean limit. To extend the misfire limit, the combustion chamber is redesigned to promote turbulence and swirl. An experimental study has been conducted in a constant volume vessel to investigate the effects of the swirling flow, the spark location, the spark energy, the spark gap and the equivalence ratio on misfire. The relationship between spark location and misfire is investigated for the three following ignition locations: quarter radius from the wall, half radius from the wall and three quarter radius from the wall. The instantaneous velocities are measured using hot wire anemometer. Mixtures of propane and air with equivalence ratios between 0.5 and 0.64 have been tested. Misfire was determined using the pressure trace and by visually inspecting the flame through the quartz glass.

The misfire probability decreases as the mean swirling velocity and turbulence intensity decay. Also the misfire probability decreases as the ignition point is nearer to the center even though the turbulence intensity is higher than that near the wall. It is postulated that the rate of growth of the flame area (flame stretching) is higher near the wall, therefore the lean misfire limit is richer.

Acknowledgement

I wish to express my sincere gratitude to Professor Roger Milane for his full supervision, continual patience, guidance, encouragement and many instructive discussions. I also wish to thank Professors Stavros Tavoularis and E. Plett for reading and commenting on this thesis.

I also thanks Dr. A. Sohrabi from the Department of Mechanical Engineer, Amirkabir University, Iran for his help during his visit at the University of Ottawa, the Faculty, the Staff and Graduate Students in the Department of Mechanical Engineering for their support and assistance.

Finally I am extremely thankful to my father, mother, brothers, sisters and my wife for their support and patience which contributed towards my success.

Contents

List of Tables

List of Figures

Notation

A	area of flame surface
B_o	specific rate of growth in quiescent mixture
C	capacitance of the capacity
C_p	specific heat at constant pressure
C_1	constant of the order 0.5 to 1.0
C_2	constant
C_3	constant has a negative value
d	kernel diameter
E	spark energy
F_k	dimensionless frequency
g_b	boundary velocity gradient
J	Joule
K	Karlovitz factor
k	thermal conductivity
kV	killovolt
KPa	killopascale
L	integral length scale
L_e	Lewis number
mJ	millijoule
m_a	mole fraction of air
m_f	mole fraction of fuel
M_a	molecular weight of air
M_f	molecular weight of fuel

MPa	migapascale
P_p	partial pressure of fuel
P_a	partial pressure of air
P_t	total pressure
R	universal gas constant
r_c	critical radius
R_e	Reynolds number
R_s	operating resistance for hot wire
R_c	cold resistance for hot wire
R_t	total resistance
T_a	adiabatic flame temperature
T_b	burned gas temperature
T_u	unburned gas temperature
T_g	gas fLow temperature
T_s	sensor temperature
t	time
U_i	instantaneous velocity
u_l	laminar burning velocity
$u^{'}$	turbulence intensity
u_t	turbulent flame speed
u_i	fluctuation velocity
$u_k^{'}$	effective root mean square turbulence velocity
V	voltage
X	fuel concentration

Greek Letters

μf	microfarad
μs	microsecond
ρ	density of unburned mixture
δ_l	laminar flame thickness
λ	Taylor microscale
ρ_b	density of burned gas
Γ_k	Kovasznay parameter
ϕ	equivalence ratio
β	constant for a given hot wire

Subscripts and Superscripts

$\overline{()}$	ensemble average value
$()'$	root mean square value

Chapter 1

INTRODUCTION

1.1 General Overview

In recent years the automotive industry has devoted considerable efforts towards improving the performance of spark ignition internal combustion engines. The new emphasis on engine efficiency is a result of the rapid rise in the price of gasoline and stringent federal government regulations on exhaust emissions and fuel economy. The present focus in the auto industry is to run the engine with a lean air-fuel ratio. There are, however, several problems associated with operating an engine in the lean fuel region, such as large cyclic variation, long combustion duration and misfire (unreliable ignition of mixture in the cylinder). There are several ways to deal with these problems such as redesigning the combustion chamber to promote

turbulence and swirl, stratifying the charge in an engine, precise metering of the air and fuel entering the cylinder to ensure optimum air - fuel ratio (e.g., electronic fuel injection), and accurate ignition timing control (e.g., closed loop feedback ignition control).

Misfire which is related to flammability limits was first recognized by Humbolt and Gay Lussac (1804) and first determined by Dovy (1816). The empirical observation that flammability limits are apparatus dependent was well summarized by Coward and Jones (1952). At that time, they proposed a long vertical tube as the standard apparatus for determining flammability limits having 51 mm in diameter, 1.8 m long, closed at the upper end and open to the atmosphere at the bottom. If a flame propagates to the top, the mixture is said to be flammable. However, if the flame is extinguished before reaching the top, the mixture is said to be nonflammable. Prior to 35 years ago, there was very little theoretical effort directed towards analyzing the extinction mechanism and the effect of boundary and initial conditions on the extinction process. A number of theories for flammability limits have been proposed. Each of these have focused on a single mechanism responsible for flame extinction such as heat loss from an one-dimension of flame (Spalding, 1957; Mayer, 1957) and flame stretch (Strehlow, 1978; Hertzberg, 1976).

1.2 Literature Review

Misfire in spark ignition engines, which is an important consideration facing combustion investigators, has been of interest for many years. Researchers have attempted to investigate the effect of engine operating variables and mixture motion within the combustion chamber on misfire. Misfire in engine is defined as the percent of cycles that does not ignite.

Quader (1976) investigated whether the lean limit occurred at ignition or during flame propagation. He described two lean misfire limits, the ignition limit and the partial-burn limit. The ignition limit is reached if the spark fails to ignite a sufficiently large flame kernel which will sustain flame propagation by the heat release from combustion. On the other hand, the partial burn limit is reached when the flame has not traversed the entire combustion chamber when the exhaust valve opens. His study showed that for early spark timing, misfire occured at ignition and that it can be avoided by retarding the spark advance. However, at late spark timing misfire occured during flame propagation and the partial burn limit was reached. Earlier Quader (1974), performed extensive experimental studies on lean misfire limit using mixtures of propane and air, and isooctane and air. His results indicated that the lean misfire limit was extended by increasing compression ratio and intake temperature, improving mixture homogeneity and decreasing charge dilution and engine speed.

There are many parameters affecting misfire limit; ignition system, spark gap and orientation, ignition energy, equivalence ratio, temperature and pressure, turbulence, quenching due to heat transfer and quenching due to stretching. In the following sections, the influence of the above mentioned factors on the misfire limit will be surveyed.

1.2.1 Ignition System

An electrical discharge spark is produced between the spark plug electrodes when a sufficiently high voltage is applied. The high temperature plasma kernel created by this spark develops into a self sustaining and propagating flame having a thin reaction sheet where exothermic chemical reactions occur. The energy which is available in the spark gap is about 7% of the total supplied electrical energy (Saggau, 1981).

Ziegler and Maly (1981) investigated the effect of two ignition systems on misfire using a mixture of methane - air for equivalence ratios between 0.59 to 0.65 incremented by 0.1 in stagnant and flowing mixtures. The two ignition systems tested were the TCI which has a long discharge duration (1.5 ms) and the VFZ which has an extremely short duration (100 ns). They found a distinct decrease in misfire probability when the VFZ system (short duration) is used for both stagnant and highly turbulent mixtures. Therefore, the VFZ system improves the lean combustion process as compared to TCI. In more recent work, Ziegler and Maly (1983) investigated

the effect of the two ignition systems, VFZ and TCI in turbulent mixture for equivalence ratios between 0.6 and 0.85 incremented by .05 for methane fuel and for an energy range between 6.5 and 32.4 mJ. For the TCI system (long duration) the lean limit attains an optimum value at low flow velocity (U = 5-7 m/s) and gets richer quickly with further increase in flow velocity. For the VFZ system (short duration) there is no flow effect on the spark duration and the spark energy at low velocity and less effect at very high flow velocities. Thus the lean limit characteristics of the VFZ system (short duration) is much less dependent on the flow field than the TCI system (long duration).

1.2.2 Spark Gap and Orientation

Ballal and Lefebvre (1977) discussed experimentally the relationship between the spark gap and the minimum energy at which a lean mixture could be ignited for a given spark advance. The minimum energy condition is the amount of energy which the spark must supply for the hot kernel to attain the critical size. At this critical size the rate of heat release in the reaction zone surrounding the hot kernel just exceeds the rate of heat loss from the kernel. Reducing the spark gap increases the heat loss to the spark electrode and the flame would be quenched. On the other hand, increasing the spark gap increases the heat loss to the unburned gas and the flame would also be quenched.

Bjorge and Rosengren (1987) found that when the spark gap is decreased the lean ignition limit is richer because of the large quenching effect caused by the electrode, and because the input electrical energy is also reduced. For a spark gap of the same size or larger than the quenching distance, the lean ignition limit will become richer with increasing velocity. Bjorge and Max (1987) found that at sufficiently high velocity (18 m/s) the influence of electrode diameter (0.3 to 1 mm) and electrode gap (0.1 to 1 mm) on the lean ignition is negligible as compared to the volume quenching by the mass flow of the unburned mixture. At these high velocities the lean ignition limit is independent of the electrode size and the spark gap. The authors also investigated the effect of electrode orientation. Three different orientations of the spark ground were used; the ground facing the upstream flow ($-90°$), the ground in crossflow ($0°$) and the ground facing the downstream flow ($+90°$). The measuring points all lie in a plane passing through the center of the spark gap. The crossflow orientation ($0°$) is slightly better than the downstream because of the quenching effect of the ground electrode in the downstream position. The upstream electrode orientation ($-90°$) gives the richer lean limit because it creates a wake in the spark gap which produces excessive quenching by the electrodes.

1.2.3 Ignition Energy

It is well recognized that in order for the flame to propagates through a stream of a homogeneous mixtures of fuel and oxidant, a sufficient amount

of energy must be released in such a way that a critical volume of the mixture is heated long enough to a sufficiently high temperature. This will enable this critical mass to react and release sufficient energy and active species. Such releases must then be communicated to adjacent layers in such a way that the reaction propagates to a regions of a fresh mixture.

Karim and Wierzba (1984) investigated the flammability of homogeneous mixture of methane and hydrogen in air. This was done in a circular tubular reactor 12.7 mm diameter and 609 mm length for both a low velocity stream (0.5 m/s) ignited with a pilot flame and for a high velocity stream ignited with a spark plug. In the high velocity stream, a greater energy would be required primarily due to an increase of loss and active species from the kernel to the surrounding. Also a greater energy is needed to allow for a successful flame initiation as the mixture is leaned. Ho and Santavicca (1987) investigated the effect of ignition energy (7 mJ and 30 mJ) on kernel growth using laser pulsed as an ignition source. The heat loss to the electrodes and the disturbance of the flow field by electrodes were eliminated. The initial flame kernel size and the growth rate were strongly affected by the level of the ignition energy. A higher energy resulted in a faster growth rate and a larger initial flame kernel size attributed to a faster initial expansion velocity. This will eventually delay the quenching effect of turbulence on flame kernel growth because the initial flame size is greater than a critical size (Lewis and Von Elbe, 1961).

Bradley and Lung (1987) found that the spread of the energy outward from the narrow discharge channel is accelerated by a high energy input in the early stage. A high initial power input produces a strong shock that rapidly moves away from the discharge channel, the high outward velocity behind the shock front enhances the convection of the energy and of the thermal spreading. The thermal spread is found to be the greatest with the short duration spark. After localized ignition, extra energy is necessary to overcome the effects of flame straining particularly in a turbulent flow. The high spark energy should be sufficient to decrease the chemical time below the reciprocal strain rate in the region of high strain rate. Pischinger and Heywood (1990) plotted the measured flame radius versus the electrical energy released at the time of flash in a square engine using a schlieren technique. They found that the higher electrical energy leads to a faster initial rate of flame growth. Ko et al (1991) studied the developing kernel growth in lean propane-air for several equivalence ratios (0.6, 0.7, 0.8), several gap sizes (0.5 - 2 mm) and several discharge duration (550 μs - 3.5 ms) in a constant volume bomb using a high - speed laser schlieren system. The equivalent kernel radius was measured near the minimum ignition energy assuming the spherical shape, and a good agreement was found with the critical radius calculated using an asymptotic analysis by Champion et al. (1986). The critical radius r_c is given by

$$r_c = \frac{(k)_{T_a}}{C_p T_a \rho T_u u_l} \frac{T_a}{T_b Le_A} exp\left[\frac{E}{2R}\left(\frac{1}{T_b} - \frac{1}{T_a}\right)\right] \qquad (1.1)$$

where T_a is the adiabatic flame temperature, T_b is the burned gas temperature, T_u is the unburned gas temperature, u_l is the adiabatic laminar burning velocity, ρ is the density of unburned gas, C_p is the specific heat at constant pressure, k is the thermal conductivity, Le_A is the Lewis number of the reactant A, E is the activation energy and R is the universal gas constant. Their data indicate that near the minimum ignition energy, the flame speed decreases from a very large value at the early stage when the radius of the flame kernel is less than the critical radius. As the flame kernel radius becomes larger than the critical radius, the speed increases and eventually approaches the adiabatic flame speed. For the nonignition case, the kernel growth rate near the minimum ignition energy is the same as the ignition case but the kernel stops growing at radius smaller than the critical radius and eventually it is extinguished. They also found that the ignition probability increases with increasing energy level and that the contact of the flame kernel with the electrodes results in heat loss. The correlation between the radius of the kernel and ignition energy for equivalence ratio richer than the misfire limit has been investigated by Thomas (1983); the radius of the kernel is found to be proportional to the ignition energy raised to the power two thirds ($\frac{2}{3}$).

1.2.4 Equivalence Ratio

Ho and Santavicca (1987) found that increasing the turbulence beyond a certain level reduces the mean flame kernel growth rate due to the flame

stretch effect for equivalence ratios between 0.5 and 0.7. For higher equivalence ratio, the mean flame kernel growth increases with turbulence due to enhanced mass burning rates. Ko et al (1991) calculated the critical radius (the radius of the kernel that must be reached for successful ignition) using a high-speed laser schlieren system. The spark current and voltage are simultaneously recorded. The critical radius increases rapidly with decreasing equivalence ratio, which will also result in a significant increase in the minimum ignition energy. Increasing the equivalence ratio results in a faster growth rate of the flame and the speed will approach the adiabatic flame speed. Maly (1981) found that the expansion velocity decreases with decreasing equivalence ratio which will eventually lead to misfire. Ballal and Lefebvre (1974) found that the minimum energy required to ignite a premixed fuel-air mixture increases rapidly as the mixture is leaned out. The inflammation process, the thickness and the rate of propagation of the resulting flame are strongly affected by the chemical energy of the mixture. The flame temperature decreases as the mixture is leaned out, the flame speed decreases and the flame becomes thicker.

1.2.5 Temperature and Pressure

Bradley and Lung (1987) found that as the kernel spreads, the temperature of its center initially decreases, then remains almost constant, and decreases when the discharge ends. The relationship between the temperature dis-

trubution and misfire was not investigated, however it is believed that this decaying trend in temperature affects misfire. The studies of Bjorge and Rosengren (1987) and of Bjorge and Max (1987) found that the lean ignition limit was leaner when gas temperature was increased. The lean limit is lowered by about 10% when the temperature is increased from $100°C$ to $200°C$. Also the lean ignition limit is lowered by a reduction in the gas pressure (5 to 10 bars). In a single cylinder engine experiments, Arici et al (1983) found that the lean limit was richer when the temperature of the mixture was colder. They proposed a correlation based on heat balance that includes a mass burning rate calculated based on the chemical and the eddy lifetimes. They developed a misfire model that assumed a fully developed turbulence flame structure immediately after the spark occurs. They formulated a singularity (misfire) condition to exist when the rate of heat gained by the initial kernel due to combustion just equals the rate of heat lost by thermal and turbulent diffusion.

1.2.6 Turbulence

Cole and Swords (1980) investigated the relationship between the fluctuations in the flow field in the region of the spark plug and the efficiency of combustion in a lean-burning engine. They found a strong correlation between the horizontal component of the mean velocity in the neighborhood of the spark plug just before firing and subsequent peak pressure, but little effect of the turbulence intensity. For the same crank angle and spark tim-

ing the peak pressure increases as the magnitude of the velocity decreases when the flow moves away from the spark plug. Maly (1981) developed a turbulent thermal ignition model taking into account the nonstationary character of the ignition process. For low turbulence level the flame front is enhanced by turbulence as compared to the expansion in a stagnant mixture. With increasing turbulence the reaction becomes weaker after ignition and may be quenched. Anderson and Lim (1985) studied the ignition limit as a function of equivalence ratio for two different engine speeds 1500 and 3000 RPM. They found that the effect of increased turbulence with RPM enhanced heat transfer from the initial flame kernel and caused a shift of the ignition limit to a richer mixture. Ho and Santavicca (1987) studied the effect of turbulence on flame kernel growth rate in lean propane - air mixture. The importance of turbulence depends on the ratio of the turbulence intensity to laminar flame speed plus the expansion velocity. As turbulence is increased the mean flame kernel growth rate decreases at equivalence ratio of 0.58 and increases at equivalence ratio greater than 0.8. Baritaud (1987) studied the early flame propagation from spark to a 4 mm flame radius using a schlieren technique in lean propane-air mixture. The flame is turbulent immediately after initiation, with no laminar phase. After 0.5 ms the effect of turbulence is very strong, and the kernel expansion rate increases with the engine speed (higher turbulence). This implies that the turbulence plays a role in misfire at the earliest stage of combustion.

Abdel-Gayed et al (1986) found that the thickness of the turbulent flame increases as the flame radius increases and the burning velocity u_t increases

with kernel radius and turbulence. The rate of increase of u_t with turbulence declines after a certain level of turbulence then u_t falls and finally explosion is quenched. The burning velocity and mass burning velocity increase with turbulent intensity prior to the quenching regime. Santavicca et al (1990) suggested that the local burning rate can be affected by turbulent flame stretch and that a sufficiently intense turbulence can result in local extinction. Arici et al (1983) found that at higher RPM (higher turbulence) the lean limit is richer.

1.2.7 Quenching due to Heat Losses

Jarosinski et al (1982) found that the extinction process for the downward propagating flame consists first of heat loss to walls which cools the gas in the region near the walls to the point where the flame can not propagate near the wall. After that, buoyancy carries cooler product gases ahead of the flame and consequently the flame is extinguished. On the other hand, upward propagating flame extinguishes by a stretch mechanism. The flame in the centerline is stretched, in such a way that the area of the flame is increasing with time as it is being washed from the tip towards the skirt of the flame. The heat losses to the wall are of no importance during this extinction process. Bjorge and Max (1987) found a richer ignition limit when the spark gap width is reduced below the quenching distance of the mixture because of the increase in heat and radical loss to the electrodes. This behavior is clearer when large electrodes are used.

Poschinger and Heywood (1990) investigated how the electrode geometry affects the heat losses to the electrode and the electrical performance of the ignition system, and how this affects the flame development process in a square engine using a schlieren technique. The heat loss to the electrode results in a significant cyclic variation in the initial flame kernel growth due to the variation in the contact area between flame kernel and the electrodes. When the heat loss from the flame kernel is higher than to the rate of energy gain from combustion, the flame growth rate is reduced significantly. The contact area is controlled by the local flow. A large flow velocity convects the flame kernel away from the electrodes, reducing the contact area and heat loss to the electrodes. When the velocity is small, the contact area will be very large, the heat loss increases and therefore the ignition is unsuccessful.

1.2.8 Quenching due to Stretching

The flame stretching factor has been introduced by Karlovitz et al (1953) as a mechanism of flame quenching in two dimensional laminar flame as:

$$K = \left(\frac{\delta_l}{U}\right)\left(\frac{dU}{dy}\right) \tag{1.2}$$

where δ_l is the thickness of flame, U is the local velocity of the gas and $\frac{dU}{dy}$ is the velocity gradient. For large values of Karlovitz stretch factor (K $\geq$1), the flame is disrupted by velocity gradient and quenching occurs. Later Karlovitz (1954) extented his work to a turbulent flow and postulated that

the flame is quenched if:

$$\frac{\delta_l}{u_l}\frac{u'}{L} \geq 1 \tag{1.3}$$

where L is the integral scale for turbulence, u' is the turbulent intensity and u_l is the laminar flame speed. The expression (1.3) implies that when the eddy lifetime $\frac{L}{u'}$ is shorter than the chemical lifetime $\frac{\delta_l}{u_l}$ misfire occurs. Klimov (1963) and Williams (1975) investigated flame propagation in a shear flow using the stretch factor:

$$K = \left(\frac{\delta_l}{u_l}\right)\left(\frac{1}{A}\frac{dA}{dt}\right) \tag{1.4}$$

where A is the area of flame surface and $\frac{dA}{dt}$ is the area growth rate. They found that for high values of K the flame may be extinguished. In a recent work, Abdel-Gayed and Bradley (1985) suggested two different expressions for the stretch factor depending on the Reynolds number. For low Reynolds numbers, the stretch factor is

$$K = \left(\frac{u'}{L}\right)\left(\frac{\delta_l}{u_l}\right) \tag{1.5}$$

and for a high Reynolds number, the stretch factor is:

$$K = \left(\frac{u'}{\lambda}\right)\left(\frac{\delta_l}{u_l}\right) \tag{1.6}$$

Quenching occurs for high values of $\frac{u'}{L}$ or $\frac{u'}{\lambda}$.

Quenching due to the flame stretching concept has been used by Reed (1967) to correlate the blow-off data of burner flames in terms of the Karlovitz similarity criterion:

$$g_b = (0.23\rho C_p u_l^2/k)(I - (I - X^{6.4})\alpha) \tag{1.7}$$

Where g_b is the boundary velocity gradient at blow-off, ρ is the density of the gas mixture in the unburned, C_p is the specific heat at constant pressure of the unburned, u_l is the burning velocity, k is the thermal conductivity of the unburned, X is the fuel concentration and α is a constant equal to zero for flames with no secondary combustion and unity for flames with secondary combustion. It has been shown that the experimental data are in agreement with the hypothesis that blow-off results from excessive quenching of the flow arising from the effect of the shear flow.

The bulk quenching of flame in an expanding chamber using schlieren photographs was analyzed by Smith et al (1977). Their study showed that the bulk quenching depended on the amount of the volume expansion rather than the rate of volume expansion. Therefore the unburned gas density was a critical parameter when bulk quenching occurred. They correlated the lean limit with the Karlovitz number for different ignition timing. The Karlovitz number was expressed in terms of the fluid and flow properties as follows

$$K = \frac{2\delta_l \rho}{d\rho_b} \tag{1.8}$$

Where d is the kernel diameter, ρ and ρ_b are the densities of the unburned and burned gases respectively and δ_l is the laminar flame thickness which is related to the laminar flame speed and to the density of the unburned gases. They found that bulk quenching occurs when ignition timing was retarded as found by Quader (1976) and that misfire occurs when Karlovitz number is greater than 0.15.

Wakisaka and Hamamoto (1979) proposed a criterion for flame extinction in the turbulent flow based on the Kovasznay parameter

$$\Gamma_k = \left(\frac{u'}{L}\right) / \left(\frac{u_l}{\delta_l}\right) \tag{1.9}$$

where u' is the turbulence intensity, L is the integral scale of turbulence, u_l is the laminar burning velocity and δ_l is the laminar flame thickness. When the value of the parameter Γ_k exceeds unity, the turbulence flame front will break up into numerous flamelets smaller than the minimal flame diameter in the mixture. Then the flamelets are quenched due to the heat loss to the unburned gas. Success or failure in flame propagation is judged by visual observation and by referring to ionization current signals. The minimum ignition energy increases with increasing flow velocity and turbulence intensity. A linear relationship holds between u'/L (reciprocal of the characteristic time of turbulent gas motion) and u_l/δ_l (reciprocal of the characteristic time of chemical reaction in the laminar flame zone). The criterion for the limits of flame propagation is expressed by the relation

$$\Gamma = (u'/L)/((u_l/\delta_l) - (u_l/\delta_l)_o) \tag{1.10}$$

where $(u_l/\delta_l)_O$ is the characteristic value of the minimum reaction rate in the quiescent mixture to overcome the heat loss to the combustion chamber wall owing to conduction or radiation. When $\Gamma \geq 1$, the flame zone is disturbed faster than the reaction proceeds and consequently the flame front breaks up and quenching occurs.

Quenching of the laminar flame in a region of intense turbulence with zero mean flow was investigated using instantaneous temperature measurements, global and local chemiluminescence measurements and schlieren technique by Chomiak and Jarosinski (1982). They found that the flame is quenched by turbulence for a critical value of the Karlovitz-Kovasznay criterion:

$$K = (u'/L)(\delta_l/u_l) \tag{1.11}$$

This value is between 7 and 20 other calculations indicate a range of 0.5 - 3.0. The coincidence of laminar and turbulent flame quenching data indicates that the extinction of flames by the flow has a universal character and is caused by an excessive stretch of the local combustion regions.

De Soete (1984) studied the effects of geometrical stretch in gases at rest (expansion due to the heat released) and aerodynamical stretch (expansion due to the velocity) in flames ignited at the stagnation point of concentric opposed jet flow on the flame speed and the surface flam growth during the early stages of flame propagation using laser shadowgraphy. Geometrical stretch causes periodically decaying fluctuation of the flame speed. Aerodynamical stretch has negative (decrease) effect on flame speed during early the stage of propagation when the spark is ignited. Aerodynamical and geometrical stretch have also positive effect on the growth rate of the flame surface becouse they cause an increase in the volumetric combustion rate.

Thomas (1983) developed a theory to identify the basic factors governing the combustion duration in a lean mixture. There are two factors that influence the combustion duration: the burning velocity and the velocity field. Therefore the success of a lean burning engine depends almost entirely on the nature of the fluid motion in the combustion chamber. A linear dependence between the rate of change of the flame area $\frac{1}{A}\frac{dA}{dt}$ (flame stretching) and the mean velocity gradient is suggested. The combustion time is inversely proportional to the flame stretching which depends linearly on the velocity gradient.

1.2.9 Correlations

Abdel-Gayed and Bradley (1980) have proposed a new analysis for the turbulent burning velocity. The spectrum of turbulence is divided into two eddies sizes: large eddies and small eddies. A correlation between u_t/u_l, u'/u_l and Reynolds number (R_e) is investigated. The influence of R_e appears to be important only for lower values of R_e. For large values, u_t/u_l varies linearly with u'/u_l. In a more recent work Abdel-Gayed et al (1984) have extended their previous work to a higher range of values of u'/u_l and R_e close to the flame quenching. The correlation proposed by Abdel-Gayed and Bradley (1980) does not predict the data for high values of u_t because at high localized rates of strain, the laminar flame velocity is reduced, with an associated reduction in u_l. If the Lewis number for the deficient reactant is close to unity, the strain field increases the temperature and the

concentration gradients; the heat source and reactant sink cannot support them and consequently the burning velocity falls. The effect of R_e resides in its effect upon the strain rate and less upon the turbulent transport processes. Later Abdel-Gayed et al (1984) included the effect of straining in their model. They measured u_t/u_l versus u'/u_l for high R_e for a range of mixture of propane-air at different equivalence ratios ($\phi = 0.7$, 0.8 and 0.9). As quenching is approached, there is a decrease in the values of u_t/u_l with an increase in u'/u_l. Quenching effects are greater with leaner hydrocarbon mixtures and can be ascribed to the effects of Lewis number ($L_e \geq 1$) in the strained laminar flame speed. Also quenching is associated with higher values of Karlovitz stretch factor (expression 1.5). Abdel-Gayed and Bradley (1985) reviewed available experimental data on the limits of the turbulent flame propagation, and proposed quenching by the turbulent straining as the controlling factor. They proposed a correlation between the turbulent and the laminar burning velocities, the Lewis and the Karlovitz numbers. They suggested two different quenching regimes one at low Reynolds number $R_e \leq 300$

$$u'/u_l \geq 0.71 R_e^{.5} \tag{1.12}$$

and the other at high Reynolds number $R_e \geq 300$

$$u'/u_l \geq 3.1(R_e/Le^2)^{.25} \tag{1.13}$$

In a recent work Abdel-Gayed and Bradley (1987) suggested that the turbulence spectrum influences both the flame propagation and the flame strain rate. In their previous work, Abdel-Gayed and Bradley (1985) correlated turbulent flame speed with u'/u_l. In this study, they found that u'_k/u_l is

more appropriate, u_k' is the effective root-mean-square turbulent velocity contribution of the frequencies aboveF_k, where F_k is the lower limit dimensionless frequency. The Karlovitz number is more appropriate than the Reynolds number R_e to describe the range of quenching both because of the influence of flame straining and because in some practical conditions, the turbulent explosion flames may grow at a constant strain rate. Abdel-Gayed and Bradley (1989) delineated continous regimes for the turbulent flame propagation. The influence of strain is coupled with the molecular thermal-diffusion processes usually embodied in a Lewis number, Le. A large Lewis number leads to a greater influence of the flame straining. They correlated flame quenching conditions with the product K.Le. At a low strain rate (K.Le $\leq$ 0.15), flame straining results in a continuous wrinkled laminar flame sheet. At a higher strain rate (K.Le $\geq$ 0.15 up to 0.3), the flame sheet starts to breakup. At higher values up to K.Le =1.5, partial quenching is observed in a fragmented reaction zone. Complete quenching occurs when K.Le $\geq$ 1.5. They found that the regimes of turbulent flame propagation are similar to the regimes defined by Borghi (1985).

Ballal and Lefebvre (1977) correlated the quenching distance with the minimum critical size (the rate of heat release in the reaction zone just exceeds the rate of heat losses from the kernel) in turbulence flowing mixture for methane and propane. They found two different mechanisms depending on the level of turbulence. For low turbulence, the quenching distance is given by:

$$d_q = \frac{A(k/\rho C_p)}{(u_l - 0.16u')} \tag{1.14}$$

where A is a constant determined experimentally, k is the thermal conductivity, ρ is the gas density, u_l is the laminar flame speed, u' is the turbulence intensity and C_p is the specific heat at constant pressure. For high level of turbulence, the quenching distance is given by:

$$d_q = \frac{B(k/\rho C_p)}{(u_t - 0.63u')} \tag{1.15}$$

where B is the ratio of quenching distance to flame thickness and u_t is the turbulent flame speed. An expression for the minimum energy E_{min} delivered to the gas was derived assuming spherical flame shape.

$$E_{min} = (\Pi/6)d_q^3 \rho C_p (T_a - T_u) \tag{1.16}$$

where T_a is the adiabatic flame temperature, T_u is the temperature of unburned gas at the time of spark. Anderson and Lim (1985) used the model of Ballal and Lefebvre (1977) to investigate misfire in internal combustion engines. The effects of equivalence ratio, intake temperature, pressure, turbulence (engine speed), spark advance, spark gap and ignition energy were investigated. The model failed to predict the effect of engine speed.

1.2.10 Swirling

It is well known that swirl leads to faster burning, to a decrease in cyclic variation and to an extension of the lean misfire limit.

Witze and Vilchis (1981) studied the effect of varying the swirl rates and turbulence level on flame propagation in an engine using laser Doppler velocimetry to characterize fluid motion and a laser shadowgraph to visualize the flame. Their mixture equivalence ratios were $\phi = 0.55$, 0.6, 0.8 and 1.1. They found for the higher swirl that the burning rate faster and that the cyclic variation is less. For no swirl the burning rate is slower and the cyclic variation is higher. In a more recent work, Witze (1982) investigated the effect of the swirl level and the spark location on the burn duration in a homogenous charge engine. The burn duration was a direct function of the flame travel distance to the combustion center when no swirl is used, therefore the central ignition is preferable. For a high swirl level, the burn duration decreases as the ignition point is moved towards the cylinder wall due to the flame holding effect that enhances the combustion by stretching the flame area. For lower swirl level central ignition is still preferable because flame holding effect is not significant. Witze (1982) concluded that when ignition is near the wall the combustion duration is shorter when swirl is high. However it is not yet known whether this result holds as the mixture gets near the lean limit. In particular, it is not known whether the lean limit is leaner or richer as the spark location is moved towards the wall.

Furthermore Hanson and Thomas (1984) have investigated combustion in a rotating disk shape vessel with off-center and centeral ignitions for

mixtures with equivalence ratios $\phi = 0.7$ and 1.0. Photographs of the explosions are taken using a high speed camera and the flame area is measured. The combustion duration is longer for central ignition becouse the centrifugal effect causes the elongation (penciling) of the flame along the axis and results in flame quenching by the end plates. The combustion duration is further increased for centeral ignition as the swirling flow is increased becouse the flame area is reduced. For off-center ignition, the combustion duration decreases as the swirling increases becouse quenching to the cylinder walls is reduced. However it is not known whether for off-center ignition combustion duration is still shorter near the lean limit. Specifically, it is not known whether the lean limit is the leaner as ignition point is the farthest from the center.

1.3 Objectives

The approach taken in this project to deal with the problems of the lean combustion is to increase combustion efficiency using swirling flow. Since the trend in misfire limit is not yet well known as the swirling flow is varied and the spark location is changed, an experimental study will be conducted to investigate the relationship between the lean misfire limit, the swirling flow and spark location. A constant volume vessel simulating the top-dead-center of an internal combustion engine will be used. The swirling flow will be varied by igniting at different delay times between the closing of the intake valve and the ignition time. Three radial ignition locations will be

investigated: quarter radius from the wall, half radius from the wall and three quarter radius from the wall. The turbulence characterstic will be measured using a single hot wire sensor. The misfire will be determined using the pressure trace and by visually inspecting the flame through the quartz glass.

Chapter 2

EXPERIMENTAL APPARATUS

2.1 Description of the Apparatus

A constant volume vessel of disc shape with a shrouded intake valve and variable lift, has been designed and constructed by Lei (1986) to closely simulate the essential features of the combustion process occurring near top dead center (T.D.C) in a conventional spark ignition engine. The complete device, illustrated in figure 1 consists of the cylindrical chamber, the intake system, the solenoid control valve, the electronic unit, the capacitor discharge ignition system (C.D.I.), a high pressure air tank supplying air to activate the air cylinder of the intake valve, a tank containing the mixture

of propane and air of volume $4.326 \times 10^{-2}\ m^3$, an injection tank connected to the vessel having a volume of $0.3523 \times 10^{-2}\ m^3$ and a vacuum pump.

2.1.1 Cylinderical Vessel

The vessel is made of stainless steel 316. In order to accommodate the intake system while saving material, the combustion chamber location is off-center. This cylindrical vessel is fitted with 25.4 mm thick quartz glass discs on each end to obtain a visual access figure 2. These two quartz glasses are attached to the cylindrical vessel by two clamps of 25.4 mm thickness each. Each clamp uses six bolts with diameter equal to 12.7 mm. The intake system, the pressure transducer and the exhaust valve are flush fitted along the wall of the cylinder.

2.1.2 Intake System

The intake valve shroud is used to produce a swirling flow figure 3. A half cut valve shroud is welded on the valve. An "O" ring sits in the groove in the intake to prevent leaking when the valve is closed and to reduce the impact load when the valve hits the intake port during closure.

The injection tank is connected to the combustion chamber through an inlet tube welded to the side of the intake system. The fuel mixture flows into the vessel through an inlet tube. The intake valve has a rod running

through the whole intake system. Two U-cups seals are used between the rod, the upper port and the shroud orientation angle selector to prevent leakage while the system is pressurized or evacuated. At the end of the rod, a flange is screwed on the rod with a flange lock nut to prevent the flange from rotating. The valve lift is controlled by the position of the flange with respect to the rod. The flange is connected to the air cylinder that controls the opening and the closure of the intake valve.

Because of the inertia of the valve, a delay period between the triggering of the signal and the actual valve opening occurs. This delay is determined directly from the pressure trace, since the pressure starts building up when the valve opens. The event was started at a time t = 0, the intake valve opened at t = 40 ms and the pressure starts building up with a constant rate till the valve starts closing, then the pressure rate decreases. When the valves closes (t = 120 ms) the pressure decreases because of the heat transfer to the chamber walls. The actual valve opening time is determined experimentally from the pressure trace.

2.1.3 Spark Plug Electrodes

In order to minimize the flow disturbance, the electrodes are pointed near the ignition point. The spark energy (E) is calculated using

$$E = \frac{CV^2}{2} \tag{2.1}$$

where C is the capacitance and V is the voltage across the capacitors. The energy is changed by changing the capacitors in the control unit. Several different capacitors having different capacity have been used: 47 μf, 100 μf, 220 μf and 470 μf. The voltage across the capacitor connected to the primary of the coil was maintained at 163 volts for two capacitors each $47\mu f$ in series to get energy 312 mJ.

2.1.4 Electronic Control Unit

The electronic control unit was designed by Mr. George Faris, former graduate student in the Department of Electrical Engineering of the University of Ottawa. This unit controls the duration of injection of the mixture and the ignition timing. The first signal sent activates the solenoid so that the intake is opened. At the end of this signal, the solenoid is deactivated and the intake closes. The valve opening time is adjustable from 55 ms to 200 ms. A second signal triggers the capacitor discharge ignition system. The time delay separating the closure of the valve and the ignition of the mixture is adjustable.

2.1.5 Mixture Preparation

The mixture global chemical reaction describing the combustion of propane and air is:

$$C_3H_8+\frac{5}{\phi}O_2+\frac{5\times 3.76}{\phi}N_2 \rightarrow (\frac{5}{\phi}-5)O_2+3CO_2+4H_2O+\frac{5\times 3.76}{\phi}N_2 \quad (2.2)$$

where ϕ is the equivalence ratio. Using this equation the mole fraction of propane and air is calculated. To prepare a mixture of predetermined propane and air ratio, the partial pressure method is used and the equivalence ratio is defined as

$$\phi = \left[\frac{\left(\frac{m_a}{m_f}\right)}{\left(\frac{m_a}{m_f}\right)_s}\right] \quad (2.3)$$

where $(m_a/m_f)_s$ is the stoichiometric air - fuel ratio, equal to 0.0642 for propane and air. The equation of state for propane assuming perfect gas is

$$P_f V = \frac{m_f}{M_f} RT \quad (2.4)$$

and for air is

$$P_a V = \frac{m_a}{M_a} RT \quad (2.5)$$

Dividing equation 2.5 by equation 2.4

$$\frac{P_f}{P_a} = \left(\frac{m_f}{m_a}\right)\left(\frac{M_a}{M_f}\right) \quad (2.6)$$

Rearranging equation 2.6

$$\frac{m_f}{m_a} = \left(\frac{P_f}{P_a}\right)\left(\frac{M_f}{M_a}\right) \quad (2.7)$$

Substituting equation 2.7 in equation 2.3 the equivalence ratio is

$$\phi = \frac{\left(\frac{P_f}{P_a}\right)\left(\frac{M_f}{M_a}\right)}{\left(\frac{m_f}{m_a}\right)_s} \quad (2.8)$$

Let A be defined as

$$A \equiv \frac{\left(\frac{M_f}{M_a}\right)}{\left(\frac{m_f}{m_a}\right)_s} \tag{2.9}$$

Therefore

$$\phi = A\frac{P_f}{P_a} \tag{2.10}$$

The molecular weight for propane is 44 gram/mole and for air is 28.84 gram/mole, therefore the constant A is equal to 23.76. In order to find out whether the mixture of gases can be assumed to be a perfect gas the compressibility factor (Z) has been found. The compressibility factor of a species can be found in a generalized compressibility chart (Van Wylen and Sonntag, 1985). The critical temperature of propane is 370 K, therefore the reduced temperature is 0.8. The critical pressure of propane is 4.3 MPa; for a total pressure of 1.03 MPa in the mixture tank, the partial pressure of propane is around 0.028 MPa. Therefore the reduced pressure is 0.0065 and the compressibility factor is equal to 1, and consequently the propane gas behaves as ano the ideal gas. The critical temperature of air is 143.41 K, the reduced temperature is then 2.09. The critical pressure of air is 3.77 MPa. Since the pressure in the mixture tank is 1.03 MPa, the partial pressure of air will be about 1.01 MPa. Then the reduced pressure is 0.27. From the compressibility chart, the factor Z of air is found to be around 0.995. Hence, the mixtur can be reasonably treated as an ideal gas. For the ideal gas the partial pressure of a component is

$$P_p = n_f P_t \tag{2.11}$$

where P_p is the partial pressure, P_t is the total pressure of the mixture and n_f is the mole fraction of the species.

After calculating the partial pressure of propane and air, the pressure regulator of the propane tank and the air tank was adjusted accordingly. When filling up the tank after evacuation, propane was injected first, followed by air. This procedure is taken so that the higher pressure air will not rush into the lower pressure propane tank. After preparation the mixture is allowed three days to mix and reach homogeneity. It is recommended to fill up the tank slowly to avoid the heating effect from compression, and allow it to reach ambient temperature before any re-adjustment of pressure.

The error in calculation of ϕ is obtained by taking the logarithm of equation 2.10

$$\log \phi = \log A + \log P_f - \log P_a \tag{2.12}$$

Differentiating equation 2.12

$$\frac{d\phi}{\phi} = \left(\frac{dP_f}{P_f} - \frac{dP_a}{P_a} \right) \tag{2.13}$$

The maximum relative error is

$$\frac{d\phi}{\phi} = \left(\left| \frac{dP_f}{P_f} \right| + \left| \frac{dP_a}{P_a} \right| \right) \tag{2.14}$$

The error in pressure reading is $\pm$ 0.138 MPa, therefore for a mixture with ϕ the relative error is $\pm$ 5.062 $\times$ 10^{-3}

Chapter 3

MEASUREMENTS TECHNIQUES

3.1 Temperature Measurements

Thermocouples manufactured by Namac corporation Florida U. S. A., were used to measure the temperature needed to correct the data for the difference between the calibration temperature and the actual temperature of the hot wire sensor. The thermocouple is of type E (chromel and constantan). The thermocouple time response is given by the manufacturer to be between 2 ms and 5 ms. The Namac thermocouples have 0.051 mm junction thickness. A DC millivolt amplifier model OMNI IIA has been used to amplify the voltage from the thermocouple by a factor of 91. The amplifier is con-

nected to the thermocouple by a copper wire and the junction is immerged in ice water (0^0C) as a reference. When the thermocouple and the junctions are placed in air the voltage output is zero as expected. To improve the efficiency, the two junctions (chromel and copper) and (constantan and copper) are placed in two tubes filled up with glycerine to avoid the ionization in the gap between the two junction figure 4. The temperature versus time are plotted for the three locations: quarter radius from the wall, half radius from the wall and three quarter radius from the wall. The decay in temperature shown in figure 1 results directly from the heat transfer to the wall. Figure 5 also indicates that there is a significant temperature gradients within the vessel resulting from a combination of charging procedure (compression effect) and wall heat transfer. The temperature decreases as the location of measurement was closer to the wall.

3.2 Pressure Measurements

In combustion, the piezoelectric pressure transducer is the most commonly used. However, the pressure measurements may suffer from error due to the thermal loading if transducers are unprotected. To minimize these errors, investigators have suggested the application of an insulating rubber coating (e.g RTV) over the transducer diaphragm. In the present experiment, the pressure was measured using a Kistler Model 601B1 piezoelectric pressure transducer with high impedance charge signal output. The transducer diaphragm was coated by the manufacturer with a high temperature sili-

cone rubber compound (GERTV12) after having been primed and cleaned with solvent. The transducer was connected to a Kistler charge amplifier Model No. 5004. The ampilifier was set for a long duration time, the transducer sensitivity range was 10-110 and the scale is 5 $\frac{bars}{volt}$. The transducer sensitivity is adjusted according to the calibration data supplied by the manufacturer. Since the expected peak combustion pressure was around 2.533 MPa, the calibration factor sensitivity was set to -1.08 as suggested by the manufacturer. A sample of the pressure history during intake is shown in figure 6.

3.3 Hot Wire Measurements

In order to calculate the turbulence characteristics of air swirl within the combustion chamber a single hot wire anemometer was used figure 7. To compensate for the effect of the air pressure and the temperature different from ones during calibration, on the output of the hot wire anemometer, a correction (Milane et al 1987) is made that requires the measurements of the pressure and temperature. The hot wire and thermocouple probes are inserted in the spark plug port and the hot wire sensor is parallel to the combustion chamber axis figure 8.

3.4 Hot Wire Calibration

Before calibrating the hot wire, the operating resistance R_s should be calculated. The resistance of the unheated wire sensor R_c is determined at the ambient temperature directly using the bridge on the anemometer. The operating resistance R_s of the wire is selected in such a way that the wire operating temperature T_s is equal to $250°C$. The operating resistance is given by the following formula:

$$R_s = R_c(1 + \alpha_c(T_s - T_c)) \tag{3.1}$$

where α_c is the thermal resistivity of the wire and T_c is the ambient temperature. By changing the flow termperature and adjusting the operating resistance R_s (the anemometer resistance), α_c and R_s are calculated using ALFARS program (Appendix A). The values used are $\alpha_c = 3.6176 \times 10^{-3}$ and $R_s = 9.36\ \Omega$.

The single hot wire anemometer is calibrated at the room temperature and the atmospheric pressure. The voltage across the sensor is calibrated versus the flow velocity measured by a pressure transducer (Validyne Model DP108). The experimental set-up used to calibrates located in the fluid lab (E005 CBY). The calibration experiments conducted in a low turbulence calibration unit. This set-up consists mainly of a yaw-pitch turntable frame and a low turbulence jet. The velocity of the jet is regulated by an intake valve and maintained constant to an accuracy of $\pm$ 0.1 %. The hot wire sensor is made of a tungsten wire platinum plated, having 5 μm diameter

and 1.3 mm length. The voltage V_o recorded by the anemometer device is equal to the sum of the voltage across the sensor, the prongs, the probe, the cable and the leg of the Wheatstone bridge. Therefore, the voltages across the sensor is expressed as:

$$V_s = \frac{V_o R_s}{R_t} \tag{3.2}$$

where

$$R_t = 40 + R_{probe} + R_{prong} + R_s \tag{3.3}$$

The velocity of the jet was given by the following relation, which is a modified Bernoulli equation,

$$U = 14.39\sqrt{(\Delta V_{tapping} - E_{off})} - 0.01478 \tag{3.4}$$

where E_{off} is the offset voltage of the pressure transducer (the voltage at zero velocity) and $\Delta V_{tapping}$ is the voltage output of the pressure transducer corresponding to a pressure difference between tapping in the calibration jet. The conversion from the hot wire voltage to the velocity is done according to the modified King's law

$$V_s^2 = A + BU^n \tag{3.5}$$

where V_s is the voltage across the wire and U is the velocity. The constants A, B and n are determined in such a way that the maximum error in the calculated values of V_s^2 is minimum using a least-square-fit for a polynomial of order 1. The program used is BEALN (Appendix A). The calibration curve for V_s^2 versus $U^{.42}$ is shown in figure 9, the value of n is 0.42. In order to correct for pressure and temperature differences from those during

calibration, the following form for the output voltage across the sensor was used (Milane et al, 1987)

$$V_s^2 = \beta(T_s - T_g)T_g^{.8} + \alpha(T_s - T_g)\frac{P_g^n}{T_g^{1.76n-0.8}}U^n \tag{3.6}$$

where the α, β and n are constants for a given wire. By comparing equations 3.5 and 3.6, the values of α and β are calculated as

$$\alpha = \frac{BT_g^{1.76n-0.8}}{(T_s - T_g)P_g^n} \tag{3.7}$$

and

$$\beta = \frac{A}{(T_s - T_g)T_g^{0.8}} \tag{3.8}$$

where α is 3.514×10^{-6} and β is 8.912×10^{-6}.

3.5 Data Acquisition

For each experiment, signals from the hot wire anemometer, pressure transducer and thermocouple are digitized on a Nicolet digital oscilloscope model 3091. The digitizing rate is 50 kHz, which enables data to be obtained over a time period of 80 ms. For each experiment, 4000 digitized data are transferred and stored on a floppy disc of a microcomputer using program STRM-91 (Appendix A). Three radial locations are tested: quarter radius from the wall, half radius from the wall and three quarter radius from the wall. For each case, hot wire data, temperature data and pressure data are gathered for 40 cycles. The measurements are taken 15 ms after closing the intake valve over a period of 80 ms.

Chapter 4

TURBULENCE CHARACTERISTICS

4.1 Definitions of Turbulence Characteristics

After taking the flow measurements, the voltage across the sensor is used to calculate the instantaneous velocity using program HHH-91 (Appendix B). Then the turbulence characteristics are calculated using ensemble average analysis using program MVT-91 (Appendix A). The instantaneous velocities are computed from the hot wire signals at each of the 4000 data points with temperature and pressure corrections according to equation 3.6.

4.1.1 Swirling Flow Measurements

In an engine the flow direction is not well known, therefore a single hot wire is not convenient because it does not resolve the flow direction. However, since the present measurements are made in a swirling flow, the mean direction is well defined and the measurements are done by positioning the sensor perpendicular to the swirling flow. Hamamoto et al (1988), have measured the flow characteristics of a swirling flow in a constant volume vessel using a single hot wire. A comparison of their results with other results taken using a laser Doppler velocimetry suggests that the measurements of a swirling flow using a single hot wire result at least in an adequate knowledge of the gross features of the flow and of the trends of the turbulence characteristics.

Furthermore in a work by Ghorbali (thesis draft), the flow was decomposed into an axial component parallel to the axis of the vessel, a radial component coincides with the radius of the vessel, and a tangential component perpendicular to the two other components. By rotating the hot wire, Ghorbali found that the mean flow in the radial and axial directions were negligible and therefore the flow was mostly tangential.

4.1.2 Mean Velocity

The ensemble averaged swirling velocity $\overline{U_i}$ at a given time is defined as:

$$\overline{U_i(t)} = \frac{\sum_{i=1}^{N} U_i(t)}{N} \tag{4.1}$$

where $U_i(t)$ is the instantaneous velocity at time t of the i cycle and N is the number of cycles sampled. Once the ensemble averaged is calculated, the time averaged is calculated over a period of 10.24 ms, which corresponds to 512 digital points as:

$$\overline{U_t} = \frac{1}{W}\sum_{j=1}^{W}\overline{U_t(t)} \tag{4.2}$$

where W is the number of points in the time window.

4.1.3 Turbulence Intensity

Since the flow is mostly tangential, and the ratio of the turbulence intensity to mean flow is less than 10 % (Tavoularis, S. 1986), the ensemble averaged turbulence intensity u' at a given time is defined as:

$$u'(t) = \left(\frac{\sum_{i=1}^{N} U_i^2(t)}{N} - \left(\frac{\sum_{i=1}^{N} U_i(t)}{N}\right)^2\right)^{\frac{1}{2}} \tag{4.3}$$

The time averaged turbulence intensity in a time window W is calculated as:

$$u' = \left[\frac{1}{W}\sum_{j=1}^{W} u'^2(t)\right]^{\frac{1}{2}} \tag{4.4}$$

4.1.4 Taylor Microscale

The ratio of the turbulence intensity to mean flow is less than 10% therefore Taylor approximation in which the structure of the turbulence eddies are

assumed to be frozen can be used (Tavoularis, S. 1986). The ensemble averaged Taylor microscale λ at a given time is given as:

$$\lambda(t) = \frac{u'(t)\overline{U_t(t)}}{\left[\overline{\left(\frac{\partial u_i(t)}{\partial t}\right)^2}\right]^{\frac{1}{2}}} \tag{4.5}$$

where $\frac{\partial u_i(t)}{\partial t}$ is the derivative of the instantaneous fluctuation velocity calculated as

$$\left[\overline{\left(\frac{\partial u_i(t)}{\partial t}\right)^2}\right]^{\frac{1}{2}} = \sqrt{\frac{1}{N}\sum_{i=1}^{N}\frac{(u_i(t+\Delta t)-u_i(t))^2}{(\Delta t)^2}} \tag{4.6}$$

where Δt is the time between a pair of consecutive points, $u'(t)$ is given in equation 4.3, and $\overline{U_t(t)}$ in equation 4.1. The time averaged Taylor microscale λ is calculated as:

$$\lambda = \left[\frac{1}{W}\sum_{j=1}^{W}\lambda^2(t)\right]^{\frac{1}{2}} \tag{4.7}$$

4.2 Flow Measurement Analysis

The flow characteristics at three different decay times (28 ms, 51 ms and 74 ms) and at three different locations have been measured in air. The flow characteristics namely the mean flow, the turbulence intensity and the Taylor microscale have been calculated using a computer program based on ensemble averaging MVT-91 (Appendix A). The values of the turbulence characteristics are shown in table C.1.

4.2.1 Mean Velocity

Figure 10 shows that the mean flow is higher at mid radius; it is lower at quarter radius to the wall because of the shear at the wall. The present measurements are consistent with the measurements of Hamamoto et al (1988), and Dyer (1979), made in vessels using Laser Doppler velocimetry.

4.2.2 Turbulence Intensity

Figure 11 shows that the turbulence intensity is higher at three quarter radius from the wall (near the center) and it decays as the wall is approached. This is consistent with the measurements of Dyer (1979). However the measurements of Hamamoto et al (1988), indicate that the turbulence increases from the center to one third of radius from the wall, then started by decaying as the wall is approached. The measurements of Hamamoto et al (1988), are done with the vessel initially partially filled with a quiescent mixture while the present measurement are done with the vessel initially evacuated. This can explain the difference in the turbulence trend between the present results and the results of Hamamoto et al (1988). The value of turbulence intensity to mean flow is also plotted in figure 12. This value is nearly independent of time which is an indication that the flow has relaxed to the chamber geometry (Milane et al, 1987 ; Hamamoto et al, 1988).

4.2.3 Taylor Microscale

Figure 13 shows that the Taylor microscale is the higher at mid radius. The Taylor microscale has also been calculated using the relation for isotropic turbulence

$$\frac{\lambda}{L} = \sqrt{30} R_e^{\frac{-1}{2}} \tag{4.8}$$

Where L is the longitudinal integral scale, λ is the longitudinal Taylor microscale and R_e is the turbulent Reynolds number based on the integral scale. Since the flow has relaxed to the chamber geometry. The longitudinal integral scale L is assumed to be scaled to the chamber height (44 mm). Figure 13 indicates that the values of the calculated Taylor microscale λ is about the same as the values of the measured Taylor microscale λ.

Chapter 5

COMBUSTION EXPERIMENTS

In order to investigate the effect of flow field on misfire, different flow fields are obtained by setting different delay time intervals between the end of charging (closing of the intake valve) and the spark ignition. The delay time intervals used are 28 ms, 51 ms and 74 ms. Eleven equivalence ratios ϕ are tested: 0.5, 0.52, 0.55, 0.57, 0.58, 0.59, 0.6, 0.61, 0.62, 0.63, and 0.64. Three different ignition locations are used: quarter radius from the wall, half radius from the wall and three quarter radius from the wall for all the equivalence ratios and delay times. The ignition was produced by a spark between electrodes with a gap of 2.2 mm which corresponds to the minimum probability of misfire also called "minimum ignition energy

condition" (to be discussed later). All the tests are made the using iguition energy of 312 mJ.

The initial pressure in the charging tank is the same for all experiments 0.46 MPa and the valve lift is set to 7 mm. All the experiments are done with the intake valve opening 40 ms after triggering the control unit because of the valve inertia and closing at a time equal 120 $\pm$ 2 ms. For each experiment, the charging pressure and the combustion pressure time history are recorded. Misfire is determined using the pressure trace and by visually inspecting the flame through the quartz glass. In this study, misfire is identified by those experiments that fail to ignite in the swirling flow while ignition is successful in the quiescent case. The experiments in the quiescent mixture are done by triggering the mixture while keeping the intake valve closed.

The probability of misfire was calculated by performing experiments with the same charging sequence and all parameters constants. The number of experiments required is found by comparing the statistics of 30, 35, 40 and 45 experiments (table C.2). It observed that the probability of misfire varies slightly. In the present investigation the calculations are based on 40 experiments.

5.1 Spark gap

In order to minimize heat transfer from the initial kernel to the electrodes, the electrode taped to a diameter of 0.05 mm from a base diameter of 3 mm. The quench distance for the mixture conditions found by systematically varying the spark gap and the ignition energy until the point of minimum energy required to initiate combustion is obtained as done by Lewis and Von Elbe (1961), Ballal and Lefebvre (1974, 1977) and De Soete (1970). In the present work the quench distance found by varying the spark gap and noting the probability of misfire. The point of minimum energy defined for the spark gap where the probability of misfire is lower. Eight different spark gaps were tested: 0.5, 1, 1.5, 1.7, 2, 2.2, 2.5 and 3 mm. For spark gaps of 0.5 and 1 mm the mixture does not ignite for both the swirling and quiescent cases when the ignition energy 312 mJ. Figure 14 for ignition energy of 312 mJ indicates that by increasing the spark gap to 1.5 mm the probability of misfire starts to decrease until it reached a minimum for the spark gap equal to 2.2 mm. The decaying trend due to the heat transfer to the electrodes which diminished as the gap increased. As the spark gap further increased the probability starts to increase due to heat and mass transfer from the kernel to the unburned gas. In this study the combustion experiments were conducted for a spark gap equal to 2.2 mm.

5.2 Spark Duration

The literature indicates that the flow field has an effect on the spark energy and duration. As the velocity stream gets higher a greater energy is required to ignite the mixture due to an increase of heat losses from the kernel to the surrounding (Karim and Wierzba (1984), De Soete (1983), Ziegler and Maly (1983) and Bjorge and Rosengren (1987)). Also the discharge duration changes with changing flow characteristic. However as the discharge duration is shortened the effect of the flow on the spark energy and duration are diminished as found by Ziegler and Maly (1983). The discharge duration of the present ignition system has been measured for two different energies 312 mJ and 10J using a high voltage probe Tektronix P6015, rated for a maximum voltage of 20 kV DC. The signal was collected on an oscilloscope, DL 1200A model, 7006 YOKO GAWA Electrical corporation with a basic maximum performance of 10^8 samples per second and a maximum sweep time 10 ns per division.

All these tests done at two different spark locations: three quarter radius and half radius from the wall for ignition,times of 28 ms and 74 ms. The voltage supplied to the ignition system held at 12.2 volts. Figure 15 shows the voltage time history for one case. The peak voltages and discharge duration are shown in table C.3. As can be observed the discharge duration independent of the flow field and spark location for each of the energy level 312 mJ and 10 J. The discharge duration for 312 mJ 54 μs and the maximum voltage of the signal 15 kV. The discharge duration for 10J 65 μs and the

maximum voltage 16 kV. As a consequence, the present system discharge duration and the peak voltage are considered to be independent of the flow field and when interpreting the present data it will be assumed that the discharge duration and the peak voltage do not play a role.

5.3 Effect of Spark Energy on Probability of Misfire

Six energy levels were investigated: 312 mJ, 347 mJ, 500 mJ, 600 mJ, 1 J and 10 J for the equivalence ratio of 0.6. Figure 16 shows that when the energy is increased the probability of misfire decreases. For example at the earliest ignition time of 28 ms, the probability of misfire decrease from 65% to 25 % when the ignition energy is increased from 312 mJ to 500 mJ. At the latest ignition time of 74 ms the probability of misfire decrease from 10% to 5% when the energy is increased from 312 J to 500 mJ. The probability of misfire is nil when the energy is increased from 1 J to 10 J.

Figure 17 for $\phi = 0.57$ indicates that the probability of misfire is nil only when the spark is located at three quarter radius from the wall (near the center) and when the ignition energy is 10 J. When the ignition time is delayed to 74 ms, figure 18 indicates a lower probability of misfire at the energy level of 10 J than that for the earlier ignition time 28 ms (figure 17). When the energy level is 312 mJ, the mixture does not ignite for ϕ

= 0.57 for both the swirling and quiescent cases (figures 17, 18). However when the energy was increased to 347 mJ, the mixture ignites always for the quiescent case but fail to ignite for the swirling case. In this study, the energy level selected is 312 mJ.

5.4 Effect of Equivalence Ratio on Probability of Misfire

The mixtures with equivalence ratios 0.5, 0.52, 0.55, 0.57 and 0.58 not ignite when the stored electrical energy is 312 mJ for both swirling and quiescent cases. For equivalence ratio greater than 0.58 the mixture start to ignite and the probability of misfire is less than 100%.

Results for equivalence ratio 0.59 are shown in figure 19. For ignition location at quarter radius from the wall and the earliest ignition time (28 ms), the probability of misfire is 80%. When the time of ignition is delayed to 51 ms, the probability of misfire decrease to 55% and then decrease to 20% for the time of ignition of 74 ms. If the spark location is moved away from the wall to half radius, the probability of misfire is 60% at the time of ignition of 28 ms and by delaying the time of ignition to 51 ms the probability of misfire decreases to 25 % and then decrease to 15 % for time of ignition of 74 ms. As the spark location is positioned the farthest from the wall at three quarter radius, the probability of misfire is 50% at

time of ignition of 28 ms and by delaying the time of ignition to 51 ms the probability of misfire decreased to 20% and then decreased to 10 % for time of ignition 74 ms. Figure 19 implies that when the spark location is near the wall the probability of misfire is higher. Furthermore the probability of misfire is lower when the ignition time is delayed, i.e., when the flow has decayed.

Figures 20 to 23 show results for equivalence ratios of 0.6, 0.61, 0.62 and 0.63. As discussed earlier, all the graphs indicate that the probability of misfire is higher when the ignition location is closer to the wall and when the ignition time is the earliest. It is observed that at the latest ignition time of 74 ms, the probability of misfire is identical at quarter radius from the wall and half radius from the wall for equivalence ratios greater or equal to 0.6. Also when the spark is located at three quarter radius from the wall (farthest from the wall), the probability of misfire is nil at ignition time of 51 ms and 74 ms when equivalence ratios are greater or equal to 0.61. Figure 22 for equivalence ratio 0.63 shows that the probability of misfire is nil except for the earliest ignition time of 28 ms when the spark location is at quarter radius and half radius from the wall.

For equivalence ratio of 0.64 the probability of misfire is nil for the three locations and the three times of ignition: 28 ms, 51 ms and 74 ms. Figures 24 to 26 shows the probability of misfire versus equivalence ratio for the three locations. As the equivalence ratio increases the probability of misfire decreases. Also as the ignition time is delayed, i.e. the flow has decayed,

the probability of misfire also decreases.

The present results concerning the effects of the equivalence ratios, the ignition energy and the flow decay are in agreement with the results of Ko et al (1991), Ho and Santavicca (1987), Heywood and Pischinger (1990) and Bradley and Lung (1987). Ko et al (1991) have found that for a quiescent mixture an increase in the energy decreases the probability of misfire. They also have found that increasing the equivalence ratio results in a faster growth rate of the flame kernel. Ho and Santavicca (1987) found that the greater ignition energy results in a more rapidly growing initial flame kernel size and a higher turbulence results in a higher probability of misfire. Heywood and Pischinger (1990) found that the higher electrical energy leads to a faster initial flame growth. This can be explained by the fact that as the energy increases the temperature of the kernel increases therefore the expansion velocity increases, and the kernel diameter increases beyond the quenching diameter (Lewis and Von Elbe, 1961). Bradley and Lung (1987) have found that the increase in energy produced a strong shock which enhanced the thermal spreading. However the effect of spark location in a swirling flow on misfire has not yet been discussed in the literature. In the next chapter, the results on the probability of misfire will be interpreted with a view of understanding why the probability of misfire is higher when the ignition is near to the wall.

Chapter 6

DISCUSSION

The effects of the three experimental variables on the probability of misfire are systematically studied. The variables are:

1. the ignition point positioned at three radial locations: quarter radius from the wall, half radius from the wall and three quarter radius from the wall,
2. the equivalence ratios is varied from 0.5 to 0.64 by increment of 0.01 and
3. the decay of the flow characteristics at ignition is varied by changing the ignition time to 28 ms, 51 ms and 74 ms.

It has been found that the probability of misfire decreases as:

1. the ignition position is farther from the wall of the vessel,
2. the has flow decayed and
3. the mixture is made richer.

Our flow results indicate that neither the level of the mean flow nor the turbulence intensity or the variation of the Taylor microscale can explain why near the wall the probability of misfire is higher. As discussed in the literature survey, results of previous workers (Ho and Santavicca (1987), Maly (1981) and Abdel-Gayed et al (1986)) indicate that as the turbulence intensity is increased beyond a certain level the misfire is likelier. The present flow data indicate that near the center the turbulence intensity is higher, however the combustion results indicate that near the center the probability of misfire is lower. Furthermore Bjorge and Max (1987) and Ziegler and Maly (1983) have found that as the mean flow increases the lean limit is richer, i.e. the probability of misfire is higher as the mean flow is higher. Our flow data indicate that at mid-radius the mean flow is higher, therefore according to the previous investigators the probability of misfire should be higher at mid radius. This contradicts the present results. Therefore the probability of misfire does not simply correlate separately with the mean flow or turbulence intensity.

Furthermore, misfire is correlated with the stretch factor K (Karlovitz factor) as

$$K = \left(\frac{1}{A}\frac{dA}{dt}\right)\left(\frac{\delta_l}{u_l}\right) \tag{6.1}$$

Therefore in the region of the flow where the rate of growth of the flame area $\frac{1}{A}\frac{dA}{dt}$ is higher, misfire is more likely. In isotropic homogenous turbulence with zero mean flow the value of $\frac{1}{A}\frac{dA}{dt}$ is correlated with turbulence rate of strain $\frac{u'}{\lambda}$ (also called inverse of the eddy lifetime). Table C.4 and figure 27 shows the value of $\frac{u'}{\lambda}$ for the present swirling flow at the three different spark locations and at the three different ignition times. As can be observed the value is higher at three quarter radius from the wall and lower at quarter radius from the wall. This suggests that the probability of misfire is higher near the center which contradicts the present results. Therefore in the swirling flow $\frac{1}{A}\frac{dA}{dt}$ should be influenced by the profile of the mean flow rather than the inverse of the eddy lifetime $\frac{u'}{\lambda}$. In fact Hanson and Thomas (1984) have correlated $\frac{1}{A}\frac{dA}{dt}$ in a laminar shear Couette flow with the rate of shear $\frac{dv}{dr}$ as follows:

$$\frac{1}{A}\frac{dA}{dt} = B_o + C_1\left(\frac{dv}{dr}\right) \tag{6.2}$$

where B_o is specific rate of growth in quiescent mixture, C_1 is a constant of the order 0.5 to 1 relating the extra growth induced by the shear to the shear rate and $(\frac{dv}{dr})$ is the rate of shear in the unburned gases. Since a higher rate of growth of flame area $\frac{1}{A}\frac{dA}{dt}$ leads to misfire and since it is related to shear, therefore the higher the shear rate the likelier misfire is. The expected trend in the spatial distribution of the mean shear rate for the present swirling flow will be discussed next.

For the present swirling flow, the measurements of the mean flow (figure 4) indicate a deviation from a solid body rotation. The swirling flow can be divided into two regions: forced vortex close to the center and shear flow close to the wall as shown by the experimental measurements of Hamamoto et al (1988) and Dyer (1979). Table C.5 shows that the angular velocity $\frac{\overline{U_t}}{r}$ increases as the center is approached. This suggests that the mean shear rate $(\frac{\partial U_t}{\partial r} - \frac{U_t}{r})$ is non zero at the three locations. In fact the shear rate is nil for a solid body rotation (forced vortex) only. The central region only may be approximated as a forced vortex flow. Here the mid-radius point and the quarter radius from the wall point are not located in the central region; however the three quarter radiur from the wall point may be in the central region. The shear rate are different at the three locations since they rotate at different angular velocity. Table C.5 suggests that the mean shear rate is higher near the wall since it rotates at the slower angular velocity. In fact the profile of the mean swirling flow in an engine and in constant volume vessel has been expressed as (Borgnakke et al. 1981)

$$U_t = C_2 r + C_3 r^2 \tag{6.3}$$

where C_2 and C_3 are two constant parameters, and C_3 has a negative value. The mean shear rate at any location r is equal to

$$\frac{\partial U_t}{\partial r} - \frac{U_t}{r} \tag{6.4}$$

Using equation (6.3) the mean shear rate is C_3r. Therefore the magnitude of the mean shear rate increases as the wall is approached. Since a higher shear rate implies a higher growth rate of the flame area $\frac{1}{A}\frac{dA}{dt}$ (Hanson and

Thomas 1984), therefore misfire is more likely at quarter radius from the wall.

The present results can also be explained by noting that the combustion in the swirling flow has two significant features: a centripetal movement of the flames ignited off-center due to buoyancy effect and a penciling of the flame in the axial direction once it is centered. If ignition occurs close to the wall, the flame while growing will be pushed to the center due to centripetal effect. In travelling to the center the flame will traverse a region having a spatial distribution of the shear rate and the flame area will be stretched. Therefore for flame ignited near the wall the rate of growth of the flame area $\frac{1}{A}\frac{dA}{dt}$ the higher and misfire is more likely to occur because the flame area (area of contact between burned and unburned) is higher as the mixture is ignited near the wall. This interpretation can be further validated by observing the combustion duration.

The combustion duration is defined by the time from ignition to the time of the peak combustion pressure is reached. Figure 28 for equivalence ratios of 0.59, 0.61 and 0.62 indicates that the combustion duration is shorter for mixtures ignited near the wall. Also figure 29 indicates that for the equivalence ratio 0.64, where all the cycles ignited successfully, the combustion duration is shorter when the ignition location is at quarter radius from the wall for all ignition times. Similar results have been found by Witze (1982). The author suggested that for off-center ignition the flame is driven by convection addition to the turbulent diffusion. Furthermore, the

combustion duration in a shear flow investigated by Hanson and Thomas (1984), results in shorter combustion duration becouse of the higher rate of growth of the flame area. The rate of growth of the flame area $\frac{1}{A}\frac{dA}{dt}$ is larger when the flame is ignited near the wall. The larger rate of growth of flame area $\frac{1}{A}\frac{dA}{dt}$ results in a larger area of contact between burned and unburned gases (flame area) and therefore the combustion duration is shorter. Consequently for the present swirling flow the larger the trajectory of the flame from ignition point to the center the shorter the combustion duration is because the mass and heat transfer between burned and unburned gases is higher. Figures 30, 31, and 32 confirm that with ignition near the wall the combustion duration is shorter for all three ignition times tested. The values of combustion duration are shown in table C.6.

The trend in the peak combustion pressure for successful ignition can also be inspected to further understand the different mechanisms that may affect misfire. Figure 33 indicates that at a given location the peak pressure increases with a higher swirling flow (earlier ignition). This results is compatible with the results of the combustion duration figure 29 which indicate a shorter combustion duration with a higher swirling flow. Hanson and Thomas (1984), found similar results. It is also observed in figure 33 that the peak pressure at quarter radius from the wall is always less than the peak pressure at three quarter radius from the wall, the maximum difference is about 6%. This may be surprising since the combustion duration at quarter radius from the wall is always less than the combustion duration at three quarter radius to the wall. However this is probably due to the

heat transfer to the cylinder wall from the flame ignited at quarter radius to the wall which may be higher than the heat transfer to the end plates due to penciling effect earlier in the combustion from the flame ignited at three quarter radius from the wall therefore heat transfer due to penciling effect is not large enough to reduce the peak pressure below that of the peak pressure from ignition at quarter radius from the wall.

In conclusion the trend in peak pressure and combustion duration do not contradict the postulate that the rate of growth of the flame area $\frac{1}{A}\frac{dA}{dt}$ is higher for off-center ignition. The ignition at off-center might be beneficial because it results in shorter combustion duration, even though its peak combustion pressure is lower, however it will also lead to misfire when the mixture is made leaner. In order to explore this point, the relationship between the rate of growth of the flame area $\frac{1}{A}\frac{dA}{dt}$ and the mean shear rate should be investigated. It is proposed that $\frac{1}{A}\frac{dA}{dt}$ be measured using flame photographs and that accurate measurements of flow characteristics be made using laser Doppler velocimetry. This is beyond the scope of this study.

Chapter 7

CONCLUSIONS AND RECOMMENDATIONS

7.1 Conclusions

The main conclusions drawn from the flow measurements and combustion experiments in the swirling flow are

1. The mean flow is higher at mid-radius.
2. The turbulence intensity is higher at three quarter radius from the wall (nearer to the center).
3. The probability of misfire increases as the ignition positions is closer to the wall.

4. The probability of misfire decreases as the flow decays.
5. The probability of misfire decreases as the mixture is made richer.
6. The probability of misfire decreases as the ignition energy level increases.
7. The combustion duration for successful ignition decreases as the ignition point is closer to the wall.
8. The peak pressure for successful ignition is higher as the ignition point is near the center because the heat transfer to the end plates is less than the heat transfer to the cylinder walls.
9. The discharge duration and energy of the present capacitive discharge ignition system is independent of the flow field.

7.2 Recommendations

It is recommended to investigate the various correlations for the misfire limit. Accurate measurements of the characteristics of the flow field are required, and the relation between the rate of growth of the flame area and the flow characteristics will be made. To that purpose it is recommended that the following projects be undertaken:

1. Measuring the flow characteristics using laser doppler velocimetry.
2. Taking photoghraphs of the flame to confirm that the rate of growth of the flame area is the highest as the ignition location is the closer to the wall.

Bibliography

[1] Abdel-Gayed, R. G. and Bradley, D. (1980), " A Two-Eddy Theory of Premixed Flame Propagation", Phil. Trans. Roy. Soc. Lond. vol. 301, 1-25.

[2] Abdel-Gayed, R. G., Khishali, K.J. and Bradley, D. (1984), "Turbulent burning Velocities and Flame Straining in Explosions", Proc. R. Soc. Lond. Vol. 391, 393-414

[3] Abdel-Gayed, R. G., Bradley, D., Hamid, M. N and Lawes, M. (1984), "Lewis Number effects on Turbulent Burning Velocity", Twentieth Symposium (International) On Combustion / The combustion Institute, pp. 505-512

[4] Abdel-Gayed, R. G. and Bradley, D. (1985), "Criteria for Turbulent Propagation Limits of Premixed Flames", Combustion and Flame, 62 : 61-68

[5] Abdel-Gayed, R. G., Bradley, D., Lawes. M., and Lung, F. K-K. (1986), "Premixed Turbulent Burning During Explosions", Twenty-

First Symposium (International) on Combustion / The Combustion Institute. 497-504

[6] Abdel-Gayed, R. G., Bradley, D. and Lawes, M. (1987), " Turbulent Burning Velocities : a General Correlation in Terms of Straining Rates", Proc. R. Soc. Lond. Vol. 414, 389-413

[7] Abdel-Gayed, R. G., and Bradley, D. (1989), " Short Communication: Combustion Regimes and the Straining of Turbulent Premixed Flames", Combustion and Flame Vol. 76 : 213-218

[8] Anderson, R. W. (1987), "The Effect of Ignition System Power on Fast Burn Engine Combustion", SAE Paper 840549

[9] Anderson, R.W. and Lim, M.T.(1985), " Investigation of Misfire in a Fast Burn Spark Ignition Engine", Combustion Science and Technology Vol. 43, pp. 183-196.

[10] Arici, O., Tabaczynski, R. J. and Arpaci, V. S. (1983), " A Model for the Lean Misfire Limit in Spark-Ignition Engine ", Combustion Science and Technology Vol. 30, pp. 31-45

[11] Ballal, D. R. and Lefebvre, A. H. (1974), "The Influence of Flow Parameters on Minimum Ignition Energy and Quenching Distance", Fifteenth Symposium pp. 1473 -1481 The Combustion Institute

[12] Ballal, D. R. and Lefebvre A. H. (1977), "Ignition and Flame Quenching In Flowing Gaseous Mixture", Proc. R. Soc. Lond. Vol. 357 pp. 163-181

[13] Baritaud, T. A. (1985), " High Speed Schlieren Visualization of Flame Initiation in a Lean Operation S.I. Engine", SAE Paper 820044

[14] Bjorge T. and Rosengren L. (1987), " Lean Ignition Limits of flowing Methane /Air and Methanol /Air Mixtures", ASME 87-ICE-24

[15] Bjorge T. and Max E. (1987). " Influence of Electrode orientation, Temperature, and Pressure on Lean Ignition Limits of Methane", SAE International Congress and Exposition in Detroit, February 23-27, 1987

[16] Borgnakke, C., Davis, G. C. and Tabaczynski R. J. (1981). "Prediction of in-Cylinder Swirl Velocity and Turbulence Intensity for an Open Chamber Cup in Piston Engine", SAE Paper 810224

[17] Bradley, D. and Lung, F. K-K. (1987), " Spark Ignition and the Early Stages of Turbulent Flame Propagation", Combustion and Flame Vol. 69 pp. 71-93

[18] Cole, J. B. and Swords, M. D. (1980), " An Investigation of The Ignition Process In a Lean Burning Engine Using Conditionally sampled Laser - Doppler Anemometry", SAE Paper 800043

[19] Chomiak, J. and Jarosinski, J. (1982), "Flame Quenching by Turbulence", Combustion and Flame 48 pp. 241-249

[20] Coward, H. F. and Jones, G. W. (1952), " Limits of Flammability of Gases and Vapors", Bureau of Mines Report # 503

[21] Davy, J. (1816), Phil. Trans. Roy. Soc., 106, 1

[22] De Soete, G. G. (1983), "Propagation Behavior of Spark Ignited Flames in Early Stages", Combustion in Engineering, Inst. Mech. Eng., C59/83, pp. 93

[23] De Soete, G. G. (1984), " Effects of Geometrical and Aerodynamic Induced Flame Stretch on the Propagation of Spark Fired Premixed Flames in Early Stages " Twentieth Symposium (Int.) on Combustion / the Combustion Institute pp. 161-168

[24] Dyer, T. M. (1979), "Characterization of one - and two - Dimensional Homogenous combustion Phenomena in a Constant Volume Bomb", SAE Trans. vol. 88 p.1196

[25] Durbin, E. J. and Tsai, K. C. (1983), " Extending the Lean Limit Operation of an SI Engine With a Multiple Electrode Spark Plug", SAE Paper 830476

[26] Gersten, M., and Stine, W. B. (1973), "Analytical Criteria for Flammabiliy Limits", Fourteenth Symposium (Int.) on combustion, pp.1109-1118

[27] Ghorbali A. (1993), "Cyclic Variation in Combustion in a Constant Volume Combustion Chamber" Thesis Draft

[28] Hamamoto, Y., Izumi M. and Tomita, E. (1990), "Effects of Swirl and Air-Fuel ratio On Premixed Combustion In a Closed Vessel", JSME International Journal Series II Vol 33, No 2

[29] Hamamoto, Y., Tomita, E. and Izumi, M. (1988), "The Effect of Swirl on The Combustion Of a Homogenous Mixture In a Closed Vessel", JSME International Jornal Series II, Vol. 31, No 1

[30] Hanson, R. J. and Thomas, A. (1984), " Flame Development in Swirling Flows in Closed Vessels", Combustion and Flame Vol. 55 pp. 255-277

[31] Hertezberg, M. (1976), "The Theory of Flammability Limits, Natural Convection", Bureau of Mines report # 8127

[32] Ho, C. M. and Santavica, D. A. (1987), " Turbulence Effects on Early Flame Kernel Growth", SAE Paper 872100

[33] Humbolt, A. and Gay Lussac, J. F. (1804), De Physique, 60, 129-168

[34] Jarosinski, J. , Strehlow, R. A. and Azarbarzin, A. (1982), " The Mechanisms of Lean Limit Extinguishment of an Upward and Downward Propagating Flame in a Standard Flammability Tube", Nineteenth Symposium (Int.) On Combustion ,The Combustion Institute, pp. 1549-1557

[35] Karlovitz, B., Denniston, D. W., Knapschaefer, D. H. and Wells, F. E. (1953), Fourth Symposium (Int.) on Combustion , Williams and Wilkins, Baltimore, pp. 613-620

[36] Karlovitz, B. (1954), " The Growth and Burn-Out of Flame Surface in a Turbulent Stream", Fourth Symposium on combustion, pp. 604-608

[37] Karim, G. A., Wierzba, I. and Soriano, R. (1984), "The Limits of Flame Propagation Within Homogenous Streams of Fuel And Air", ASME 84-Pet-13

[38] Ko, Y., Anderson, R. W. and Arpaci, V.S. (1991), " Spark Ignition of Propane - Air Mixture Near the Minimum Ignition Energy : Part I. An Experimental study", Combustion and Flame 83 pp. 75-87

[39] Klimov, A. M. (1963), Zh. Prikl. Mekh. i. Tekhn. Fiz. 3:49- 58.

[40] Lewis, B. and Von Elbe, G. (1961), "Combustion, Flames and Explosions of Gases" Academic Press, New York.

[41] Maly R. (1981), " Ignition Model For Spark Discharges The Early Phase of Front Growth", Proceeding of Eighteenth International Symposium on Combustion, pp. 1747-1754, The Combustion Institute.

[42] Mayer, E. (1957). Combustion and Flame, 1, 438.

[43] Milane, R. E., Evans, R. L. and Hill, P. G. (1987), " Combustion and Turbulent Structure in a Closed Chamber with Swirl", Combust. Sci. and Tech. V. 51 pp. 1-20.

[44] Milane, R. E.(1990), " Cyclic Analysis of Turbulence and the Isotropic Relation for Length Scale in a Decaying Swirling Flow", International Journal of Engineering Fluid Mechanics 3(3), 207-224.

[45] Poschinger, S. and Heywood, J. ' . (1990), " How Heat Losses To The Spark Plug Electrodes Affect Flame Kernel Development in an SI-Engine", SAE Paper 900021

[46] Quader, A. A. (1974), " Lean Combustion and The Misfire Limit in Spark Ignition Engines", SAE Paper 741055

[47] Quader, A. A. (1976), " What Limits Lean Operation in Spark Ignition Engines- Flame Initiation or Propagation", SAE Paper 760760

[48] Reed, S. B. (1967), " Flame Stretch-a Connecting Principle for Blow-off Data", Combustion and Flame Vol II pp. 177-189

[49] Santavicca, D. A., Liou, D. and North, G. (1990), "A Fractal Model of Turbulent Flame Kernel Growth", SEA Paper 900024

[50] Satoru, I. and Chung, K. L. (1982), "An Experimental Study on Extinction and Stability of Stretched Premixed Flames", Nineteenth Symposium (Int.) on Combustion / The Institute, 327-335

[51] Smith, O. I, Westbrook, C. K. and Sawyer, R. F. (1977), " Lean Limit Combustion in an Expanding Chamber", International Symposium on combustion.

[52] Spalding, D. B. (1957), Proc. Rcy. Soc. London, A - 240, 83

[53] Saggau, B. (1981), "Calorimetry of the Three Discharges Modes of the Igniting Spark", Archivfur Elektrotechnik, 64, pp. 229-235, in German

[54] Strehlow, R. A., and Savage, L. D. (1978), Combustion and flame, 31, pp. 209 - 211

[55] Thomas, A. (1983), " Flame Development in Spark - Ignition Engine", Combustion and Flame 50 pp. 305- 322

[56] Tavoularis, S. (1986), "Techniques for Turbulence Measurment", Encyclopedia of Fluid Mechanics, Vol. 1, Ch. 36, pp. 1207-1255, Gulf Publishing Company, Houston, Texas

[57] Van Wylen, G. J. and Sonntag, R. E. (1985), " Fundamentals of Classical Thermodynamics", Third Edition, John Wiley and Sons

[58] Wakisaka, T., Hamamoto, Y. and Shimamoto, Y. (1982), "Turbulence Structure of Air Swirl in Reciprocating Engine Cylinders", ASME Meeting on Flow in Internal Combustion Engines, pp. 93-100

[59] Wakisaka, T. and Hamamoto, Y. (1979), " Effects of Mixture Turbulence on the Limits of Flame Propagation", JSME. Vol.22, No. 165

[60] Williams, F. A. (1975), AGARD Conference Proceedings (164), pp. II:1-1-II:1-25

[61] Witze P. O. (1982), " The Effect of Spark Location on Combustion in a Variable - Swirl Engine", SAE Paper 820044

[62] Witze, P. O. and Matthew J. H. (1990), "Cycle-Resolved Measurments of Flame Kernel Growth and Motion Correlated with Combustion Duration", SAE Paper 900023

[63] Witze, P. O. and Vilchis F. R. (1981), " Stroboscopic Laser Shadowgraph Study of the Effect of Swirl on Homogeneous Combustion in a Spark - Ignition Engine " SAE Paper 810226

[64] Ziegler, G., Maly, R. R. and Wagner E. P. (1983), "Effect of Ignition System Design on Flammability Reguirements is Ultra-Lean Turbulent Mixture", C 47/83, I. Mech. E., pp.81-92

[65] Ziegler, G. and Maly, R. (1981), "Influence of Ignition on Inflammation and Flame Propagation", First Specialists Meeting (Int.) of The Combustion Institute, Bordeaux, The Combustion Institute, pp.89-94

Table C.1: Flow Measurements Results

Flow Parameters	Time from closing intake valve (ms)	Locations from the wall		
		quarter radius	half radius	three quarter radius
$\overline{U}(m/s)$	28	20.51	24.09	19.99
	51	20.39	19.60	15.10
	74	15.02	16.47	12.80
u' (m/s)	28	1.22	1.43	1.69
	51	0.93	1.08	1.29
	74	0.80	0.74	0.95
λ (mm)	28	1.74	1.96	1.85
	51	1.61	1.79	1.79
	74	1.34	1.80	1.60

Table C.2: Percentage of Misfire for Equivalence Ratio of 0.6

Spark Locations	Time from closing intake valve (ms)	Number of experiments			
		30	35	40	45
Quarter radius from the wall	28	66.6%	65.7%	67.5%	68.8 %
	74	10 %	8.5 %	10 %	8.8 %
Half radius from the wall	28	46.6%	45.7%	47.5%	51 %
	74	6.6%	8.5%	7.5 %	8.8%
Quarter radius from the center	28	16.6%	14.3%	15 %	15.5 %
	74	0 %	0 %	0 %	0 %

Table C.3: Ignition System Characteristics (duration is in μs and peak pressure is in MPa)

Ignition location	Time from closing intake valve (ms)	Energy level			
		312 mJ		10 J	
		Duration	Peak pressure	Duration	Peak pressure
Half radius	28	54.22	1.555	65.12	1.663
to wall	74	54.25	1.559	65.14	1.669
three quarter	28	54.24	1.558	65.13	1.662
radius to wall	74	54.25	1.558	65.18	1.668

Table C.4: Ratio of Turbulence Intensity (u') to Taylor Microscale (λ)

Time from closing intake valve (ms)	$\frac{u'}{\lambda}\ s^{-1}$		
	quarter radius	half radius	three quarter radius
28	701	729.6	913.5
51	573	603.4	720.7
74	597	411	593.8

Table C.5: Angular Velocity $w = \frac{U_t}{r}$ in Second

Time from closing intake valve (ms)	Angular velocity s^{-1}		
	quarter radius	half radius	three quarter radius
28	310.8	547.5	908.6
51	308.9	445.5	686.4
74	227.6	374.3	581.8

Table C.6: Combustion Duration (ms)

Equivalence Ratio	Spark Location from the wall	Time From Closing Valve		
		28 ms	51 ms	74 ms
0.59	quarter radius	94.13	97.22	100.16
	half radius	96.30	103	105.96
	three quarter radius	100.6	105.80	106.64
0.61	quarter radius	83.58	92.44	90.40
	half radius	86.48	94.62	92.50
	three quarter radius	87.36	95.41	96.90
0.62	quarter radius	64.90	66.08	58.66
	half radius	66.14	68.54	68.74
	three quarter radius	70.90	72.50	73.10
0.64	quarter radius	54.26	56.15	61.48
	half radius	57.10	66.97	71.65
	three quarter radius	58.20	67.70	72.10

Table C.7: Peak pressure (MPa)

Equivalence Ratio	Spark Location from the wall	Time From Closing Valve		
		28 ms	51 ms	74 ms
0.59	quarter radius	1.490	1.444	1.454
	half radius	1.464	1.434	1.449
	three quarter radius	1.492	1.481	1.492
0.61	quarter radius	1.479	1.481	1.459
	half radius	1.464	1.473	1.483
	three quarter radius	1.483	1.485	1.487
0.62	quarter radius	1.582	1.630	1.569
	half radius	1.574	1.590	1.549
	three quarter radius	1.598	1.641	1.580
0.64	quarter radius	1.569	1.546	1.517
	half radius	1.628	1.547	1.521
	three quarter radius	1.666	1.578	1.558

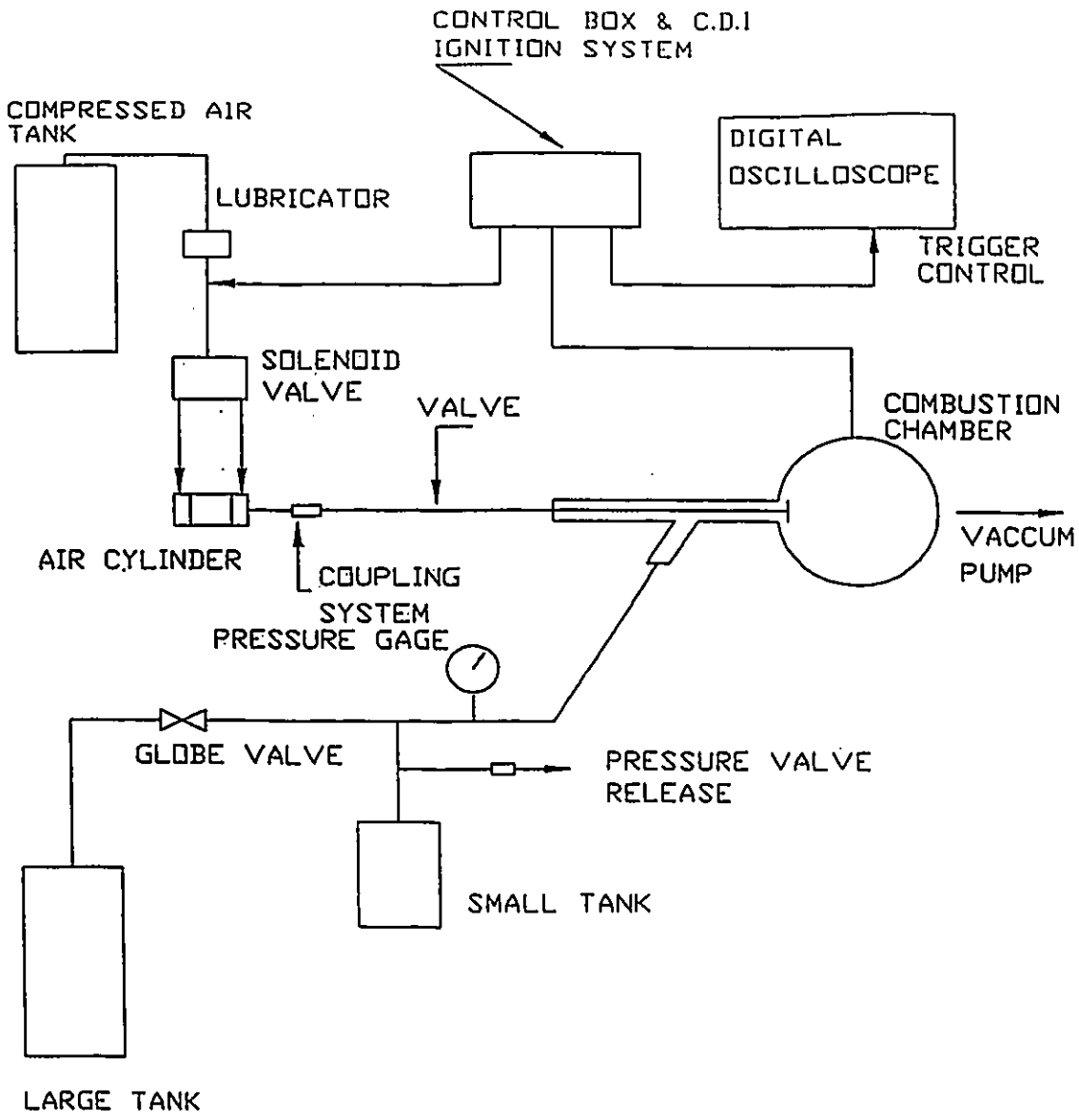

Figure 1. Schematic of experimental set-up

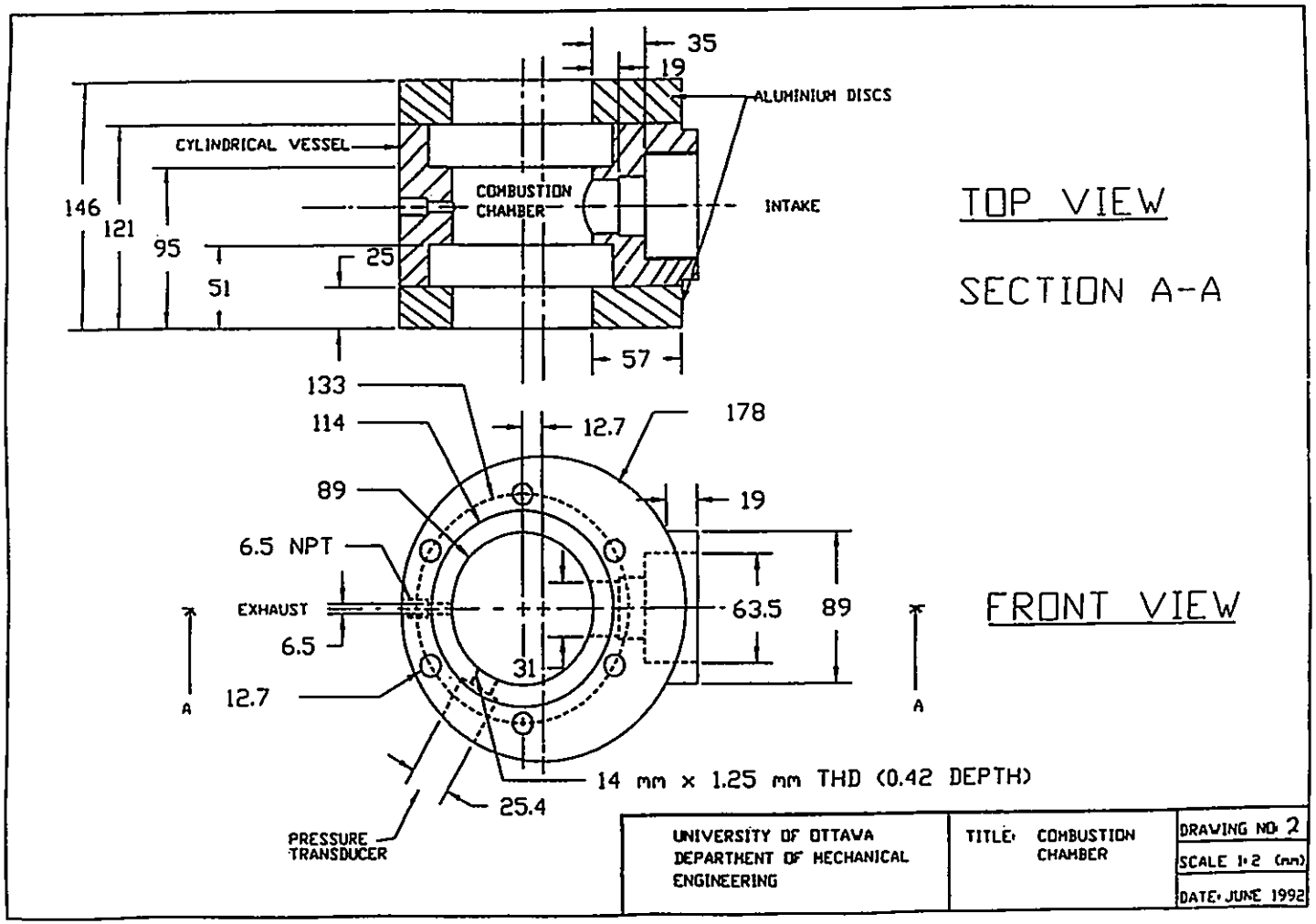

Figure 2. Cylindrical vessel

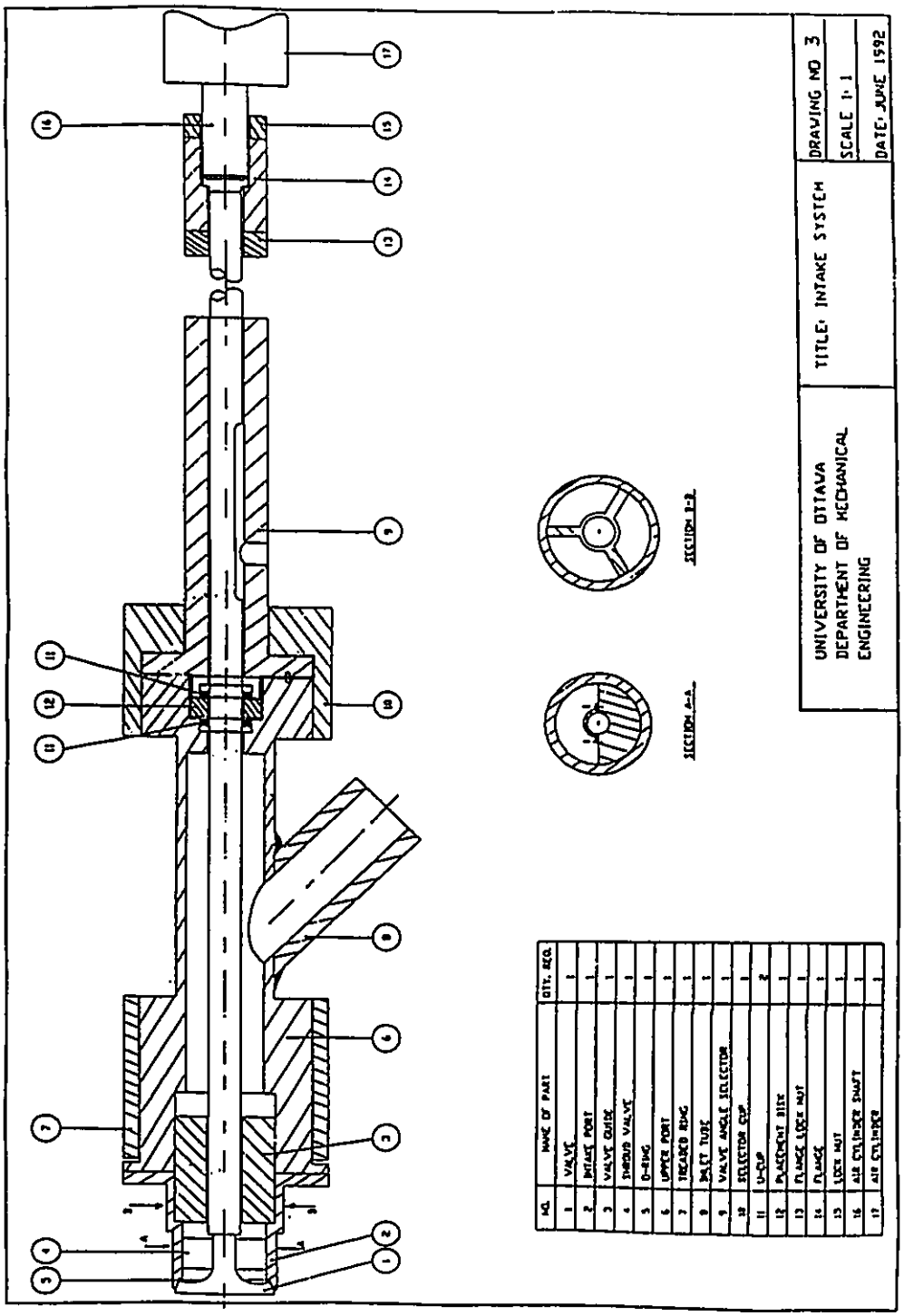

Figure 3. Intake system

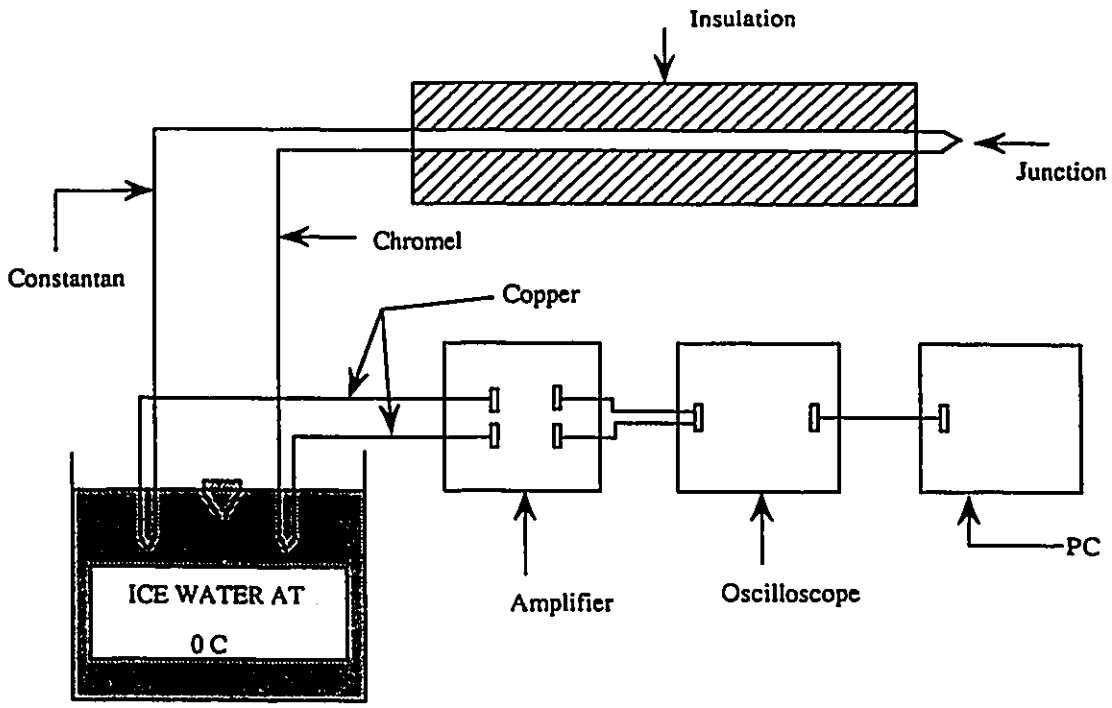

Figure 4. Thermocouple set-up

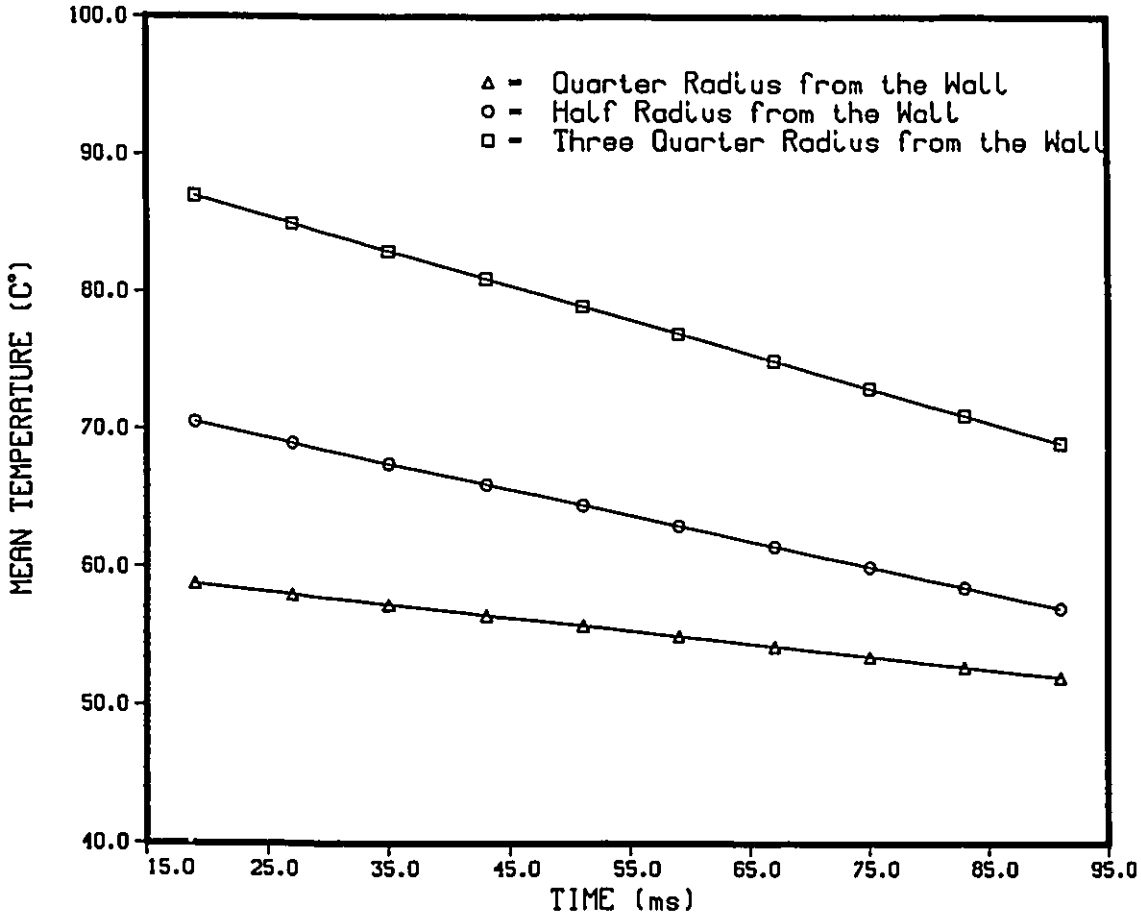

Figure 5. Mean temperature versus time for the three ignition locations

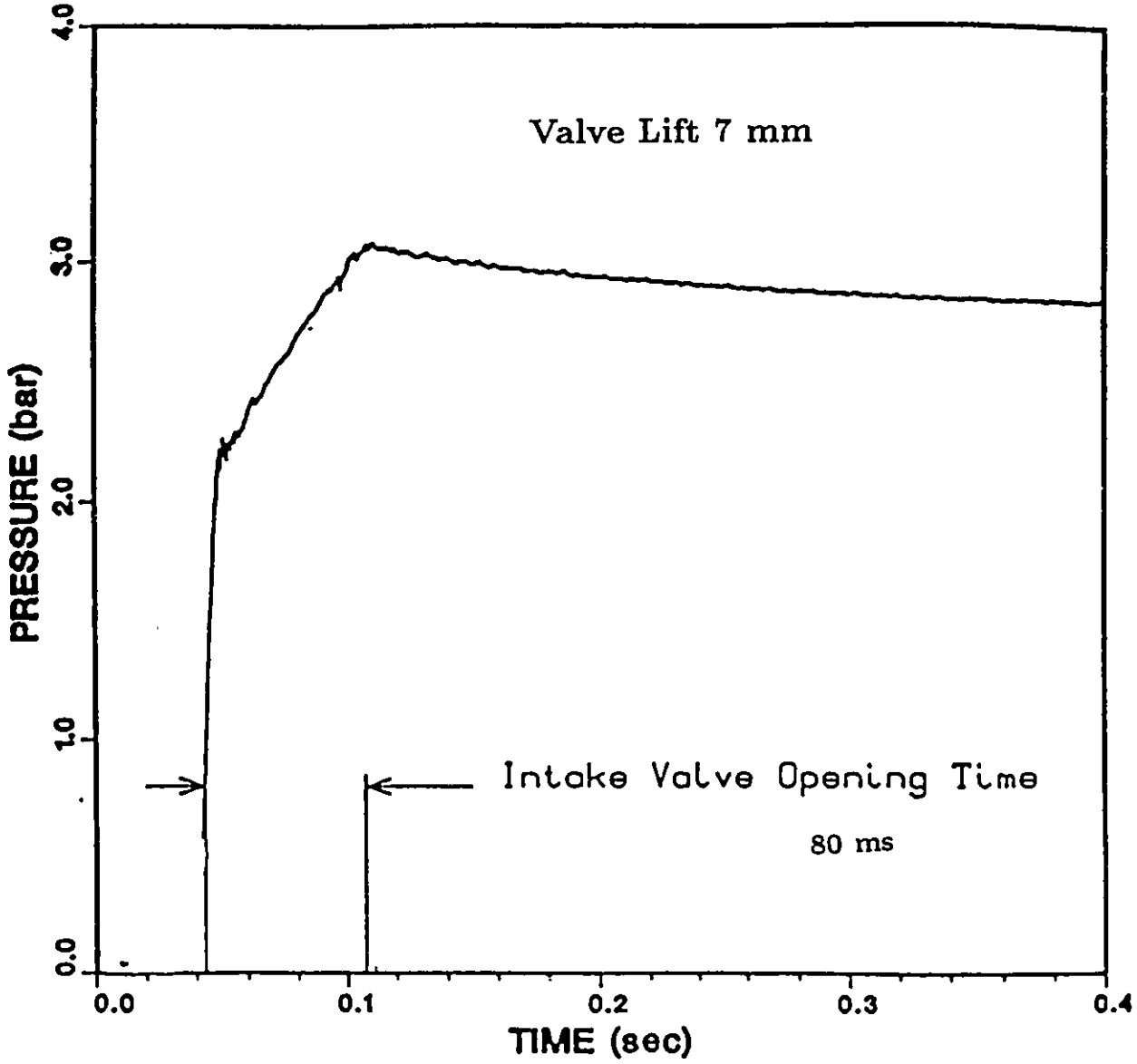

Figure 6. Pressure time history in the vessel during the intake

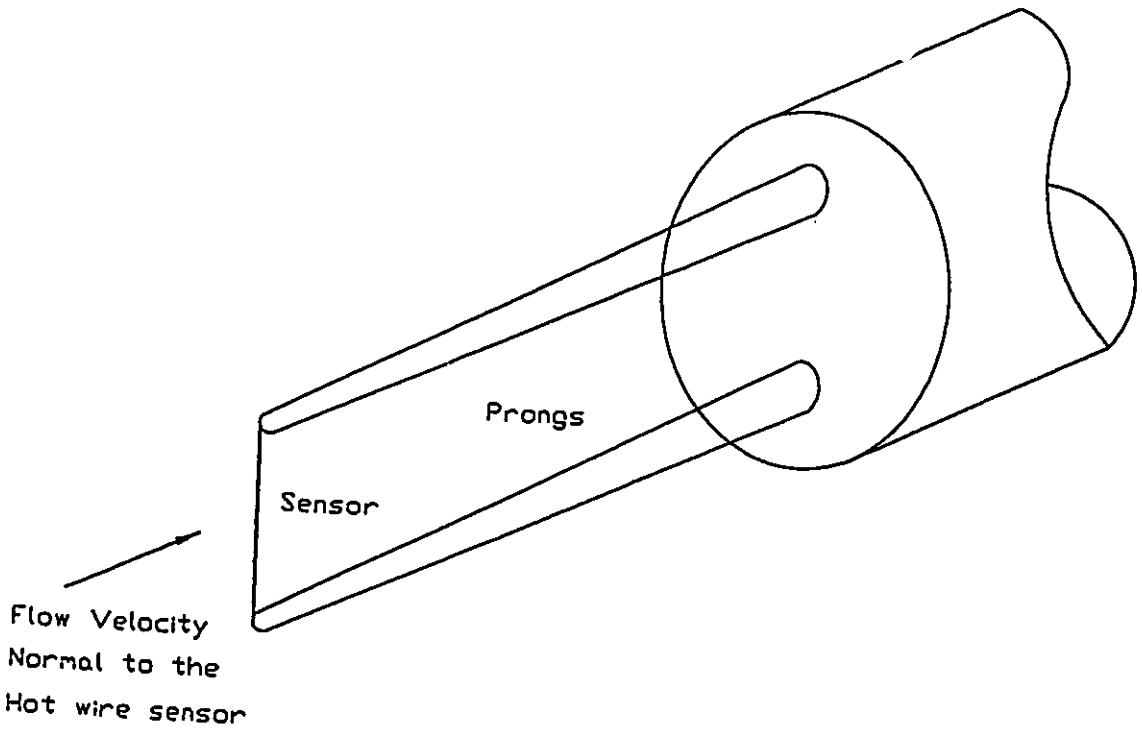

Figure 7. Single hot wire

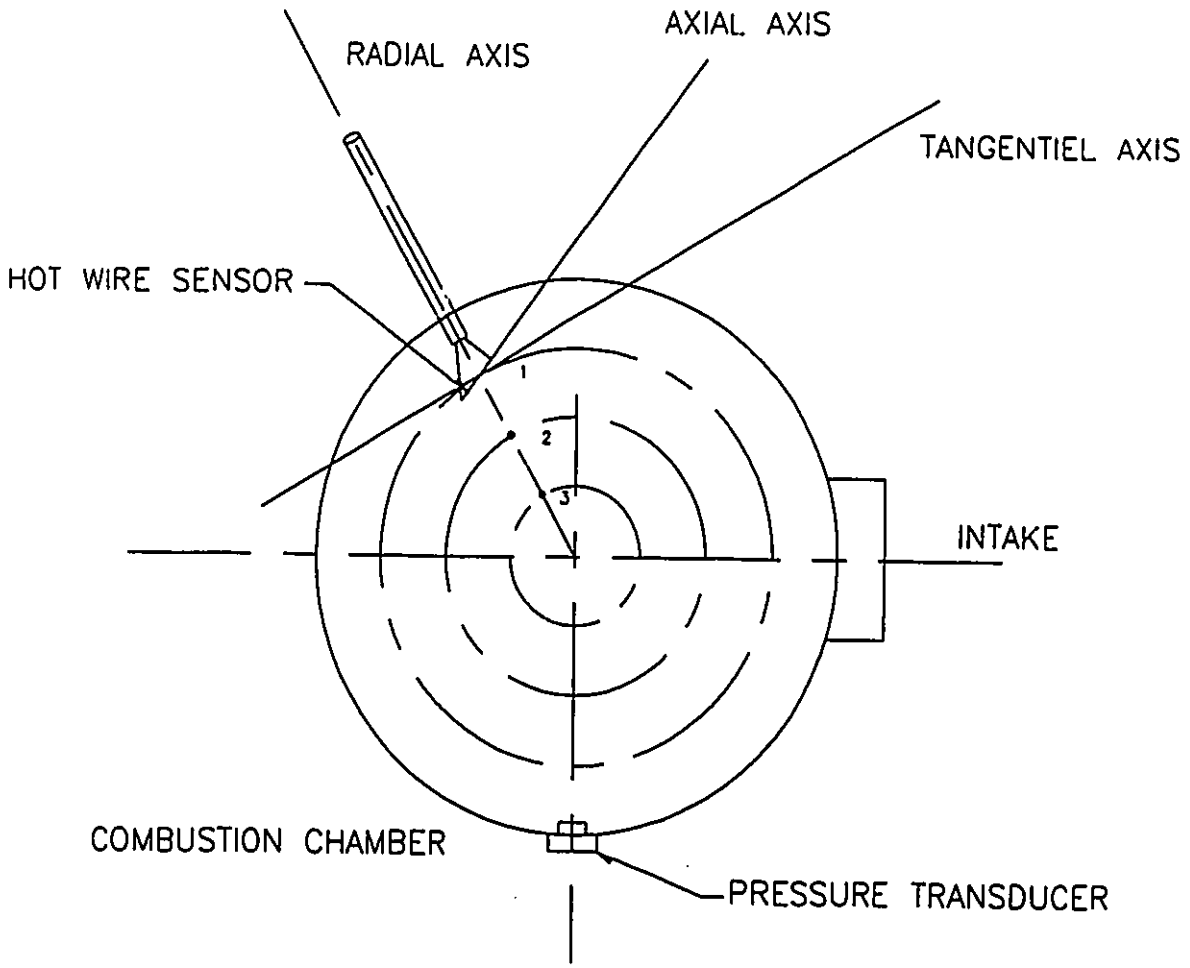

Figure 8. Measurements locations of hot wire and thermocouple

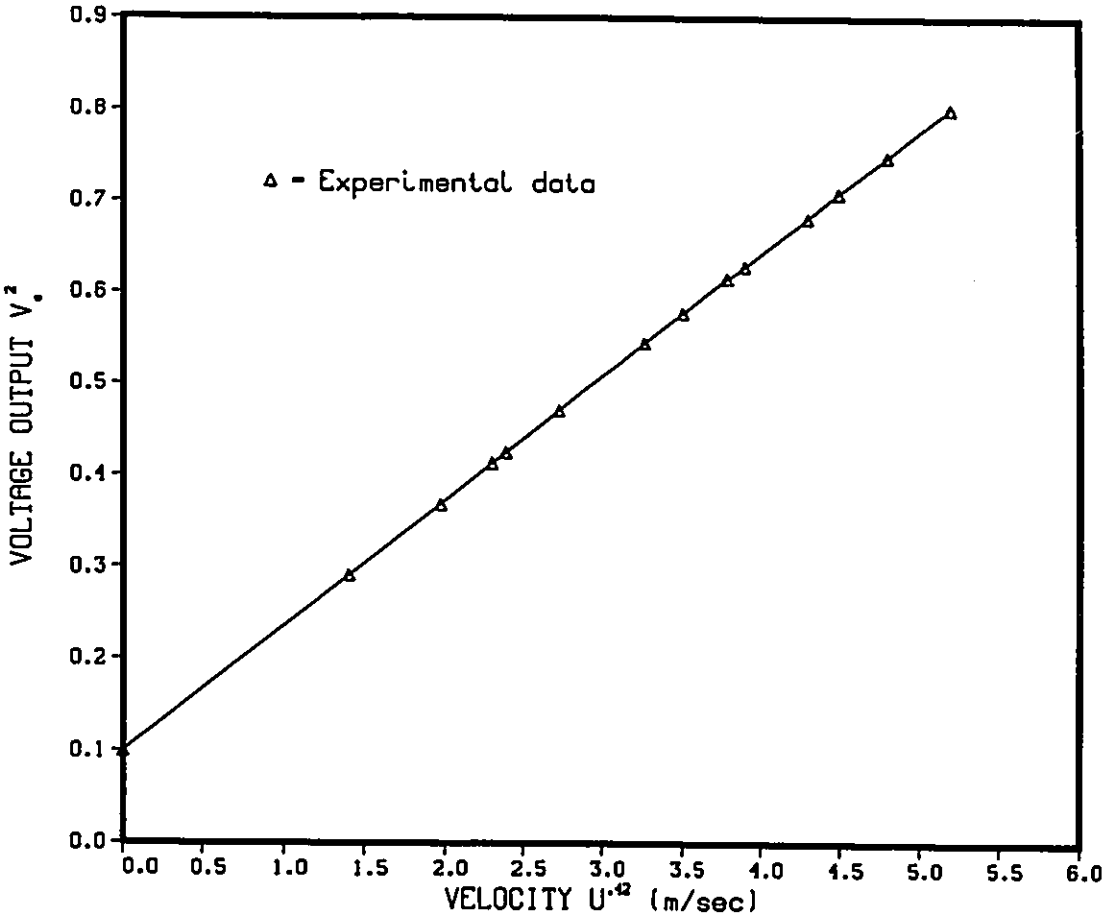

Figure 9. Hot wire calibration curve; continuous line is the polynomial fit using modified King's law

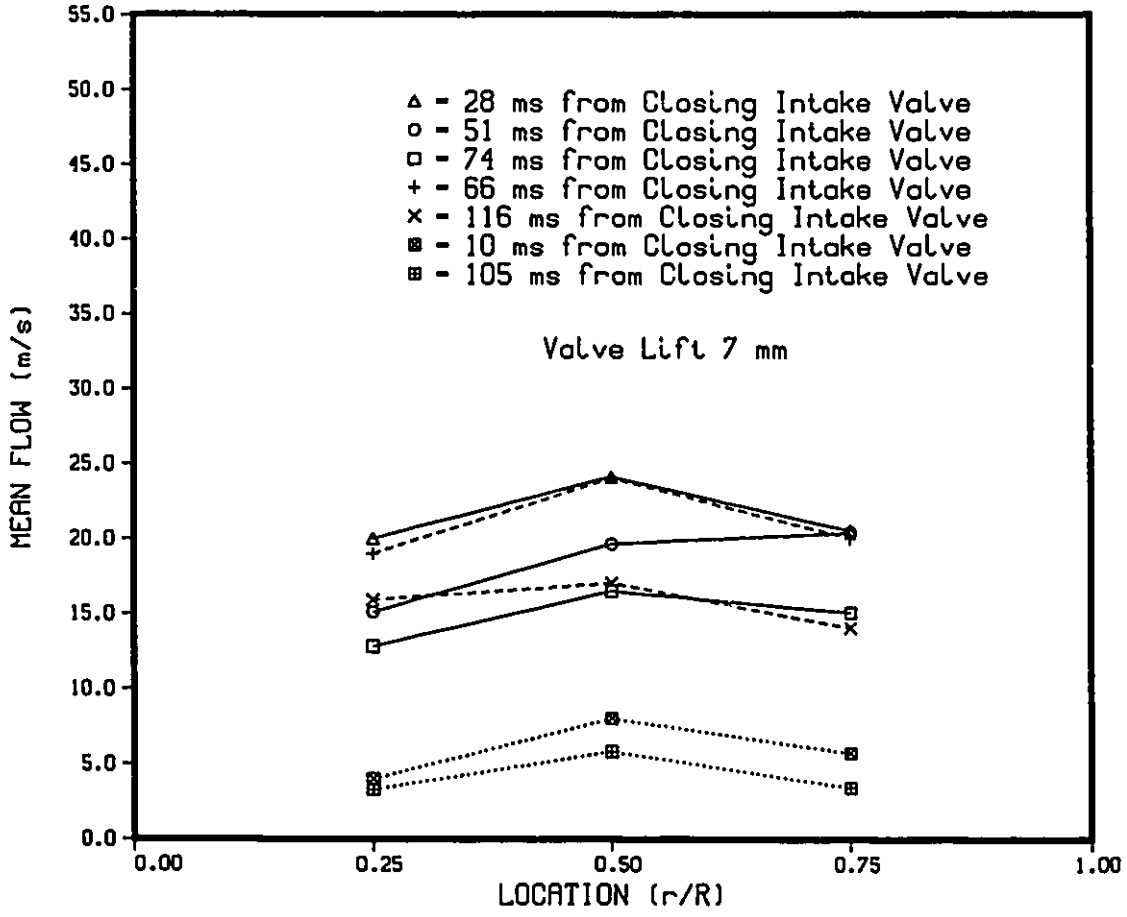

Figure 10. Mean flow versus location for three decay times and a valve lift of 7 mm. Continuous lines represent the present data, dashed lines represent Dyer's data (1979) and dotted lines represent Hamamoto's data (1988)

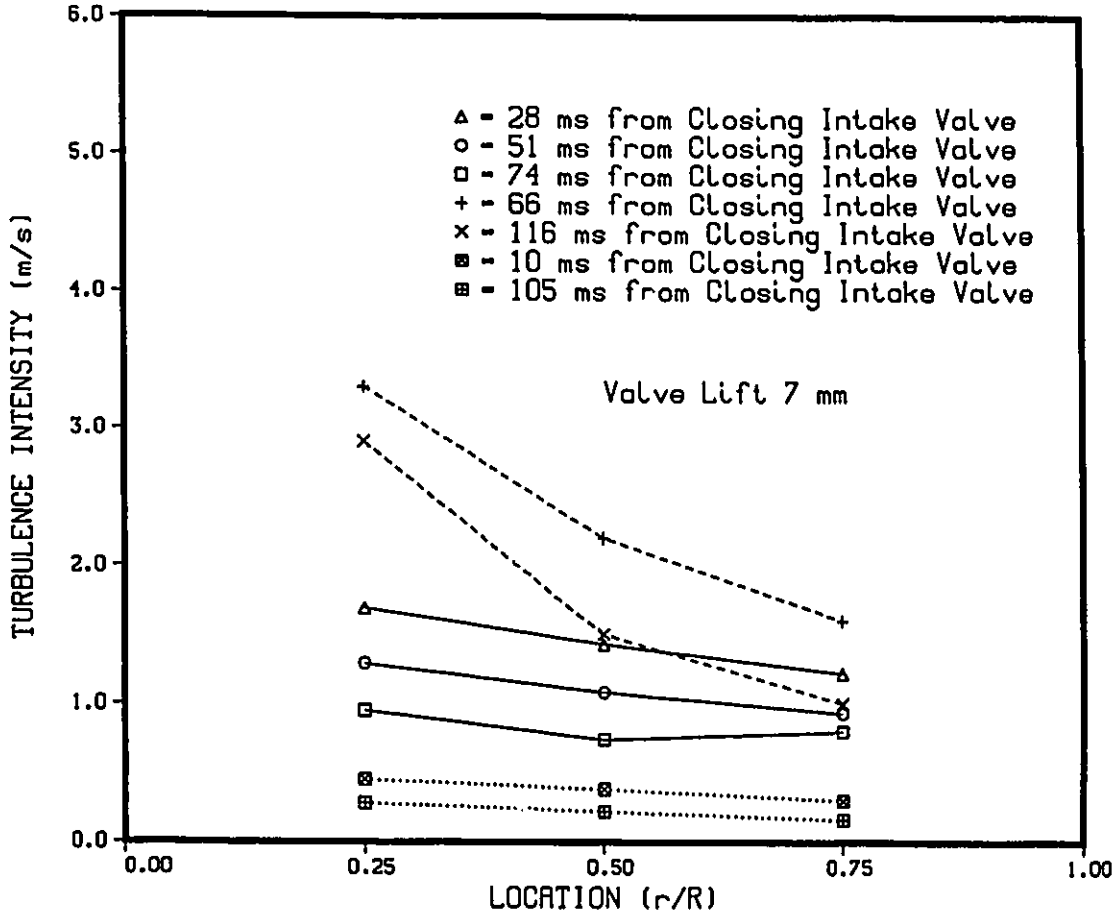

Figure 11. Turbulence intensity versus location for three decay times and a valve lift of 7 mm; Continuous lines represent the present data, dashed lines represent Dyer's data (1979) and dotted lines represent Hamamoto's data (1988)

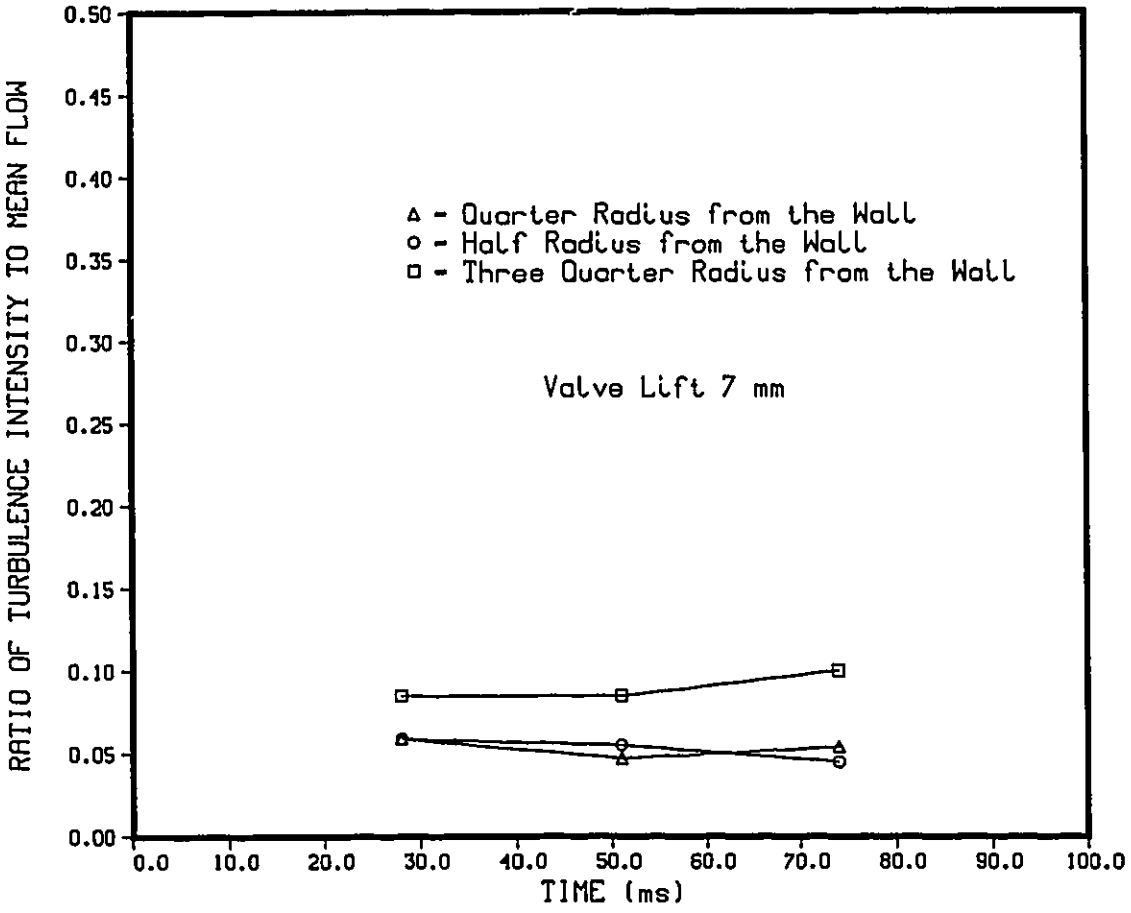

Figure 12. Ratio of turbulence intensity to mean flow $u'/\overline{U}$ for three decay times

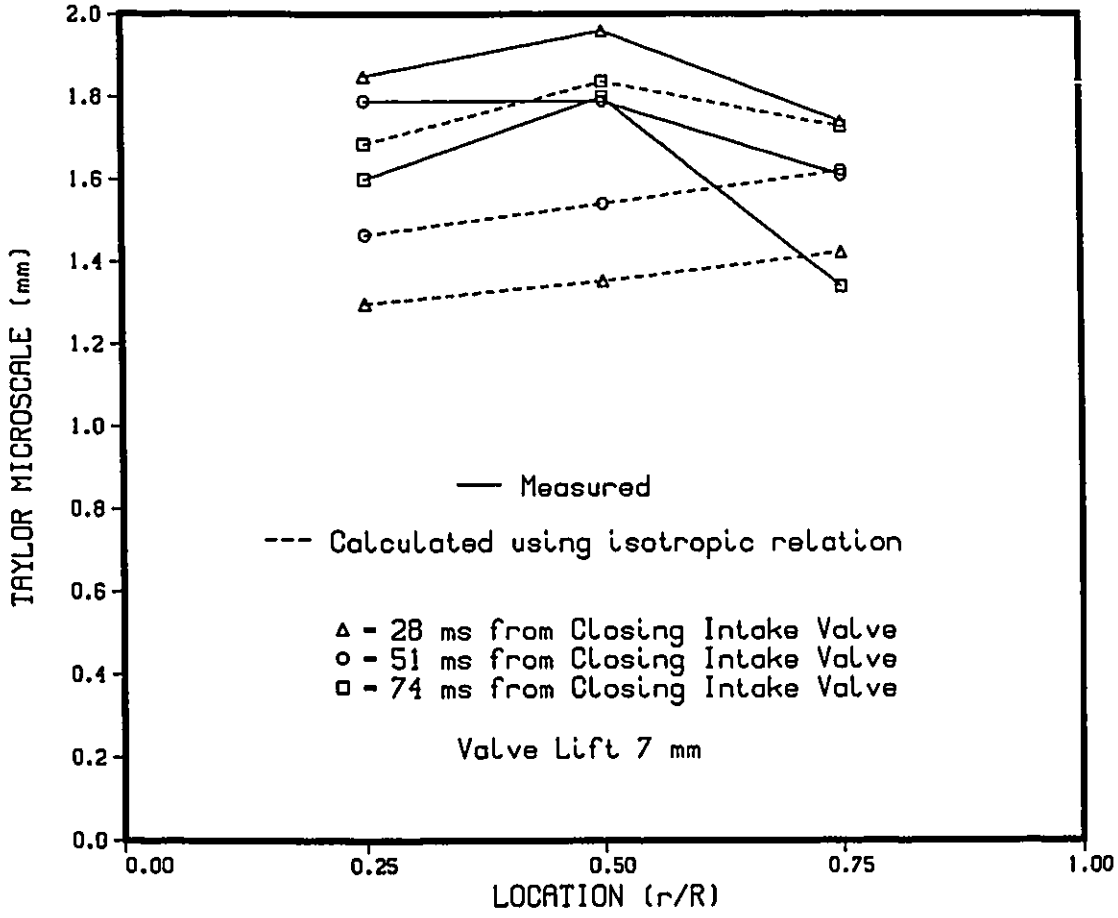

Figure 13. Taylor microscale versus location for three decay times and valve lift 7 mm

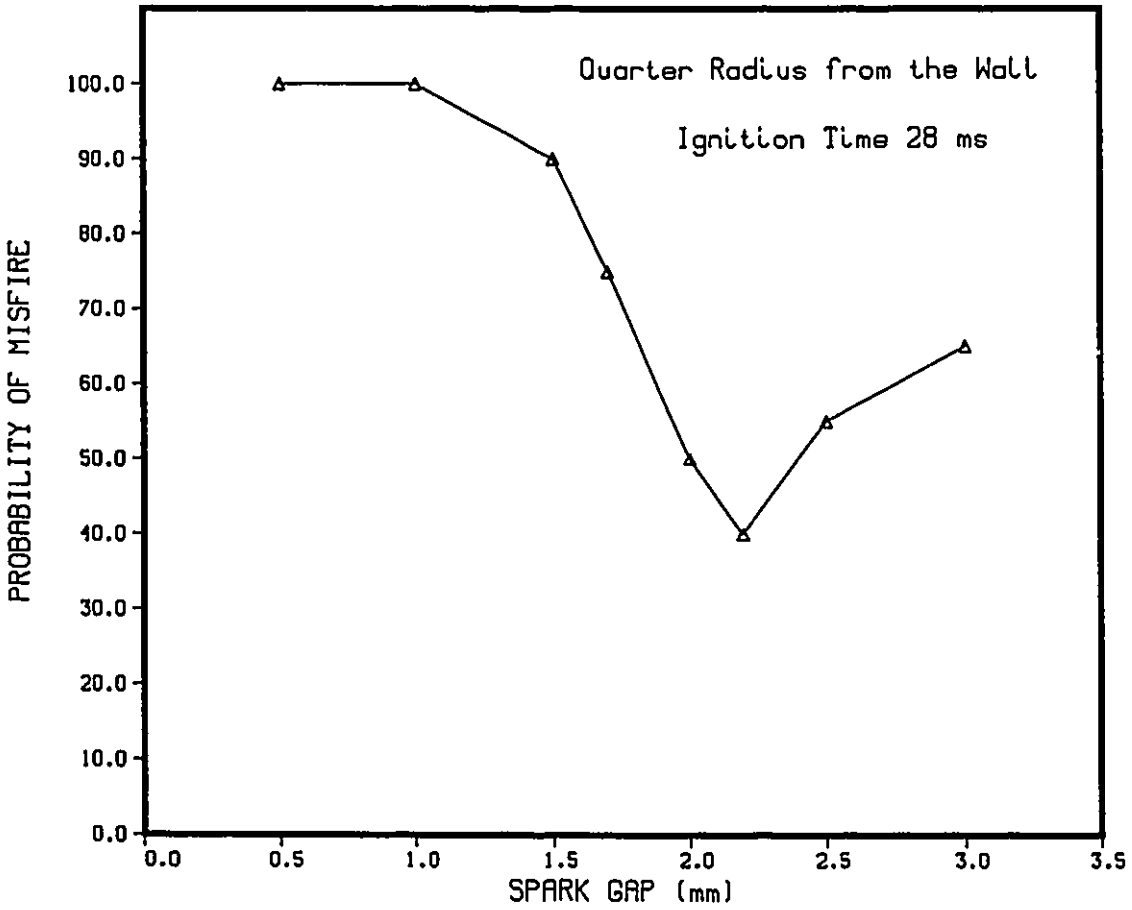

Figure 14. Probability of misfire versus spark gap for ignition at quarter radius from the wall and ignition time 28 ms

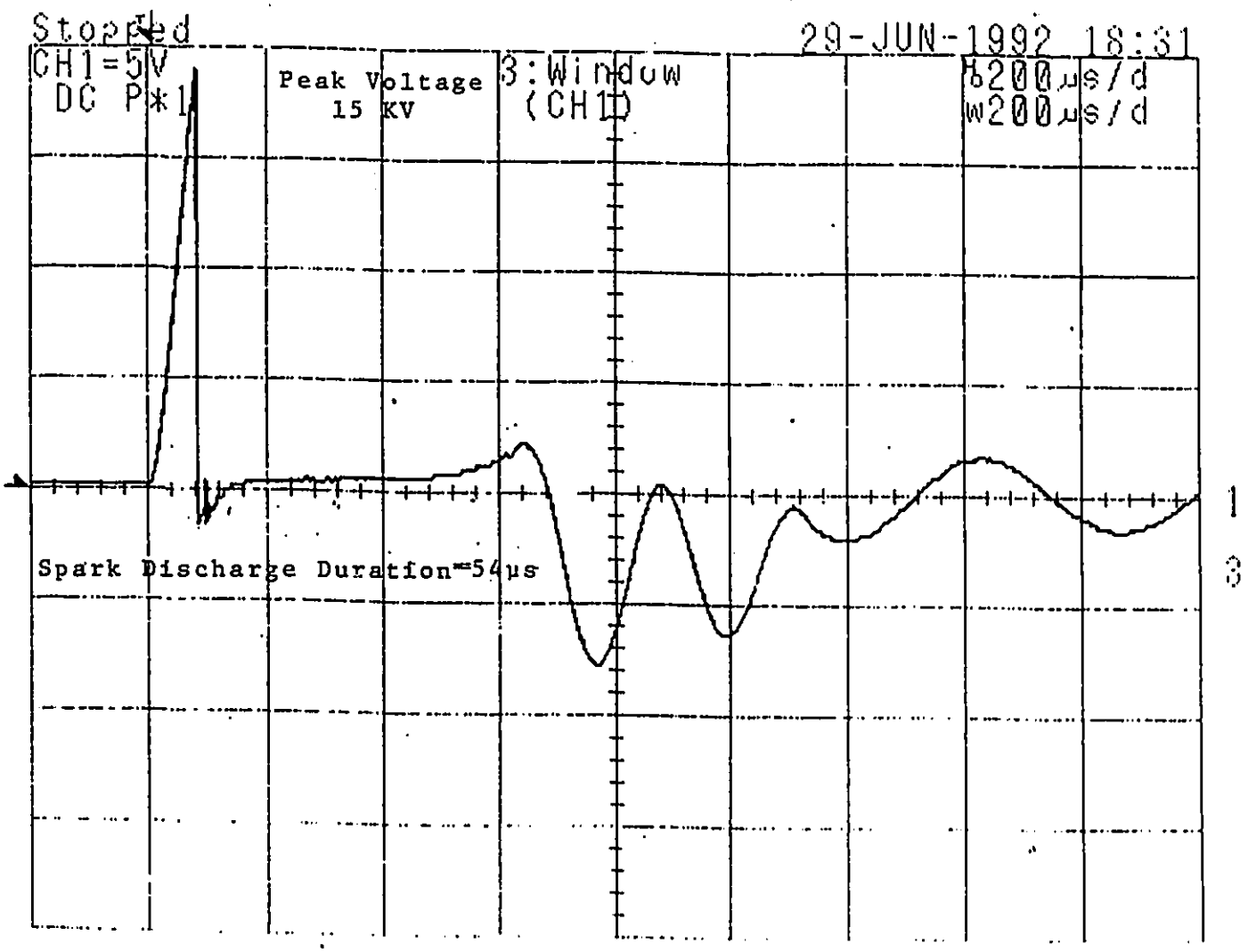

Figure 15. Voltage time history across the spark gap

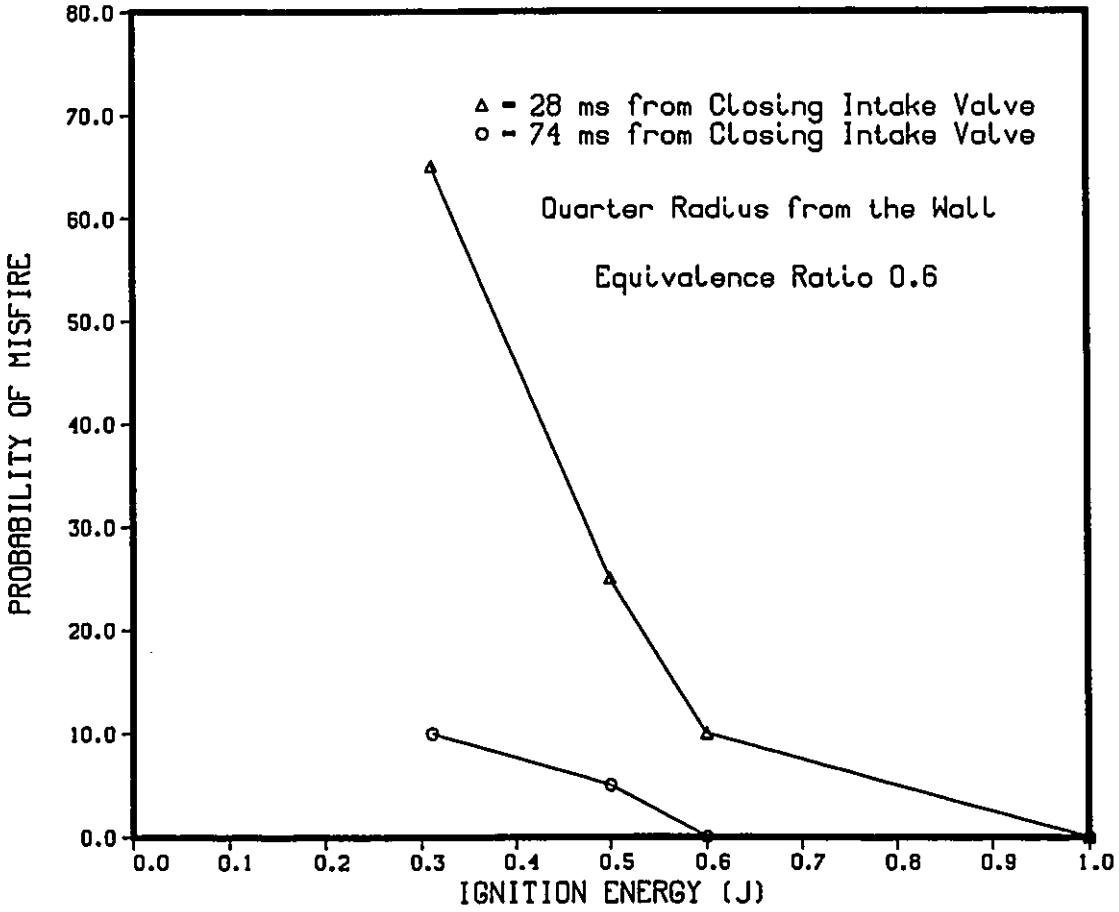

Figure 16. Probability of misfire versus ignition energy for two ignition times at quarter radius from the wall and equivalence ratio 0.6

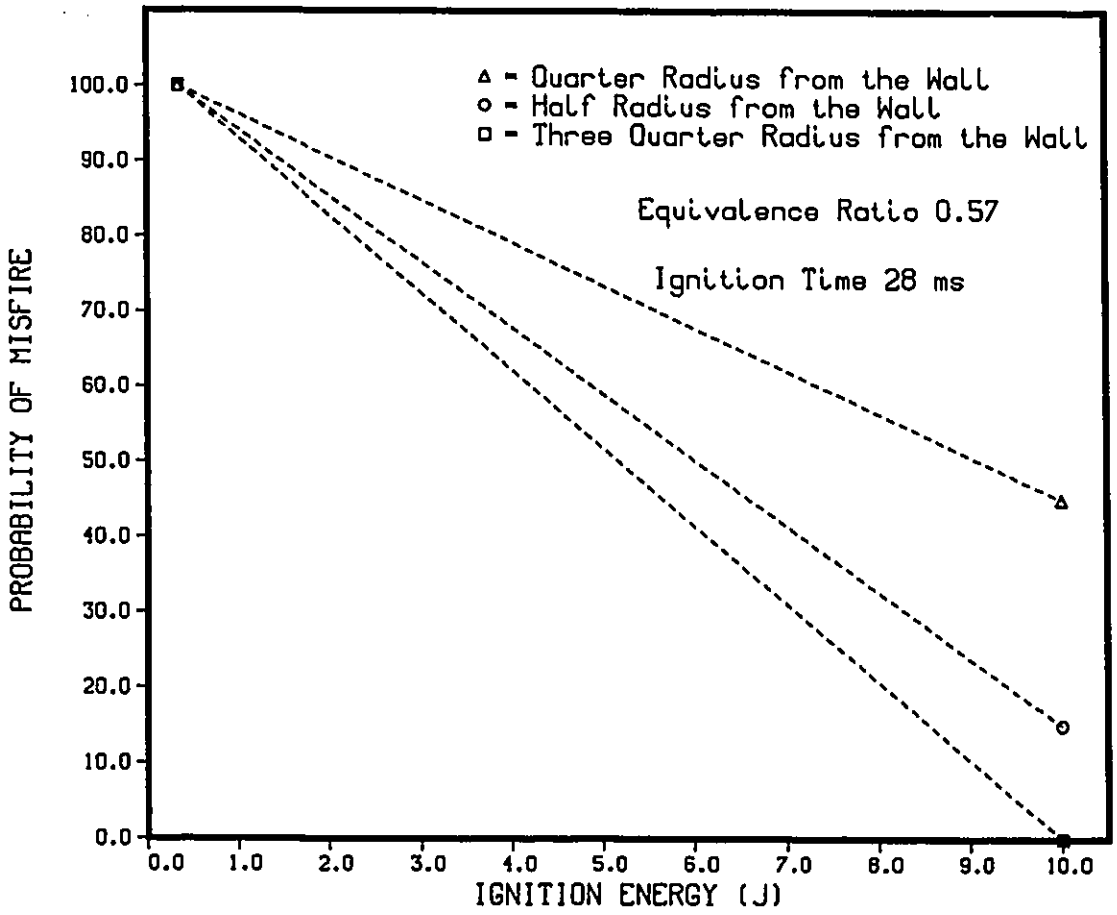

Figure 17. Probability of misfire versus ignition energy for equivalence ratio 0.57 and ignition time 28 ms

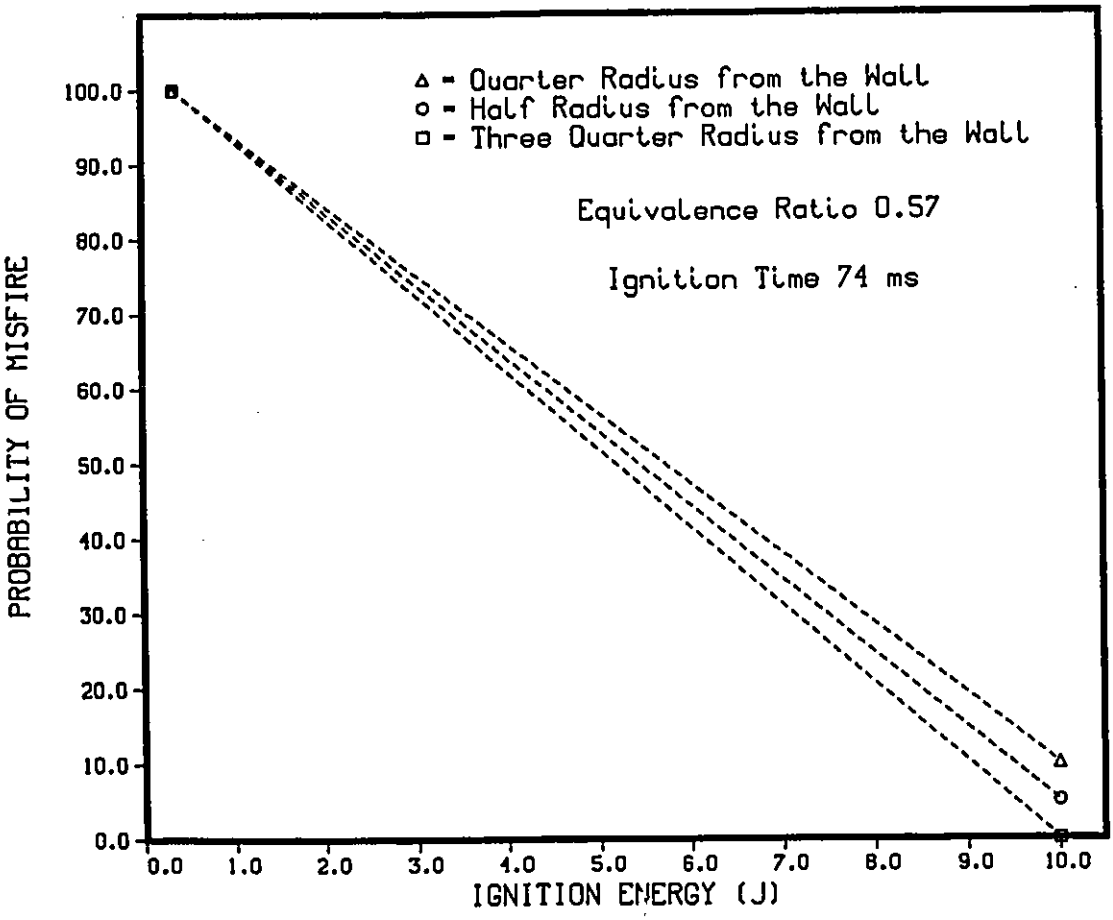

Figure 18. Probability of misfire versus ignition energy for equivalence ratio 0.57 and ignition time 74 ms

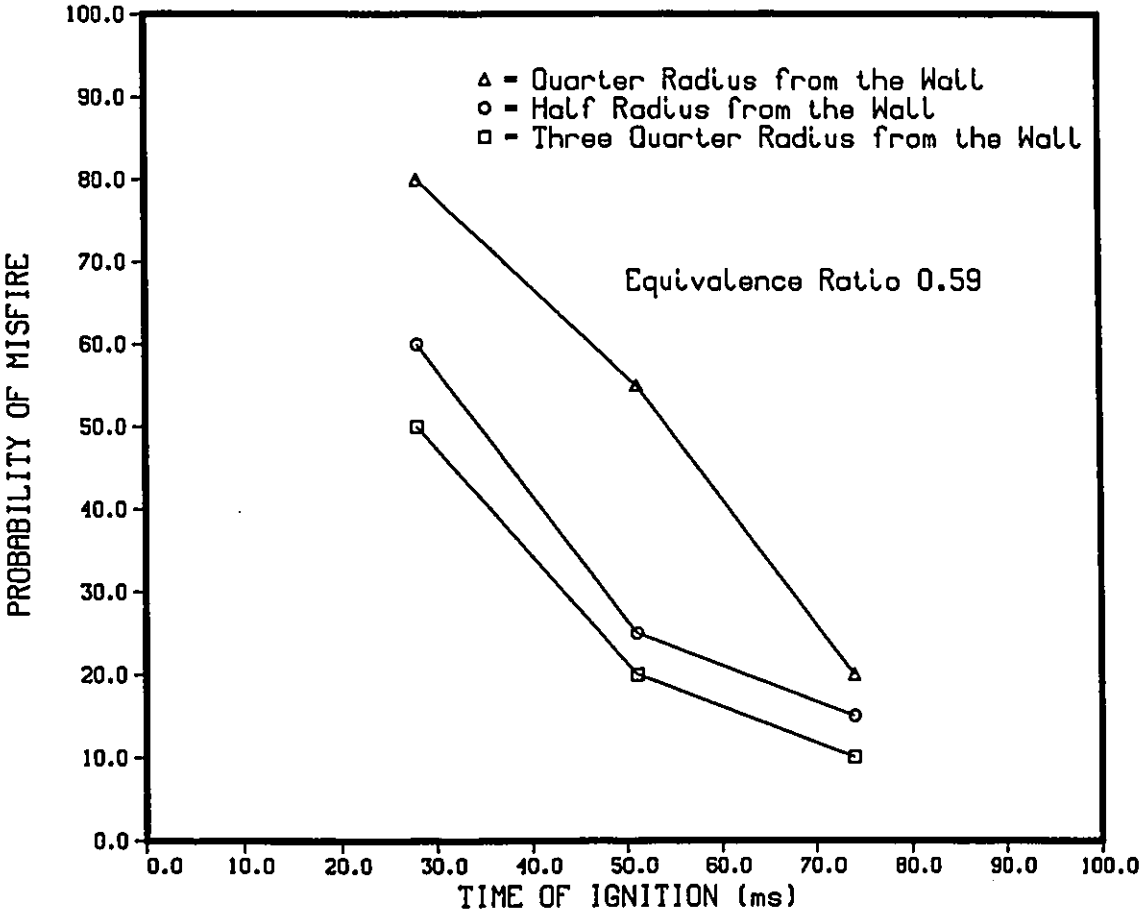

Figure 19. Probability of misfire versus ignition time for three ignition locations and equivalence ratio 0.59

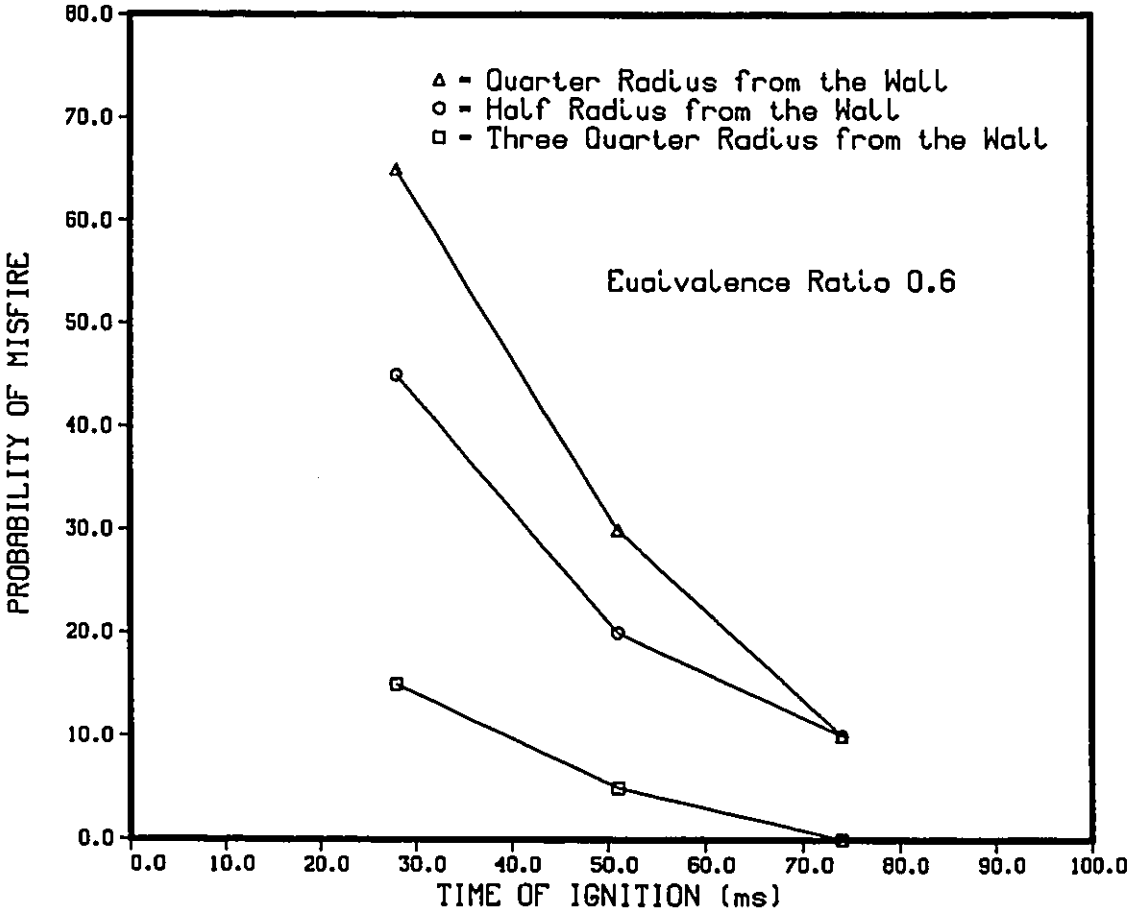

Figure 20. Probability of misfire versus ignition time for three ignition locations and equivalence ratio 0.6

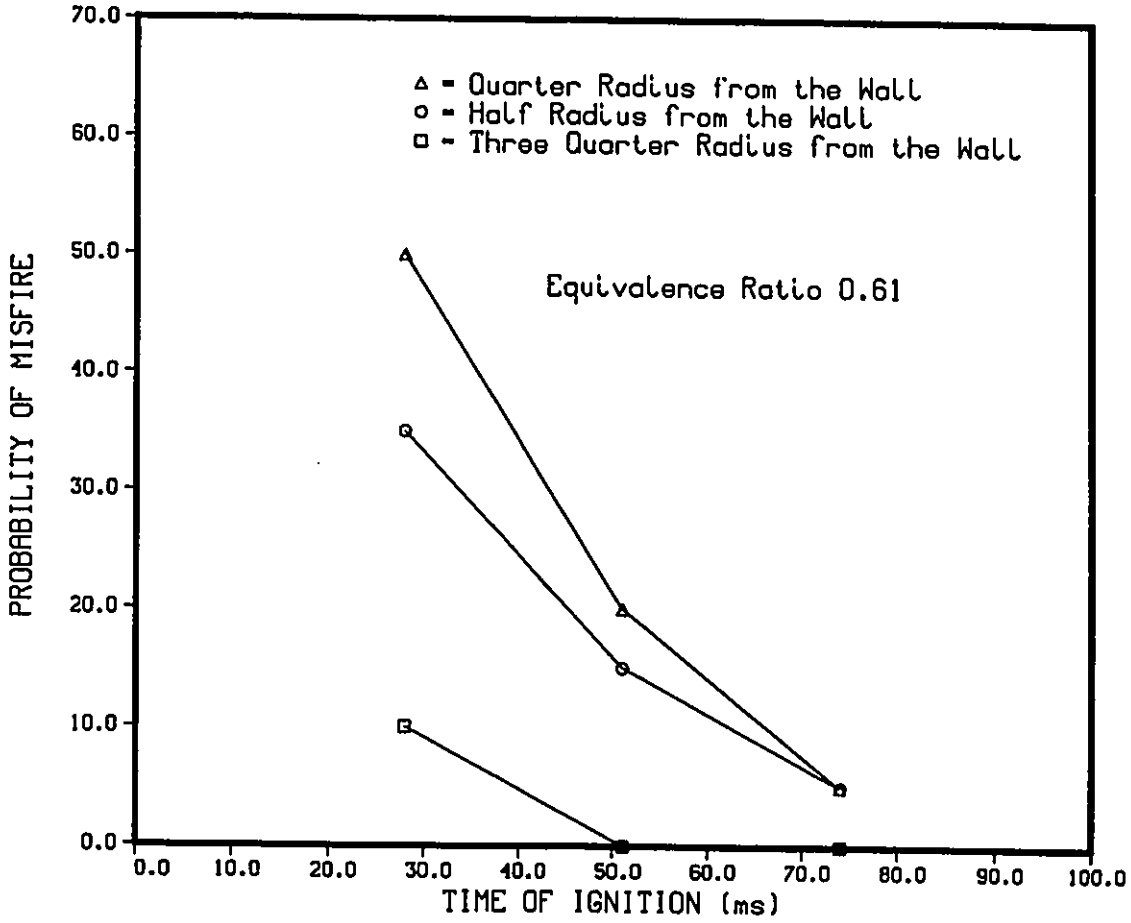

Figure 21. Probability of misfire versus ignition time for three ignition locations and equivalence ratio 0.61

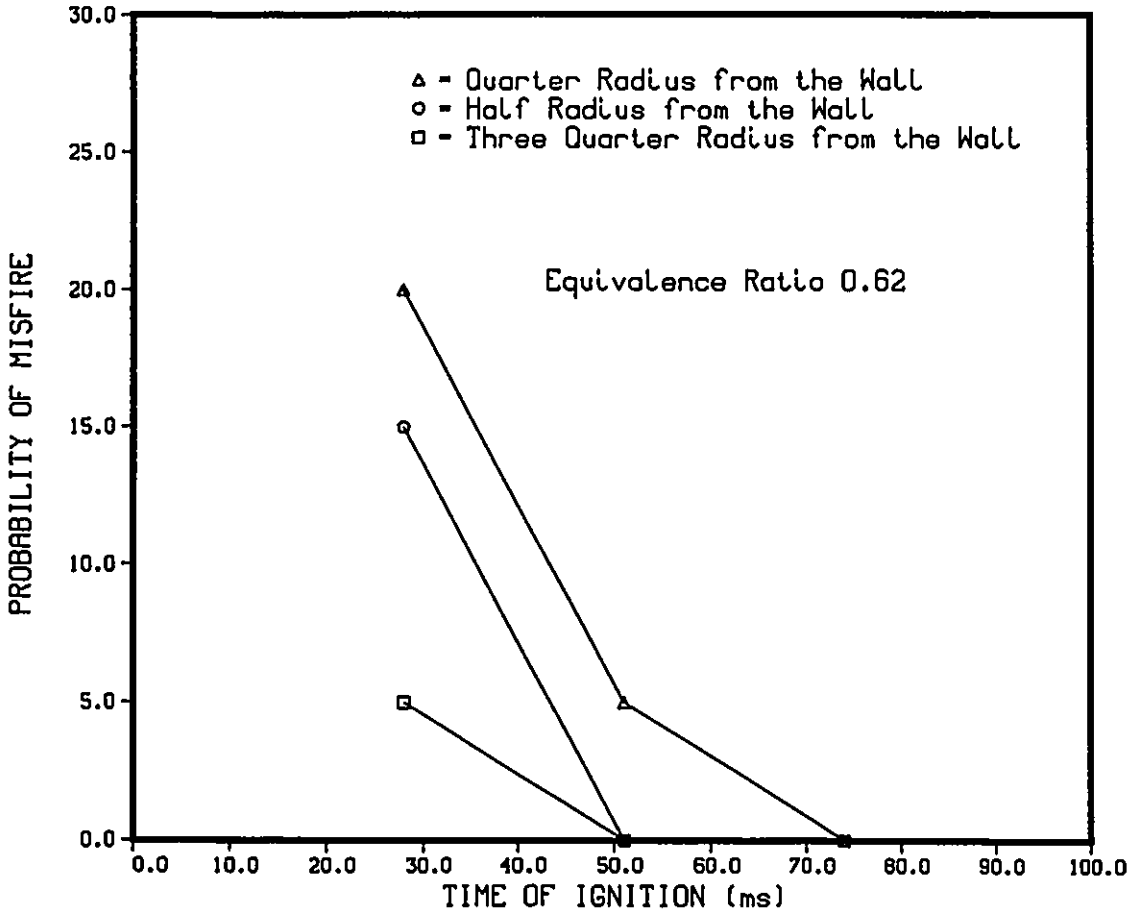

Figure 22. Probability of misfire versus ignition time for three ignition locations and equivalence ratio 0.62

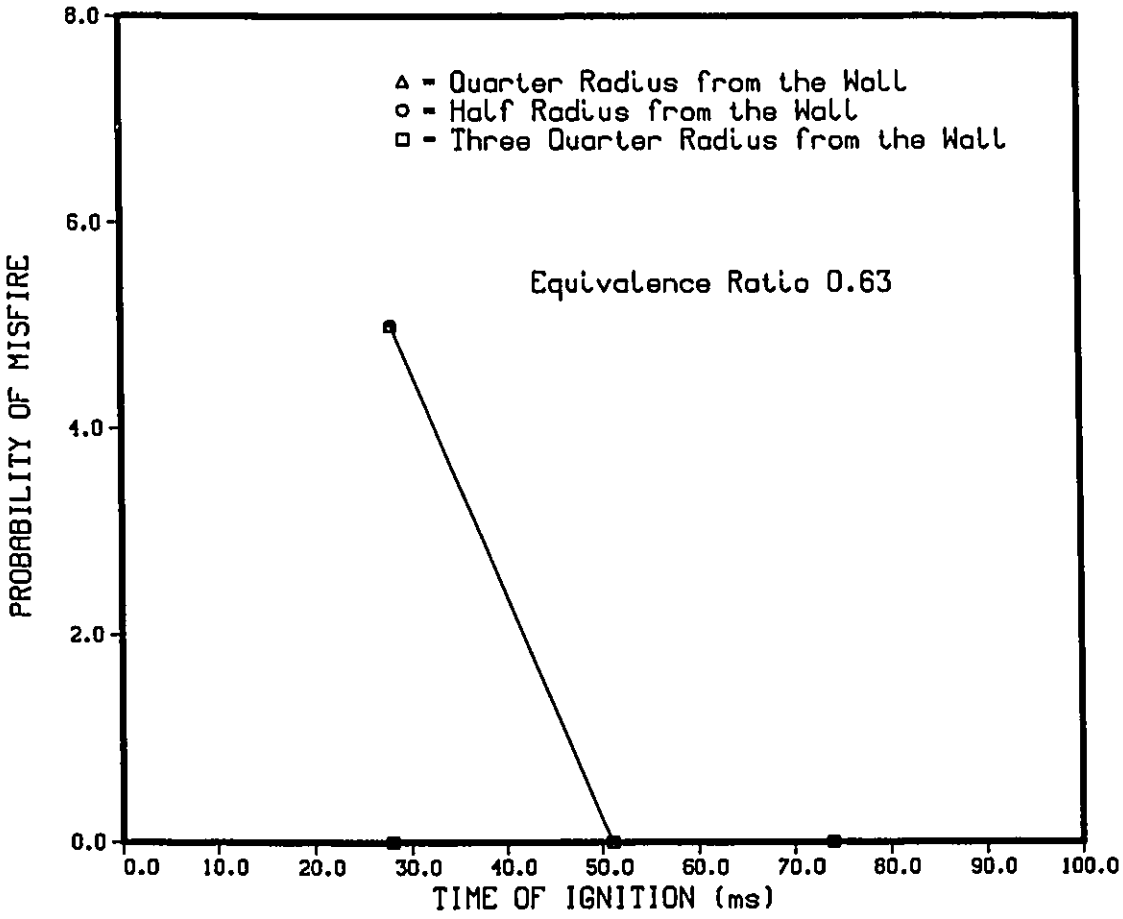

Figure 23. Probability of misfire versus ignition time for three ignition locations and equivalence ratio 0.63

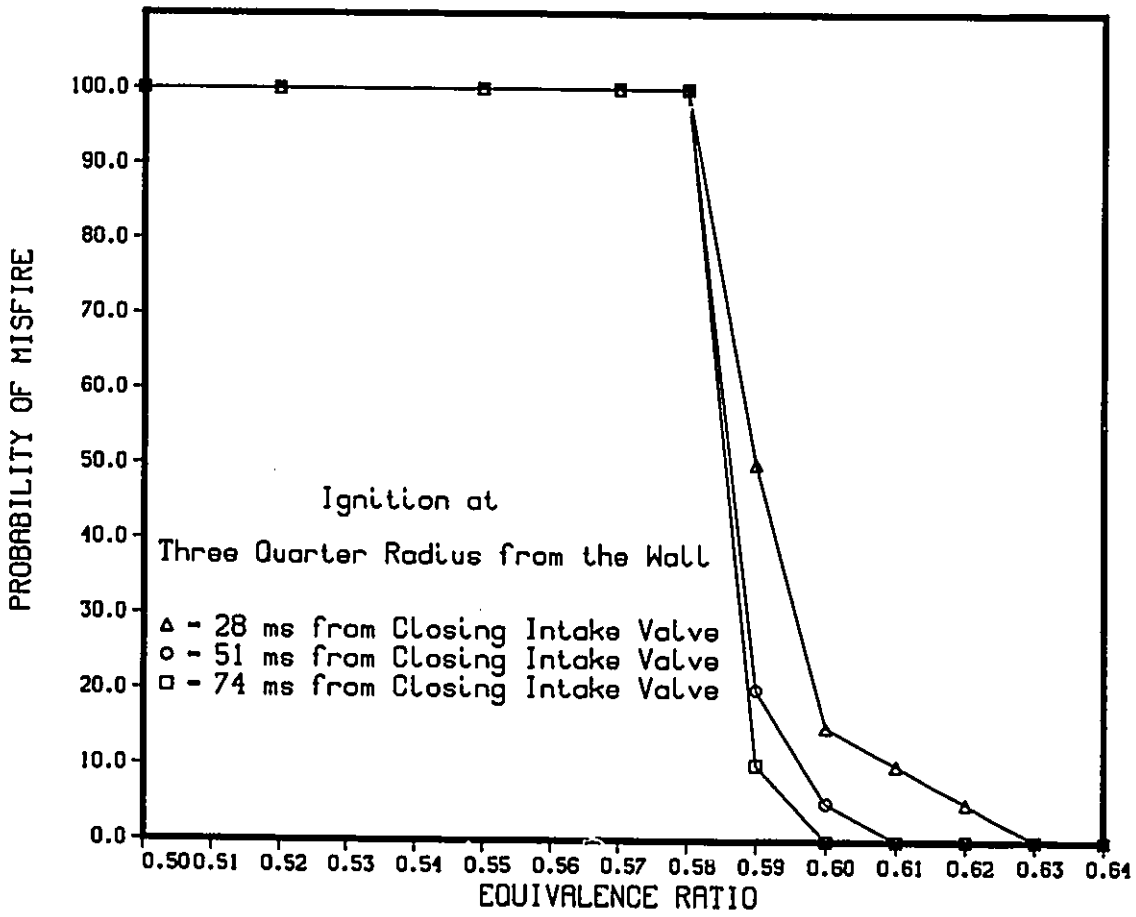

Figure 24. Probability of misfire versus equivalence ratio for three ignition times and for ignition at three quarter radius from the wall

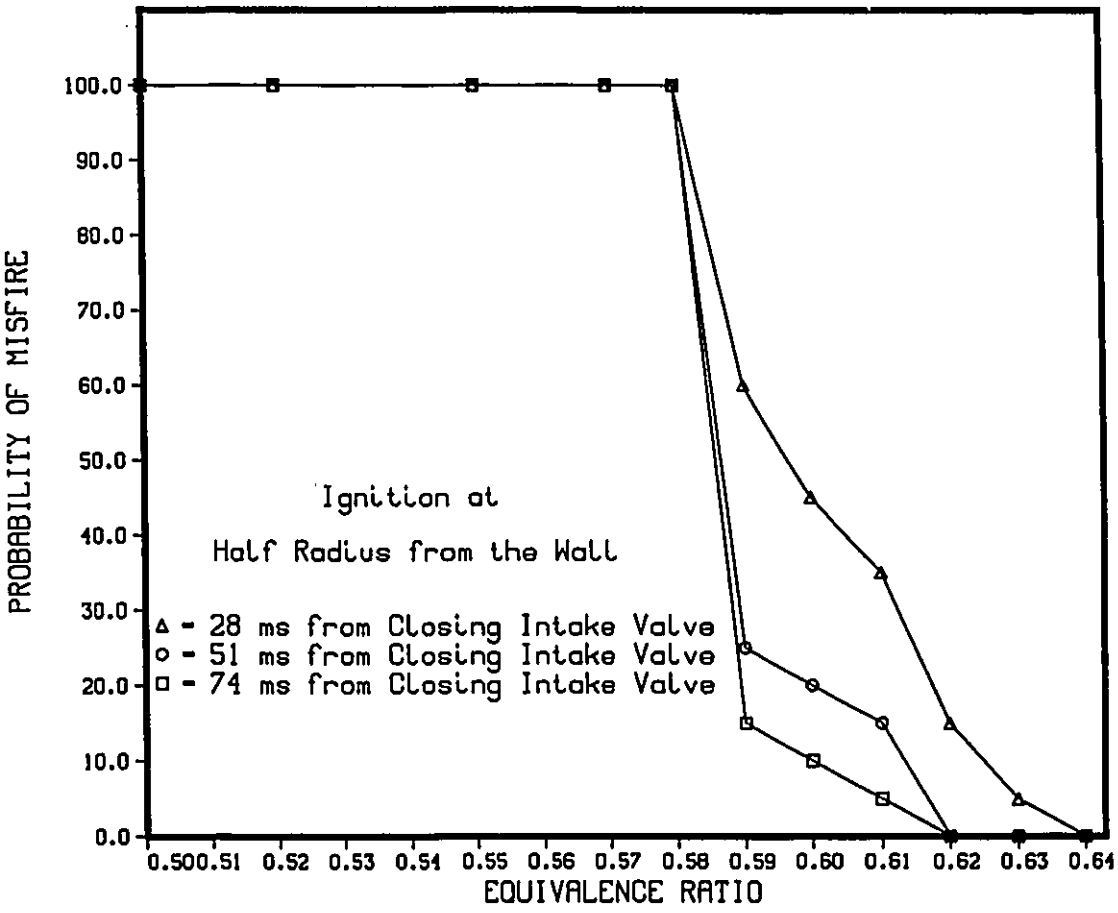

Figure 25. Probability of misfire versus equivalence ratio for three ignition times and for ignition at half radius from the wall

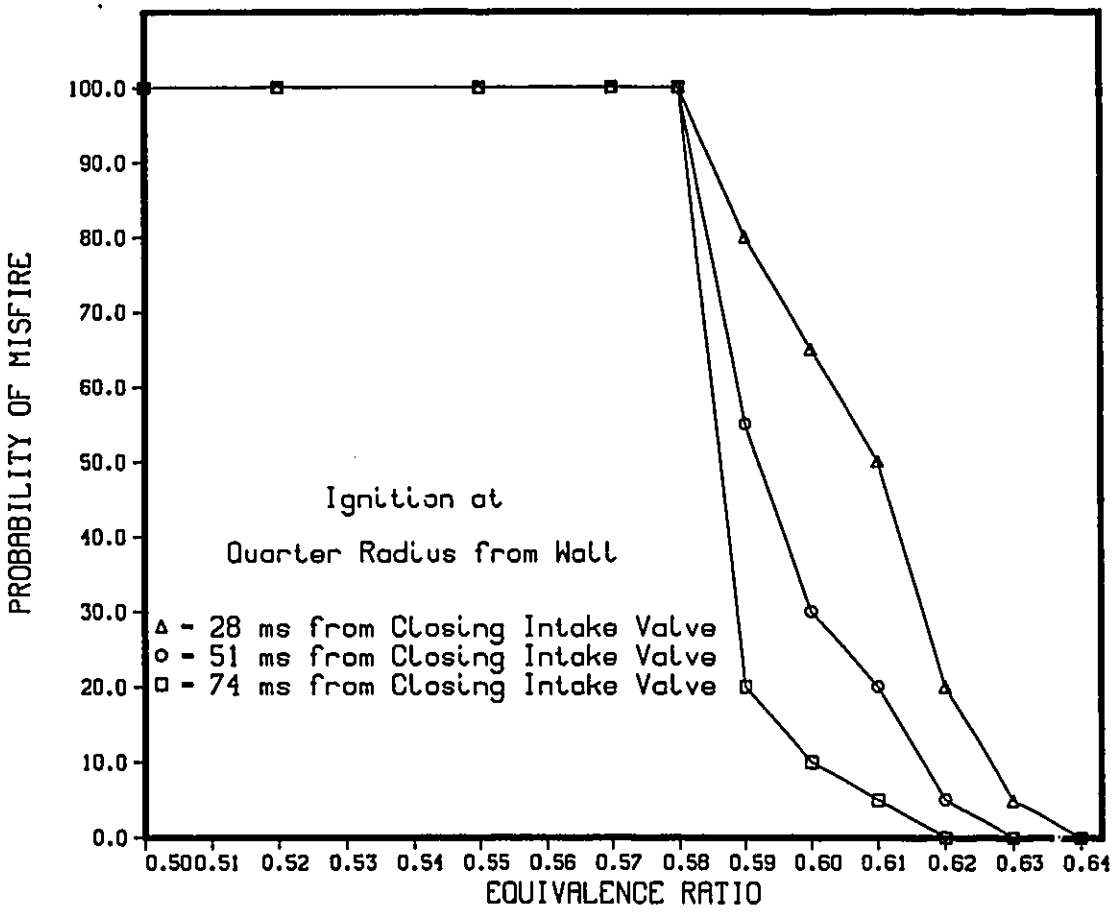

Figure 26. Probability of misfire versus equivalence ratio for three ignition times and for ignition at quarter radius from the wall

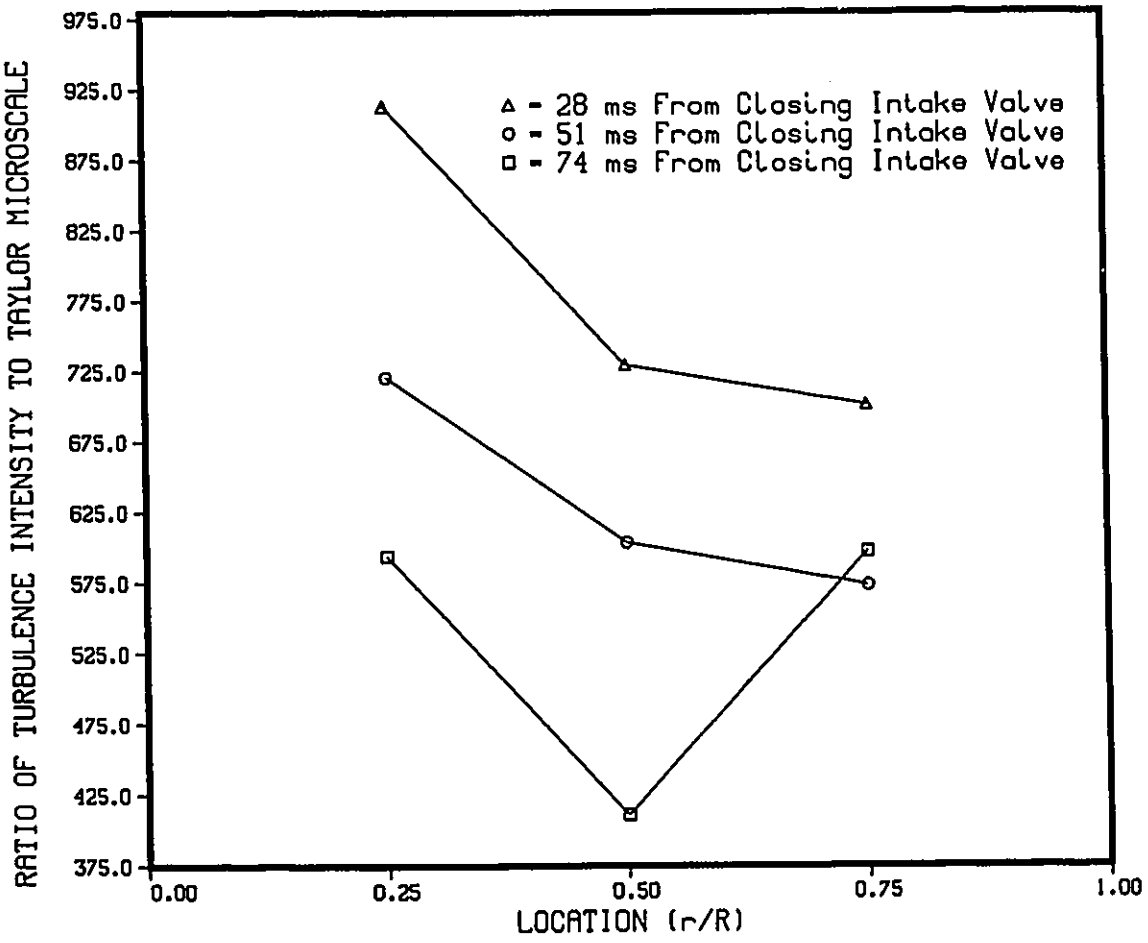

Figure 27. Ratio of turbulence intensity to Taylor microscale ($\frac{u'}{\lambda}$) at three ignition times and for three ignition locations

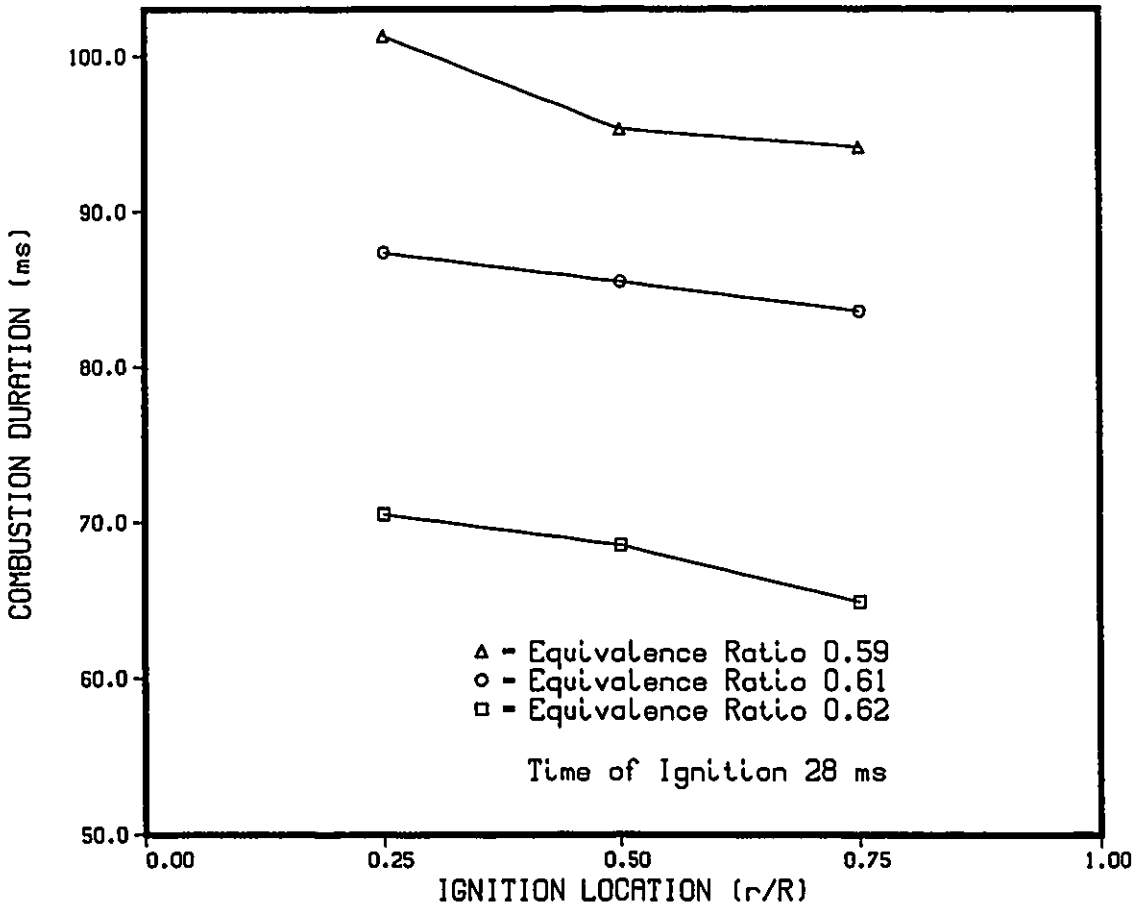

Figure 28. Combustion duration versus ignition location for three equivalence ratios (0.59, 0.61 and 0.62) and time of ignition of 28 ms

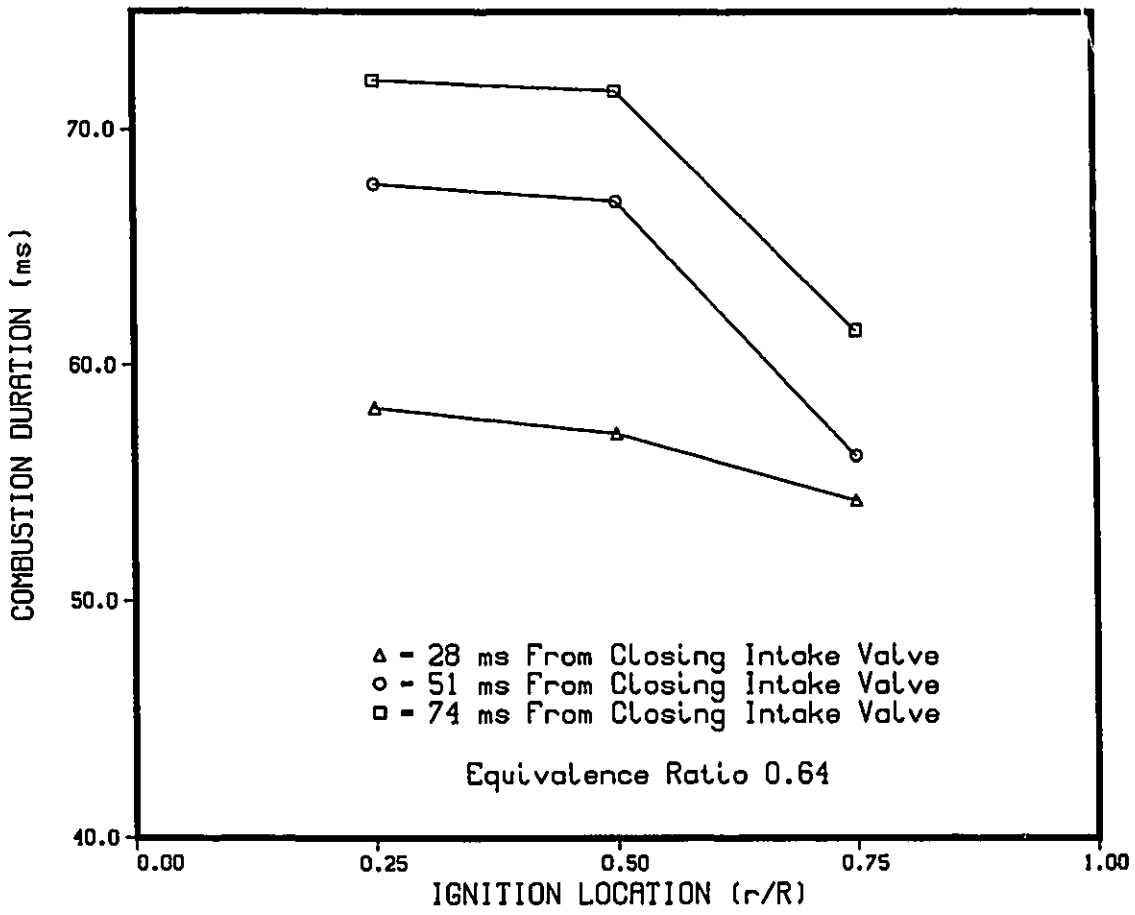

Figure 29. Combustion duration versus ignition location for three ignition times and equivalence ratio 0.64

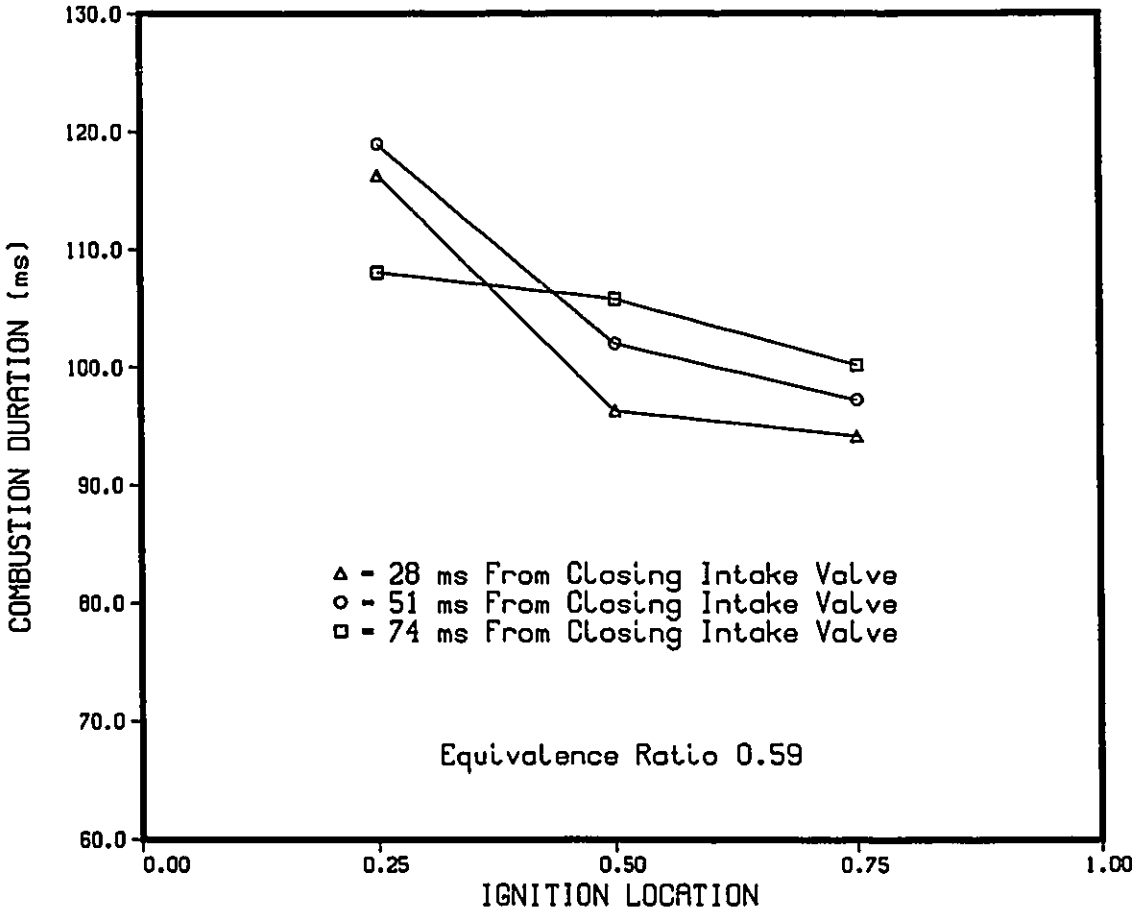

Figure 30. Combustion duration versus ignition location for three ignition times and equivalence ratio 0.59

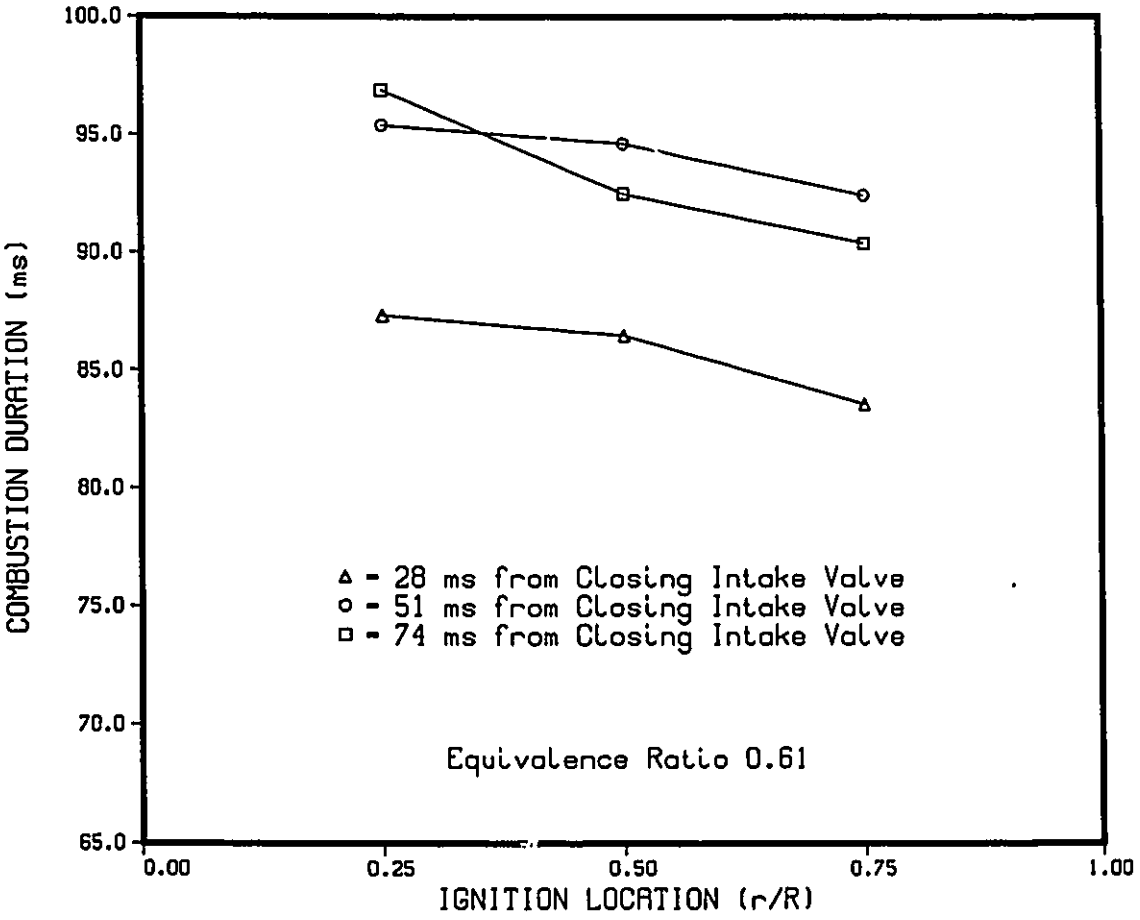

Figure 31. Combustion duration versus ignition location for three ignition times and equivalence ratio 0.61

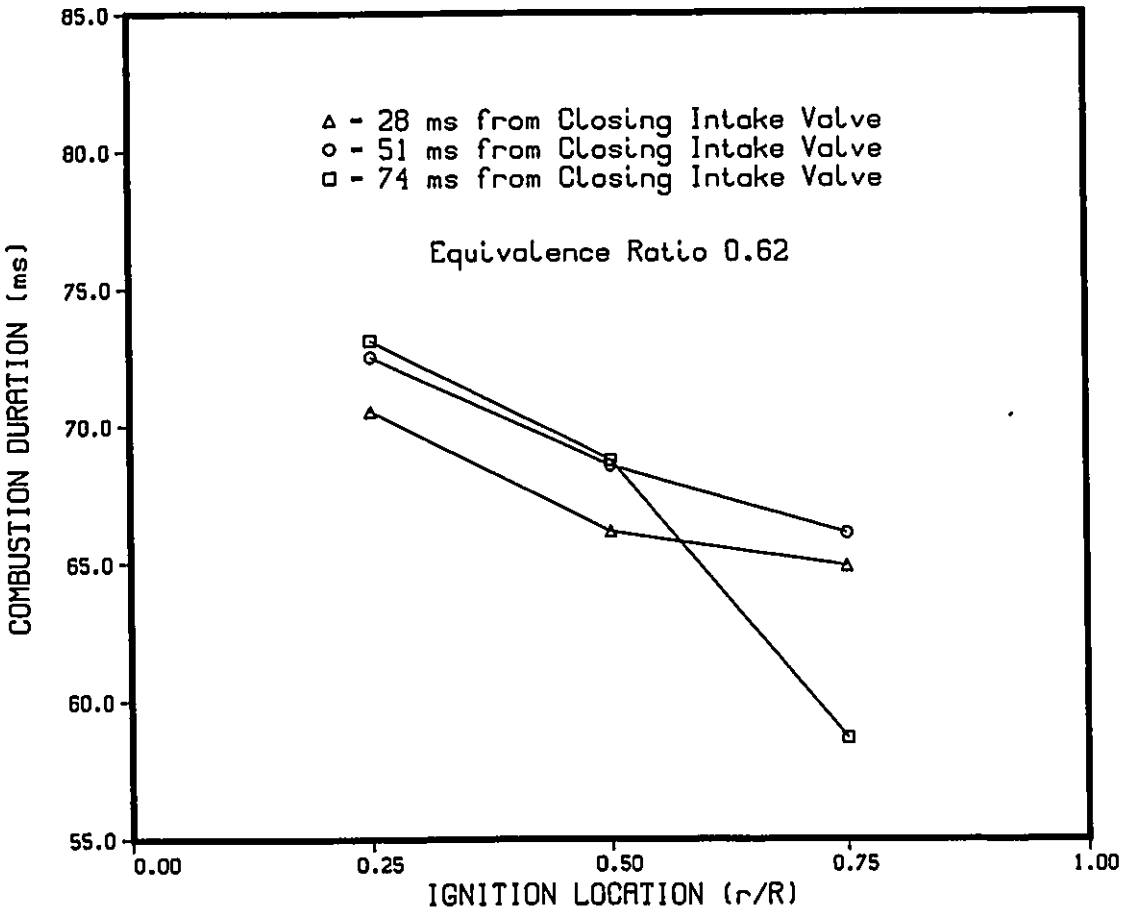

Figure 32. Combustion duration versus ignition location for three ignition times and equivalence ratio 0.62

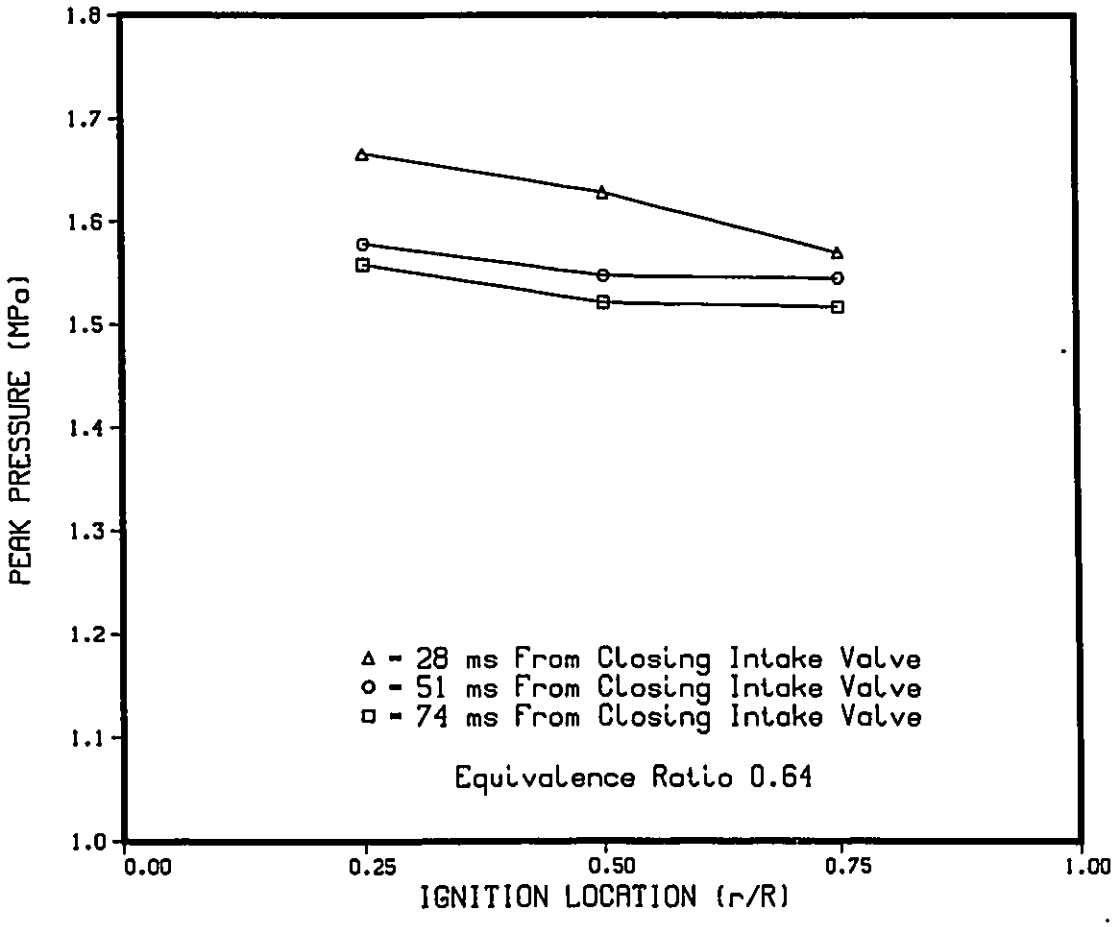

Figure 33. Peak pressure versus ignition location for three ignition times and equivalence ratio 0.64

Appendix A

Programs

ALFARS fortran program

This program read the data for ambient temperature and corresponding operating resistance in the calibration nozzle from data file and then calculating the thermal resistivity and operating resistance for the hot wire.

```
      DIMENSION XX(20),YY(20),X(20),Y(20)
      RC=5.1
      N=4
      TS= 523
      TC=292
      AN=FLOAT(N)
      SX=0.
      SY=0.
      SY2=0.
      SX2=0.
      SXY=0.
      DO 10 I=1,N
      Y(I)=YY(I)
      X(I)=XX(I)
      SX=SX+X(I)
      SX2=SX2+X(I)*X(I)
      SY=SY+Y(I)
      SY2=SY2+Y(I)*Y(I)
      SXY=SXY+Y(I)*X(I)
   10 CONTINUE
      A=(SX2*SY-SX*SXY)/(AN*SX2-SX*SX)
      B=(AN*SXY-SX*SY)/(AN*SX2-SX*SX)
      ALPHA=B/RC
      RS = RC * ( 1 + ALPHA * (TS - TC ))
      RMS=0.
      DO 5 I=1,N
      XB=((Y(I)-A)/B)
      XA=X(I)
      WRITE(3,*)Y(I),XB,XA
C     YC=A+B*X(I)
C     WRITE(3,*)YC,Y(I)
    5 RMS=RMS+(XB-XA)**2
      RMS=SQRT(RMS/AN)
      WRITE(*,2)A,B
      WRITE(2,72)A,B
    2 FORMAT(4X,'A=',F10.5,3X,'B=',F10.5)
   72 FORMAT(4X,'A=',F10.5,3X,'B=',F10.5)
      WRITE(2,9)ALPHA, RS
    9 FORMAT(4X,'ALPHA=',E10.5,3X,'RS=',E10.5)
      WRITE(*,3)ALPHA,RS
    3 FORMAT(4X,'ALPHA=',E10.5,3X,'RS=',E10.5)
      STOP
      END
```

BEALNS fortran program

```
      This program read the data for the velocity of the flow
      and corresponding voltage across the hot wire in the
      calibration nozzle and then calculated the calibration
      constants alpha, beta  and n for the hot wire
```

```
      DIMENSION XX(20),YY(20),X(20),Y(20)
      RC=5.1
      RH=9.34
      TS=523.
      TG=292.
      P=101000.
      N=8
      AN=FLOAT(N)
    3 WRITE(*,4)
    4 FORMAT(2X,'ENTER N')
      READ(*,*)EX
      IF (EX.GE.10.)GO TO 100
      SX=0.
      SY=0.
      SY2=0.
      SX2=0.
      SXY=0.
      DO 10 I=1,N
      Y(I)=YY(I)**2
      X(I)=XX(I)**EX
      WRITE(3,*)X(I),Y(I),AN
      SX=SX+X(I)
      SX2=SX2+X(I)*X(I)
      SY=SY+Y(I)
      SY2=SY2+Y(I)*Y(I)
      SXY=SXY+Y(I)*X(I)
   10 CONTINUE
      A=(SX2*SY-SX*SXY)/(AN*SX2-SX*SX)
      B=(AN*SXY-SX*SY)/(AN*SX2-SX*SX)
      BE  = A / ((TS - TG) * (TG**.8))
      AL = B * (TG**(1.76*EX - .8)) / ((TS - TG) * (P**EX))
      RMS=0.
      DO 5 I=1,N
      XB=((Y(I)-A)/B)**(1./EX)
      XA=(X(I)**(1./EX))
      WRITE(3,*)Y(I),XB,XA
C     YC=A+B*X(I)
C     WRITE(3,*)YC,Y(I)
    5 RMS=RMS+(XB-XA)**2
      RMS=SQRT(RMS/AN)
      WRITE(*,2)A,B,RMS
      WRITE(2,72)EX,A,B,RMS
    2 FORMAT(4X,'A=',F10.5,3X,'B=',F10.5,3X,'RMS=',F7.6)
   72 FORMAT(4X,'N=',F5.3,3X,'A=',F10.5,3X,'B=',F10.5,3X,'RMS=',F7.6)
      WRITE(*,8)BE,AL
    8 FORMAT(4X,'BETA=',E20.9,3X,'ALPHA=',E20.9)
      WRITE(2,9)BE,AL
```

BEALNS fortran program

```
  9   FORMAT(4X,'BETA=',E20.9,3X,'ALPHA=',E20.9)
      GOTO 3
100   STOP
      END
```

STRM-91 basic program

```
10 PRINT
30 PRINT
40 PRINT "This program acquire data (pressure,temperatures,and velocities)"
50 PRINT "and store them in various files for further manipulations in hhh"
60 PRINT "programme. measurements are first stored on oscilloscope screen"
70 PRINT "and then transferred to the computer"


550 PRINT "   File  NDAQ.BAS  inputs data from Nicolet oscilloscope."
560 PRINT "   ═══════════════════════════════════════════════════════"
570 PRINT
580 PRINT
590 PRINT "This program reads one screen full of information stored on the"
600 PRINT "Nicolet Oscilloscope and reproduces it on this monitor. "
610 PRINT "If requested a hard copy of the graph can be printed, and the "
620 PRINT "data can be stored on the hard disk in drive C."
630 DEFINT A
640 DIM A(4100)
641 DIM T(4100)
642 DIM V(4100)
643 DIM P(4100)
645 DIM N(8)
650 PRINT "In order to transfer data, check that the oscilloscope is in"
660 PRINT "the 'STORE' mode."
670 PRINT "Press 'P' to open communications, then press the RS232 button"
680 PRINT "on the oscilloscope after the tone."
690 PRINT "Communications remain open until the DATA ACQUISITION COMPLETE"
700 PRINT "message appears (this takes approx. 2 minutes)."
702 Inf = 0
704 IVF = 0
740 PRINT "   TAKE PRESSURE DATA,ENTER P AT KEYBOARD,"
750 PRINT "   THEN PRESS RS-232 ON NICOLET AFTER TONE."
760 IFLAG = 0
770 GOTO 880
780 Inf = 0
790 IVF = 0
800 PRINT "   TAKE VELOCITY DATA,ENTER P AT KEYBOARD,"
810 PRINT "   THEN PRESS RS-232 ON NICOLET AFTER TONE."
820 IFLAG = 1
830 GOTO 880
840 PRINT
850 PRINT "   TAKE TEMPERATURE DATA,ENTER P AT KEYBOARD,"
860 PRINT "   THEN PRESS RS-232 ON NICOLET AFTER TONE."
870 IFLAG = 2
880 PRINT
890 PRINT
900 B$ = INPUT$(1)
910 IF B$ = "p" THEN 930
920 IF B$ = "P" THEN 930 ELSE 900
930 PRINT "COMMUNICATIONS OPEN..."
940 ' Open line to ramdrive  C  through file #2
960 ' Open communications file to RS232 port (file #1),
970 ' 9600 baud, no parity check, 7 data bits, ignore CTS and DSR ,
980 OPEN "COM1:9600,S,7,1,CS,DS" FOR RANDOM AS #1
```

STRM-91 basic program

```
990 ' Input character string from communications buffer...
1000 ' Write character string to ramdrive (file #2)...
1010 ' Print character strings on screen...
1020 SOUND 880, 25
1030 INPUT #1, I: PRINT I
1040 FOR J = 3 TO 4002
1050 A(J) = VAL(INPUT$(5, 1))
1060 NEXT J
1070 A$ = INPUT$(1, 1)
1080 FOR L = 1 TO 8
1090 N(L) = VAL(INPUT$(5, 1))
1100 NEXT L
1220 PRINT
1225 CLOSE #1
1230 PRINT "DATA ACQUISITION COMPLETE"
1240 SOUND 880, 10
1250 PRINT
1260 HZERO = N(4)
1270 V1 = (N(5) - 5) * 10 ^ (N(6) - 12)
1280 H1 = (N(7) - 5) * 10 ^ (N(8) - 12)
1290 HEND = H1 * 4000
1300 HMID = HEND / 2
1310 VPOS = V1 * 2000
1320 VPOS2 = VPOS / 2
1330 VNEG = -VPOS
1340 VNEG2 = VNEG / 2
1350 PRINT
1420 ANS$ = "Y"
1430 TTL$ = " NICOLET OSCILLOSCOPE RECORD "
1440 YAX$ = "VOLTS"
1450 XAX$ = "TIME (SEC.)"
1460 IF ANS$ = "y" GOTO 1540
1470 IF ANS$ = "Y" GOTO 1540
1480 PRINT
1490 INPUT ; "ENTER TITLE  ", TTL$
1500 PRINT
1510 INPUT ; "X-AXIS UNITS  ", XAX$
1520 PRINT
1530 INPUT ; "Y-AXIS UNITS  ", YAX$
1540 KEY OFF
1550 SCREEN 2, , 0, 0
1560 LINE (100, 90)-(600, 90)
1570 LINE (100, 1)-(600, 1)
1580 LINE (100, 180)-(600, 180)
1590 LINE (100, 1)-(100, 180)
1600 LINE (600, 1)-(600, 180)
1610 LINE (100, 45)-(105, 45)
1620 LINE (600, 45)-(595, 45)
1630 LINE (600, 135)-(595, 135)
1640 LINE (100, 135)-(105, 135)
1650 LINE (350, 180)-(350, 176)
1660 LOCATE 12, 8, 0: PRINT "0.00";
1670 LOCATE 1, 6, 0: PRINT USING "###.##"; VPOS;
1680 LOCATE 6, 6, 0: PRINT USING "###.##"; VPOS2;
1690 LOCATE 23, 6, 0: PRINT USING "###.##"; VNEG;
```

```
1700 LOCATE 18, 6, 0: PRINT USING "###.##"; VNEG2;
1710 LOCATE 25, 52, 0: PRINT XAX$;
1720 LOCATE 9, 1, 0: PRINT YAX$;
1730 LOCATE 1, 28, 0: PRINT TTL$;
1740 LOCATE 24, 12, 0: PRINT "0.0";
1750 LOCATE 24, 42, 0: PRINT HMID;
1760 LOCATE 24, 73, 0: PRINT HEND;
1770 LOCATE 1, 1, 0
1780 FOR X = 100 TO 600
1790 Y = 90 - A((X - 99) * 8 - 5) / 22.75
1800 PSET (X, Y)
1810 NEXT X
1820 INPUT ; ST$
1830 SCREEN 0
1840 IF IFLAG = 0 GOTO 1870
1850 IF IFLAG = 1 GOTO 2220
1860 IF IFLAG = 2 GOTO 2550
1870 PRINT
1890 PRINT "PRESSURE DATA IS BEING STORED ON DISKETTE IN DRIVE B"
1900 PD$ = "B:PES91.DAT"
1910 OPEN "R", #1, PD$, 8
1920 FIELD #1, 4 AS X$
1930 FOR I = 3 TO 4002
1935 P(I) = A(I) * V1
1940 LSET X$ = MKS$(P(I))
1950 PUT #1
1960 NEXT I
1970 CLOSE #1
2100 GOTO 840
2220 PRINT
2240 PRINT "VELOCITY DATA IS BEING STORED ON DISKETTE IN DRIVE B"
2250 IVF = IVF + 1
2260 inf = inf - 1
2270 inf$ = STR$(inf)
2280 V$ = "B:V91" + inf$ + ".DAT"
2300 OPEN "R", #2, V$, 2
2301 FIELD #2, 2 AS X$
2302 FOR I = 3 TO 4002
2303 V(I) = A(I) * V1 * 1000
2307 LSET X$ = MKI$(V(I))
2310 PUT #2
2317 NEXT I
2320 CLOSE #2
2371 PRINT IVF
2373 IF IVF = 50 GOTO 3540
2375 GOTO 800
2550 PRINT
2560 PRINT "TEMPERATURE IS BEING STORED ON DISKETTE IN DRIVE B"
2562 IVF = IVF + 1
2564 inf = inf - 1
2566 inf$ = STR$(inf)
2577 T$ = "B:TS91" + inf$ + ".DAT"
2590 OPEN "R", #3, T$, 2
2600 FIELD #3, 2 AS X$
2610 FOR I = 3 TO 4002
```

```
2615 T(I) = V1 * A(I) * 1000
2620 LSET X$ = MKI$(T(I))
2630 PUT #3
2640 NEXT I
2650 CLOSE #3
2750 IF IVF = 20 GOTO 780
2760 PRINT IVF
3000 GOTO 850
3540 PRINT : PRINT "PROGRAM ENDED"
```

HHH-91 basic program

```
10 PRINT
20 PRINT "Program : HHH-91 .BAS  "
35 PRINT
40 PRINT "This program read the values of pressure and temperature"
41 PRINT "from drive C and B and correct (compensates) the velocity."
50 PRINT " since the data are in voltage, it first converts the "
60 PRINT " values to appropriate quantities."
110 PRINT
200 DIM DU(4100): DIM TS(4300)
300 DIM DUS(4100)
630 DEFINT A
632 DIM B(20)
635 DIM MT(4100)
637 DIM SMT(1000)
640 DIM ST(4100)
645 DIM N(8)
646 DIM P(4100)
647 DIM T(4100)
650 DIM V1(4100)
653 DIM V(4100)
660 FOR I = 1 TO 10
670 SMT(I) = 0
680 NEXT I
721 IVF = 0
725 INF = 0
731 TA = 19
732 GA = 3.6 * (10 ^ (-3))
733 RC = 5.1
735 RS = 9.34
738 RT = 401 + RS + .28
739 TW = (RS / RC - 1) / GA + TA + 273
740 PRINT "TW = "; TW
741 RF = RT / RS
742 CN = .38
743 BE = 4.5764 * (10 ^ (-6))
744 XKS = 01
745 Hs = 1.2
747 PHA = 3.514144 * (10 ^ (-6))
1205 B(1) = .591
1210 B(2) = 1.192
1215 B(3) = 1.801
1220 B(4) = 2.419
1225 B(5) = 3.047
1230 B(6) = 3.683
1235 B(7) = 4.329
1240 B(8) = 4.983
1245 B(9) = 5.646
1250 B(10) = 6.317
1255 B(11) = 6.996
1260 B(12) = 7.687
1265 B(13) = 8.377
1270 B(14) = 9.070
1272 B(15) = 9.787
1286 FAM = 91.25
1290 BES = 01
```

HHH-91 basic program

```
1900 PD$ = "B:PRES.DAT"
2110 OPEN PD$ FOR RANDOM AS #1 LEN = 2
2111 FIELD #1, 2 AS C$
2130 FOR J = 3 TO 4002
2160 GET #1
2165 P(J) = CVI(C$) / 1000
2170 NEXT J
2173 CLOSE #1
2185 FOR J = 3 TO 4002
2187 P(J) = P(J)
2188 PRINT P(J)
2190 NEXT J
2192 PRINT "P(50),P(100),P(150)= "; P(50), P(100), P(150), IVF
2200 IVF = IVF + 1
2210 INF = INF - 1
2240 INF$ = STR$(INF)
2260 T$ = "B:TS91" + INF$ + ".DAT"
2555 OPEN T$ FOR RANDOM AS #2 LEN = 2
2560 FIELD #2, 2 AS C$
2562  FOR J = 3 TO 4002
2564 GET #2
2566 T(J) = CVI(C$)
2568 NEXT J
2569 CLOSE #2
2571 FOR J = 3 TO 4002
2575 T(J) = T(J) / FAM
2579 I = 1: S = 15
2580 M = INT((I + S) / 2)
2582 IF T(J) <= B(M) THEN S = M ELSE I = M
2584 IF S > I + 1 THEN GOTO 2580
2590 T(J) = I * 10 + (10 / (B(S) - B(I))) * (T(J) - B(I))
2600 ST(J) = ST(J) + T(J)
2800 MT(J) = ST(J) / IVF
3000 NEXT J
3010 CLOSE #2
3015 PRINT "MT(50),MT(100),MT(150)= ", MT(50), MT(100), MT(150), IVF
3016 IF IVF = 1 GOTO 3026
3025 GOTO 2200
3026 I = 1
3030 N = 514
3031 M = 3
3032 FOR J = M TO N
3033 SMT(I) = MT(J) + SMT(I)
3034 NEXT J
3035 I = I + 1
3036 M = M + 384
3037 N = N + 384
3038 IF I = 11 GOTO 3040
3039 GOTO 3032
3040 FOR k = 1 TO I - 1
3043 NEXT k
3046 PRINT "TEMPERATURE DATA IS BEING STORED ON DISKETTE IN DRIVE C"
3048 TG$ = "C:TS.DAT"
3050 OPEN "R", #2, TG$, 4
3053 FIELD #2, 4 AS x$
```

HHH-91 basic program

```
3055 FOR J = 3 TO 4098
3060 LSET x$ = MKS$(MT(J))
3061 PUT #2
3065 NEXT J
3066 CLOSE #2
3077 IVF = 0
3080 INF = 0
3082 IVF = IVF + 1
3083 INF = INF - 1
3085 INF$ = STR$(INF)
3090 VO$ = "B:VINS" + INF$ + ".DAT"
3100 OPEN VO$ FOR RANDOM AS #3 LEN = 2
3105 FIELD #3, 2 AS C$
3106 FOR J = 3 TO 4002
3107 GET #3
3108 V(J) = CVI(C$) / 1000
3110 NEXT J
3111 CLOSE #3
3113 PRINT "V(50),V(100),V(150)="; V(50), V(100), V(150), IVF
3114 FOR J = 3 TO 4002
3115 IF P(J) = 0 THEN P(J) = .00001
3116 IF P(J) < 0 THEN P(J) = .00001
3120 V1(J) = ((((V(J) / RF) ^ 2) / (TW - MT(J) - 273) - BE * (MT(J) +
273)^.8)*(MT(J) + 273)^(1.76*CN - .8))/(PHA*(P(J)*100000)^CN)
3125 IF V1(J) < 0 THEN V1(J) = 0
3130 V(J) = (V1(J) ^ (1 / CN))
3140 NEXT J
3500 PRINT " V(50), V(100),V(150)="; V(50), V(100), V(150), IVF
4205 PRINT "VELOCITY IS BEING TRANSFERRED TO DISKETTE IN DRIVE C"
4210 U$ = "C:INSV" + INF$ + ".DAT"
4215 OPEN "R", #3, U$, 4
4216 FIELD #3, 4 AS x$
4220 FOR J = 3 TO 4098
4221 IF J > 4002 THEN V(J) = V(4002)
4225 LSET x$ = MKS$(V(J))
4228 PUT #3
4230 NEXT J
4239 CLOSE #3
2410 PRINT "V(1000)="; V(1000)
5000 IF IVF = 1 GOTO 6000
5500 GOTO 3082
6000 PRINT "PROGRAM ENDED"
```

MVT-91 basic program

```
10 PRINT
20 PRINT "Program MVT-91 "
30 PRINT
40 PRINT "This program reads data from drive C and calculates the ensemble"
50 PRINT "average ofthe velocity and turbulence intensity. It also finds  "
60 PRINT "the time average of the mean and turbulence intencity.."
70 PRINT
80 PRINT
110 PRINT
637 DIM SUE1S(4100)
638 DIM SMUE1(4100)
642 DIM SUT(4100)
649 DIM U(4100)
654 DIM TI(4100)
711 DIM SUE1(4100)
712 DIM MUE1(4100)
715 DIM MV(4100)
717 DIM UTM(4100)
719 DIM UTF(4100)
720 DIM UM(4100)
721 DIM DS(4100)
722 DIM UT(4100)
723 DIM UF(4100)
725 DIM AM(4200)
744 DT = .00002
750 IVF = 0
800 INF = 0
900 C = 0
1000 FOR J = 1 TO 4096
1100 SUE1(J) = 0
1150 SUE1S(J) = 0
1200 NEXT J
2082 IVF = IVF + 1
2083 INF = INF - 1
2084 ICF = -1
2085 INF$ = STR$(INF)
2090 V$ = "C:ISVT" + INF$ + ".DAT"
2100 OPEN V$ FOR RANDOM AS #3 LEN = 4
2105 FIELD #3, 4 AS X$
2110 FOR J = 1 TO 4096
2120 GET #3
2125 U(J) = CVS(X$)
2130 NEXT J
2131 CLOSE #3
3142 PRINT "Velocity: "; U(512); U(1000); U(1590); U(2000); U(3500); ",IVF= "; IVF
3180 FOR J = 1 TO 4096
3190 SUE1(J) = U(J) + SUE1(J)
3192 SUE1S(J) = U(J) ^ 2 + SUE1S(J)
3202 MUE1(J) = SUE1(J) / (IVF - C)
3203 UT(J) = (SUE1S(J) / (IVF - C) - MUE1(J) ^ 2)
3204 IF UT(J) < 0 THEN UT(J) = 0
3205 UT(J) = UT(J) ^ .5
3207 NEXT J
3245 IF IVF = 3 GOTO 4200
```

MVT-91 basic program

```
3250 GOTO 2082
4200 PRINT "VELOCITY IS BEING TRANSFERRED TO DISKETTE IN DRIVE B"
4210 MV$ = "B:MVO.DAT"
4215 OPEN MV$ FOR OUTPUT ACCESS WRITE AS #4
4220 FOR J = 1 TO 4096
4225 PRINT #4, USING "######.###### "; MUE1(J), UT(J)
4230 NEXT J
4240 CLOSE #4
5000 M = 1
5005 N = 512
5010 I = 1
5015 FOR J = M TO N
5020 UM(I) = MUE1(J) + UM(I)
5025 UF(I) = UM(I) / 512
5030 UTM(I) = UTM(I) + UT(J) ^ 2
5040 UTF(I) = (UTM(I) / 512) ^ .5
5045 NEXT J
5050 M = M + 384
5053 N = N + 384
5055 I = I + 1
5057 IF I = 11 GOTO 5080
5060 GOTO 5015
5080 FOR I = 1 TO 10
5085 PRINT "time mean average ="; UF(I); "time ave.turb.int.= "; UTF(I)
5090 NEXT I
6000 PRINT "PROGRAM ENDED"
```